TOWARDS AN LMI APPROACH TO MULTICRITERIA VISUAL SERVOING IN ROBOTICS

—

COMPANION REPORT

Patrick Danès

LAAS-CNRS

7, avenue du Colonel Roche

31 077 Toulouse, France

Université Paul Sabatier

118, route de Narbonne

31 062 Toulouse, France

patrick.danes@laas.fr

Delphine Bellot

Laboratoire de Robotique de Paris

18, route du Panorama — BP61

92 265 Fontenay aux Roses, France

Université Pierre et Marie Curie

4, place Jussieu

75 005 Paris, France

bellot@robot.jussieu.fr

This paper is intented to be a companion report to the paper having the same title, which has been accepted for publication in European Journal of Control, special issue on LMIs in Control.

This work has been orally presented at the invited Workshop on Linear Matrix Inequalities in Control (LMI'04), July 1st & July 2nd 2004, LAAS-CNRS, Toulouse, France.

A slight typo error appearing in the published manuscript has been corrected here, see Figure 2.

Version of July 18, 2006

LAAS REPORT #05085

Abstract

This paper attempts to propose a general framework to the multicriteria analysis and synthesis of visual servoing schemes in robotics. Two of the most prominent control strategies are unified under a common state-space representation, which is highly nonlinear and possibly uncertain. This model is then embedded into a Linear Differential Inclusion with linear fractional uncertainty, so that the problem can be tackled in a robust linear control context. Many visual servoing requirements can be dealt with, e.g. convergence, avoidance of actuators saturations, image and 3D contraints.

Existing work on the analysis and control of rational systems through quadratic Lyapunov functions is a seminal basis to the approach. As the symmetry and convexity properties of the consequent ellipsoidal invariant sets is penalizing in this robotics context, some extensions are presented, which can be of independent interest.

When possible, the criteria are dealt with through Linear Matrix Inequalities.

Keywords: visual servoing, rational systems, "global linearization", LFTs, robust linear control, linear matrix inequalities.

0 Notations

This paper uses some standard notation. If A is a matrix, then $A^{'}$, A^{-1}, rank$A$, trace$A$, det$A$, respectively term the transpose, the inverse, the rank, the trace and the determinant of A; A is assumed to have appropriate dimensions so that such operators can be applied. I_n and $0_{(n;m)}$ respectively term the identity matrix of $\mathbb{R}^{n\times n}$ and the null matrix of $\mathbb{R}^{n\times m}$; when there is no ambiguity, I and 0 are used instead. The diag$(.)$ constructor enables the definition of a block-diagonal matrix from scalars or square submatrices of appropriate dimensions. The operator col$_j(A)$ extracts the j^{th} column of the matrix A. The symbol $\stackrel{\Delta}{=}$ means "is equal to, by definition". The notation $P>0$ (resp. $P<0$) means that the square matrix P is positive definite (resp. negative definite.) Similarly, $P\geq 0$ and $P\leq 0$ are used for semidefiniteness. Without loss of generality, P is assumed symmetric.

More specific notations follow. A vector $r=(r_1,\ldots,r_{\mathsf{N}})^{'}\in\mathbb{N}^{\mathsf{N}}$ being given, $n_p(r)$ is defined as $n_p(r)\stackrel{\Delta}{=}\sum_{i=1}^{\mathsf{N}} r_i$. Besides, the following sets will often be referred to: $\mathscr{D}(r)\stackrel{\Delta}{=}\{\Delta=\text{diag}(\delta_1 I_{r_1},\ldots,\delta_{\mathsf{N}} I_{r_{\mathsf{N}}}) : \delta_i\in\mathbb{R},\ i=1,\ldots,\mathsf{N}\}$; $\blacktriangle(r)\stackrel{\Delta}{=}\{\Delta\in\mathscr{D}(r) : |\delta_i|\leq 1,\ i=1,\ldots,\mathsf{N}\}$; $\mathscr{B}(r)\stackrel{\Delta}{=}\{B=\text{diag}(B_1,\ldots,B_{\mathsf{N}}) : B_i\in\mathbb{R}^{r_i\times r_i},\ i=1,\ldots,\mathsf{N}\}$; $\mathscr{S}(r)\stackrel{\Delta}{=}\{S\in\mathscr{B}(r) : S_i=S_i^{'}>0,\ i=1,\ldots,\mathsf{N}\}$; $\mathscr{G}(r)\stackrel{\Delta}{=}\{G\in\mathscr{B}(r) : G_i=-G_i^{'},\ i=1,\ldots,\mathsf{N}\}$.

1 Introduction

The advent of fast and efficient visual sensors has led the robotics community to investigate a broader field of applications. In addition to their former use in low-frequency tasks such as pattern recognition or scene modeling and interpretation, cameras have been considered as a relevant information source for tasks operating at fast rate. Consequently, a considerable effort has been made on the problematics of optical odometry, active vision, visual-based control, to cite few. This paper takes place within the last area mentioned, which has been a very active field of research for the last fifteen years, see for example [24] and the journal special issues [27, 33].

The use of visual data in control algorithms shows many advantages compared to a solution exclusively based on proprioceptive information[†]. For instance, when considering a proprioceptive-based servo of a manipulator arm, an error-free regulation of the end-effector pose [‡] to a constant reference does not ensure that the task is properly performed, e.g. because of errors in the models of the robot or of its environment. By contrast, a visual feedback is a fundamental step towards the fulfillment of accurate positioning tasks. Visual sensors may even be mandatory for tracking moving targets.

This paper assumes that the camera is rigidly attached to the controlled robot or end-effector. Visual servocontrol schemes can be classified depending on the type of data that is transmitted to the controller [27]. The approach commonly named *position-based* —or *"3D"— visual servoing* defines the controlled variable as the *3D pose*, i.e. the relative situation between the sensor and the target. This quantity is estimated from the processed image by a localization algorithm. As localization reliability heavily depends on a good knowledge of the camera calibration parameters and —when such extra-information is used— of the model of the target, the robustness of 3D servos may happen to be fairly poor. In addition, though some feeling can be got about the camera 3D trajectory, no straight conclusion can be established concerning the 2D apparent motion in the image, so that the target may be lost. An *image-based* —or *"2D"— visual servoing* entails a control law that is directly expressed in the space of the visual sensor. In its simplest form, some dedicated *visual features* —spots, lines, etc.— are fixed to the target, which projections onto the camera image plane must reach a reference configuration. No 3D pose reconstruction is required, so that this kind of visual-based feedback is less sensible to calibration errors and can be implemented at a higher rate. However, even if the image trajectory may be approximately controlled, the consequent 3D trajectory may get contorted. More recent hybrid "$2\frac{1}{2}$D" servos avoid some drawbacks of the above schemes [30].

As one would expect, visual servocontrol raises sharp problems at the confluence of Computer Vision and Automatic Control [40]. At the sensor level, fast and reliable algorithms are needed for features

[†] *Proprioceptive sensors* —e.g. encoders, odometers, gyroscopes, etc.— provide information about a robot internal state, while *exteroceptive sensors* —e.g. visual sensors, laser telemeters, ultrasonic sensors, etc.— are involved in the perception of its environment.

[‡] The words *pose* and *situation* term the pair (*position*,*attitude*).

extraction and labelling, or for localization. On a control point of view, many strategies have been used. A pioneering work proposed by Espiau *et al.* [19] reformulates the problem in the space of a penalized output, called *task function* [36], under some regularity conditions. Numerous studies and extensions have then been developed in this framework. In [28], a robust stabilizing controller for a simplified robot is synthesized taking into account Lagrangian dynamics. An underactuated rigid body system is visually servoed using robust backstepping techniques in [23]. Adaptive, LQR and Generalized Predictive control have respectively been considered in [34] [25] and [22]. In [39], a gain-scheduled $\mathscr{H}_\infty$ controller for a pan/tilt platform is synthesized, achieving some robust performance. Problems of task singularities and convergence are recorded in [6], for strategies entailing the inverse of the Jacobian relating the camera control input to the derivatives of either 3D situation parameters or 2D parameters in the image. Stability analysis for recent strategies are presented in [29].

Despite this large amount of work, the analysis and the synthesis of visual-based positioning laws are still open with respect to convergence, avoidance of actuators' and sensors' saturations and guarantee of 3D constraints, when all those criteria are simultaneously taken into account. So it is, both in situation-based and feature-based approaches. Some strategies have been proposed to maintain the target into the camera field of view, through path-planning [33, 43], navigation functions [10], circular-like trajectories [8] or decoupling issues [42, 9]. A controller is designed in [41] so as to quadratically stabilize a polytopic system which locally embeds a task-function based representation while taking into account actuators velocities bounds and visibility constraints. However, the avoidance of some convergence problems referred to in [6] is not ensured.

This paper attempts to propose a general framework for the solution of this whole multicriteria problem in the kinematic case, i.e. when dynamics effects are neglected. More specifically, the positioning of a 6 degrees-of-freedom (DOF) camera with respect to a fixed target is considered in an uncluttered environment. Position-based and image-based servos are unified into a common state-space model in § 2. This model is then embedded into a Linear Differential Inclusion with LFT uncertainty in § 3, so that the multicriteria analysis or synthesis can be tackled in a robust linear control context. The mere application of existing techniques, shown in § 4, does not enable the treatment of relevant visual servoing schemes. So, two extensions —which may be of independent interest— are presented in § 5 to reduce their conservatism. Perspectives and open problems are finally discussed.

2 State space modeling of interactions and Problem statement

As mentioned in the introduction, this paper tackles the multicriteria analysis and synthesis of visual-based control schemes which aim to drive a perspective camera to a unique relative situation with respect to a

fixed target. Dedicated spots serve as visual features. They are layed on the target in such a way that to any configuration of their projection onto the camera image plane corresponds a unique sensor-target relative situation. This is the case when coplanar unaligned spots are used, whose number is at least four [26]. Though the environment can be constrained, it is presumed to be free of mobile obstacles.

A noise-free model of interactions is set up first, in which all the parameters are known. The actuators, the sensor and the image processing system —particularly the extraction and the labeling of the projections of the visual features, and, when necessary, the visual-based localization algorithm— are supposed perfect and instantaneous, so that they do not explicitely appear. As is often the case in the literature, dynamic effects in the camera motion are neglected. The control input to the so-called kinematic model is thus the camera velocity screw, i.e. the vector made up of its translational and rotational velocities. The method will be further shown to easily take into account parametric uncertainties, if any.

2.1 Notations

The following frames are relevant to the forthcoming modeling, see Figure 1. $F_O = (O, \overrightarrow{x_O}, \overrightarrow{y_O}, \overrightarrow{z_O})$ is a frame linked to the world. $F_S = (S, \overrightarrow{x_S}, \overrightarrow{y_S}, \overrightarrow{z_S})$ is rigidly associated to the camera, with S the optical center and $\overrightarrow{z_S}$ positioned on the optical axis. The third frame $F_T = (T, \overrightarrow{x_T}, \overrightarrow{y_T}, \overrightarrow{z_T})$, rigidly linked to the target, is defined as the situation to be reached by F_S once the positioning is performed. Of course, all the constraints of the problem must be fulfilled when F_S and F_T coincide.

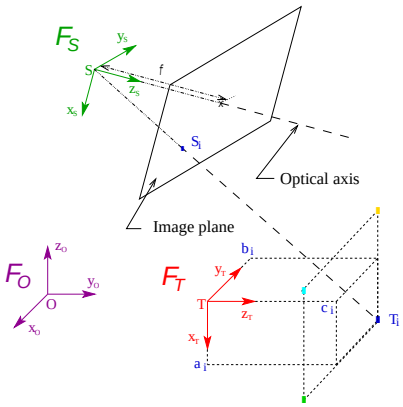

Figure 1: Frames F_O, F_S, F_T

A variable is superscripted by the symbol $*$ to depict its value at the camera reference situation.

The target is fitted with the M dedicated spots $T_1, T_2, \ldots T_M$, whose perspective projections onto the camera image plane are termed $S_1, S_2, \ldots S_M$. Let $(\overrightarrow{ST_i})_{(F_S)} = (x_i, y_i, z_i)'$ and $(\overrightarrow{TT_i})_{(F_T)} = (a_i, b_i, c_i)'$ be the coordinates of T_i, $i = 1, \ldots, M$, in frames F_S and F_T. The metric coordinates $(\overrightarrow{SS_i})_{(F_S)} = (X_i, Y_i, f)'$ of S_i, $i = 1, \ldots, M$, in frame F_S thus satisfy $X_i = f\frac{x_i}{z_i}$ and $Y_i = f\frac{y_i}{z_i}$, with f the camera focal length. In addition, one has $X_i^* = f\frac{a_i}{c_i}$ and $Y_i^* = f\frac{b_i}{c_i}$.

2.2 Open-loop model

Assume first that a 6DOF "free-flying" camera is considered. As previously outlined, the control signal vector u is the velocity screw of the camera with respect to the world. Equivalently, one states

$u \triangleq (V_x, V_y, V_z, \Omega_x, \Omega_y, \Omega_z)'$, with $(V_x, V_y, V_z)'$ and $(\Omega_x, \Omega_y, \Omega_z)'$ the entries in F_S of the translational and rotational velocities of F_S w.r.t. F_O.

No dynamic effect is assumed in the camera motion and the target is motionless, so that every variable of the open-loop system can be determined through a memoryless mapping of the sensor-target relative situation. The state vector is therefore defined as $x = (\mathscr{T}', \mathscr{R}')'$ with $\mathscr{T}$ (resp. $\mathscr{R}$) a parametrization of the relative translation (resp. of the relative attitude) between F_S and F_T. $\mathscr{T}$ can be naturally made up with the entries $(\overrightarrow{ST})_{(F_S)} = (t_x, t_y, t_z)'$ in frame F_S of the vector joining the origins S and T of F_S and F_T. As the Special Orthogonal Group of rotations is not isomorphic to $\mathbb{R}^3$, the definition of $\mathscr{R}$ as a 3-tuple of independent angles is somewhat more involved: care must indeed be taken in order to avoid the singularities of this representation during the completion of the task. A convenient choice is the set of Bryant angles [§] $\mathscr{R} = (\lambda, \mu, \nu)'$. This 3-tuple of attitude parameters is indeed multivalued only when $\mu \equiv \pm \frac{\pi}{2} [2\pi]$, in which case the camera optical axis $\overrightarrow{z_S}$ is orthogonal to $\overrightarrow{z_T}$. Such a configuration cannot happen in a visual servocontrol task, lest the target would be out of the camera field of view [3].

The output vector y is defined as the input to the controller. If the control under study is of the position-based type, y is merely the state vector x. When considering an image-based servo, y must be a function of the vector $s \triangleq (X_1, Y_1, \ldots, X_{\mathsf{M}}, Y_{\mathsf{M}})'$ made of the projections coordinates of the visual features. Besides, y must be a function of the reference coordinates s^*. Lastly, in order to enable the global linearization step explained in § 3.3, y must be 0 when $x = 0$. So, for an image-based servo, one sets $y = s - s^*$.

The state equation depicts the effect of the velocity screw onto the relative sensor-target situation. It is obtained by applying the translational and rotational velocities composition rule. For image-based servos, the output equation accounts for the interaction between the sensor-target relative situation and the coordinates of the features' perspective projections. An outline of the computations concerning the 6DOF case is given in Appendix A. They lead to the open-loop state space equations (1)–(2) in Figure 2. When the camera degrees of freedom are restricted, the open-loop state vector x and the control vector u lie in $\mathbb{R}^n$ and $\mathbb{R}^{n_u}$. Though the results will henceforth be presented telling n from n_u, these two dimensions will be assumed equal. Also recall that y belongs to $\mathbb{R}^{2\mathsf{M}}$.

2.3 Closed-loop system and Problem statement

The open-loop equations (1)–(2) were shown to be highly nonlinear. Moreover, though it hasn't been supposed so far, they are often affected by some uncertainty, e.g. on the focal length f of the camera, on the coefficients a_i, b_i, c_i of the target model, etc.

[§] The relative attitude between $F_S = (S, \overrightarrow{x_S}, \overrightarrow{y_S}, \overrightarrow{z_S})$ and $F_T = (T, \overrightarrow{x_T}, \overrightarrow{y_T}, \overrightarrow{z_T})$ is depicted through the 3-tuple (λ, μ, ν) as follows: an intermediate frame F_2 is first obtained by rotating F_S of the angle λ around $\overrightarrow{x_S}$; rotating F_2 of the angle μ around $\overrightarrow{y_2}$ leads to a secondary intermediate frame F_3, the image of which through the rotation of angle ν around $\overrightarrow{z_3}$ is $(S, \overrightarrow{x_T}, \overrightarrow{y_T}, \overrightarrow{z_T})$.

$$\begin{pmatrix} \dot{t_x} \\ \dot{t_y} \\ \dot{t_z} \\ \dot{\lambda} \\ \dot{\mu} \\ \dot{\nu} \end{pmatrix} = \begin{pmatrix} -1 & 0 & 0 & 0 & -t_z & t_y \\ 0 & -1 & 0 & t_z & 0 & -t_x \\ 0 & 0 & -1 & -t_y & t_x & 0 \\ 0 & 0 & 0 & -1 & -\sin\lambda\tan\mu & \cos\lambda\tan\mu \\ 0 & 0 & 0 & 0 & -\cos\lambda & -\sin\lambda \\ 0 & 0 & 0 & 0 & \frac{\sin\lambda}{\cos\mu} & \frac{-\cos\lambda}{\cos\mu} \end{pmatrix} \begin{pmatrix} V_x \\ V_y \\ V_z \\ \Omega_x \\ \Omega_y \\ \Omega_z \end{pmatrix} \tag{1}$$

$$y = x \text{ (position-based servo)} \quad | \quad y = (X_1 - X_1^*, Y_1 - Y_1^*, \ldots, Y_{\mathsf{M}} - Y_{\mathsf{M}}^*)' \text{ (image-based servo)} \tag{2}$$

with $\begin{pmatrix} X_i - X_i^* \\ Y_i - Y_i^* \end{pmatrix} = \frac{f}{c_i z_i} \begin{pmatrix} c_i x_i - a_i z_i \\ c_i y_i - b_i z_i \end{pmatrix}$ and

$$\begin{aligned} z_i &= t_z + a_i(-\cos\lambda\sin\mu\cos\nu + \sin\lambda\sin\nu) + b_i(\cos\lambda\sin\mu\sin\nu + \sin\lambda\cos\nu) + c_i\cos\lambda\cos\mu \\ c_i x_i - a_i z_i &= c_i t_x - a_i t_z - a_i^2(-\cos\lambda\sin\mu\cos\nu + \sin\lambda\sin\nu) + c_i^2\sin\mu - b_i c_i\cos\mu\sin\nu \\ &\quad -a_i b_i(\cos\lambda\sin\mu\sin\nu + \sin\lambda\cos\nu) + a_i c_i\cos\mu(\cos\nu - \cos\lambda) \\ c_i y_i - b_i z_i &= c_i t_y - b_i t_z - b_i^2(\cos\lambda\sin\mu\sin\nu + \sin\lambda\cos\nu) - c_i^2\sin\lambda\cos\mu \\ &\quad -a_i b_i(-\cos\lambda\sin\mu\cos\nu + \sin\lambda\sin\nu) + a_i c_i(\sin\lambda\sin\mu\cos\nu + \cos\lambda\sin\nu) \\ &\quad +b_i c_i(\cos\lambda(\cos\nu - \cos\mu) - \sin\lambda\sin\mu\sin\nu). \end{aligned}$$

Figure 2: Open-loop model (mind the typo error, corrected in red)

Let a visual-based feedback controller having no external input be connected to the above open-loop model. The first property to be checked or ensured in closed-loop is the convergence of the camera to the reference final situation. Because of the above choice of the open-loop state vector, this positioning is performed whenever the equilibrium state 0 of the —autonomous— closed-loop system is asymptotically stable[¶]. Doing so, "local minima" [6] —viz. convergence to situations such that the control vector is zero while s and s^* differ— are avoided.

The other criteria of the problem are dealt with by making some scalar so-called additional variables ζ_j, $j = 1, \ldots, n_\zeta$, lie into prescribed intervals. Without loss of generality, each such additional variable is a memoryless function $\zeta_j(\tilde{x})$ of the closed-loop state vector $\tilde{x} \stackrel{\Delta}{=} (x', x_c')'$, taking the value 0 when $\tilde{x}$ is 0. Boundedness constraints on additional variables enable the satisfaction of criteria of paramount importance. For instance, the visual features' projections can be restricted to the physical limits of the camera image plane by defining $\zeta_j = s_j - s_j^*$, including for 3D servos. Actuators saturations can be dealt with as well, e.g. by defining some ζ_j's as entries of the velocity screw u or norms of subvectors extracted from u. 3D constraints, such as constraining the camera to move inside a corridor without hitting its walls, can be handled even for 2D servos by bounding some distances $\zeta_j = d_{3\mathrm{D}_j}$. Last, imposing bounds on the control signal u or the differences $s_j - s_j^*$ can enable the avoidance of differential singularities in the loop transfers,

[¶]In fact, the attractivity of 0 is sufficient to ensure the positioning. Nevertheless, asymptotic stability is wanted to prevent, for instance, camera round-trips through infinity, e.g. as these described by [6] in the case of some image-based inverse Jacobian controllers.

e.g. when using some 2D inverse Jacobian control schemes.

Such a statement can be viewed as a first step towards a "standard" problem in visual servoing. For instance, a penalized output z can be introduced having in some way the meaning of a task function. Despite the problem is not fully reformulated in the task space as in [19, 36], it can be associated to the minimization of a criterion on z or on the transfer from a relevant input signal w to z. In principle, any type of controller can be considered, whether 3D or 2D, static or dynamic, or even gain-scheduled (e.g. 2D controllers scheduled by 3D data, which would be a special kind of $2\frac{1}{2}$D controllers.) Also note that dynamic effects could be taken into account in the open-loop model, by building u with the forces and torques which cause the camera motion, and by defining x with pose parameters and velocities. Besides, a finer modeling of the camera could be used, including all its intrinsic parameters rather than just the focal f, so that s and s^* would be expressed in pixel coordinates. Uncertainties on the camera parameters, on the measurements, or on the coefficients a_i, b_i, c_i of the target model can be considered as well.

3 Towards a robust linear control problem

The problem is dealt with in the linear robust control framework, as many results have been developed for the multicriteria analysis and synthesis of linear uncertain systems. They sometimes lead to convex optimization problems —e.g. entailing Linear Matrix Inequalities (LMIs) [5]— which enjoy nice tractability properties and can thus be solved with efficient solvers.

The possibly uncertain genuine nonlinear closed-loop system is "embedded" into an uncertain system described by a linear differential inclusion. So, when dealing with analysis, a property is proved true for the nonlinear closed-loop system whenever it is satisfied by this embedding inclusion. As for the synthesis, one may endow the actual closed-loop system with a given property by bestowing this property to each realization of the uncertain system. Such a linerization technique, referred to as "global linearization" in [5], handles nonlinearities and uncertainties in a unified manner. Of course, it induces conservatism, in that many trajectories of the uncertain system —henceforth termed "spurious"— are physically meaningless. So, the analysis/synthesis conditions, which are only sufficient, may be far too pessimistic. At worst, their conjunction may lead to a poor performance, or even be void.

The proposed methodology relies on the seminal work of El Ghaoui *et al*. concerning the analysis and control of rational systems [18, 17, 14, 13]. In this context, the global linearization step leads to an embedding linear system with strongly structured uncertainty, hopefully limiting the conservatism.

3.1 Rational systems

Definition 3.1 (Rational system [18]) *A system is said* rational *if its state space representation has the form*[‖]

$$\begin{pmatrix}\dot{x}\\ y\end{pmatrix} = \begin{pmatrix}\mathbf{A}(\Phi_x(x),\Phi_\chi(\chi)) & \mathbf{B}(\Phi_x(x),\Phi_\chi(\chi))\\ \mathbf{C}(\Phi_x(x),\Phi_\chi(\chi)) & \mathbf{D}(\Phi_x(x),\Phi_\chi(\chi))\end{pmatrix}\begin{pmatrix}x\\ u\end{pmatrix}, \tag{3}$$

where $\Phi_x(.)$ *and* $\Phi_\chi(.)$ *are some vector-valued functions, and* $\mathbf{A}(.,.)$, $\mathbf{B}(.,.)$, $\mathbf{C}(.,.)$, $\mathbf{D}(.,.)$ *term some matrix functions which depend rationally on their arguments and are well-defined in* $(\Phi_x,\Phi_\chi)=(0,0)$. *When inserted, the vector* χ *accounts for parametric uncertainties.*

In the context of visual servoing, all the attitude coordinates appear as the arguments of trigonometric functions. Provided that $\lambda \in [-\frac{\pi}{2};\frac{\pi}{2}]$, $\mu \in]-\frac{\pi}{2};\frac{\pi}{2}[$ and $\nu \in [-\pi;\pi]$, a bijective change of variables can be applied to the state vector, respectively turning λ, μ and ν into L, M, N, with

$$L \triangleq \tan(\frac{\lambda}{2}),\ M \triangleq \tan(\frac{\mu}{2}),\ N \triangleq \tan(\frac{\nu}{4}), \tag{4}$$

so as to get the following equivalent rational representation of the open-loop system (1)–(2):

$$\begin{pmatrix}\dot{x}\\ y\end{pmatrix} = \begin{pmatrix}0 & \mathbf{B}(\Phi_x(x))\\ \mathbf{C}(\Phi_x(x)) & 0\end{pmatrix}\begin{pmatrix}x\\ u\end{pmatrix},\ x\in\mathbb{R}^n,\ \Phi_x(x)\in\mathbb{R}^{\mathsf{N}_x}. \tag{5}$$

The interconnection of (5) with a m^{th}-order controller

$$\begin{pmatrix}\dot{x_c}\\ u\end{pmatrix} = \begin{pmatrix}\mathbf{K_c}(\Phi_{cx}(x)) & \mathbf{K_{cy}}(\Phi_{cx}(x))\\ \mathbf{K_u}(\Phi_{cx}(x)) & \mathbf{K}(\Phi_{cx}(x))\end{pmatrix}\begin{pmatrix}x_c\\ y\end{pmatrix},\ x_c\in\mathbb{R}^m,\ \Phi_{cx}(x)\in\mathbb{R}^{\mathsf{N}_{cx}}, \tag{6}$$

leads to the autonomous closed-loop rational system

$$\dot{\tilde{x}} = \tilde{\mathbf{A}}(\Phi(x))\,\tilde{x},\ \tilde{x}\in\mathbb{R}^{n+m},\ \Phi(x)\in\mathbb{R}^{\mathsf{N}}. \tag{7}$$

3.2 Equivalent Linear Fractional Transforms

Definition 3.2 (LFT of a rational system — Well-posedness) *It can be shown [18] that* (5) *can be turned into the form*

$$\begin{pmatrix}\dot{x}\\ y\end{pmatrix} = \left(\begin{pmatrix}0 & B_u^\sharp\\ C_y^\sharp & 0\end{pmatrix} + \begin{pmatrix}B_p^\sharp\\ D_{yp}^\sharp\end{pmatrix}\Delta_{ol}(\Phi_x(x))\,(I-D_{qp}^\sharp\Delta_{ol}(\Phi_x(x)))^{-1}\begin{pmatrix}C_q^\sharp & D_{qu}^\sharp\end{pmatrix}\right)\begin{pmatrix}x\\ u\end{pmatrix} \tag{8}$$

$$\text{with } \Delta_{ol}(\Phi_x(x)) = \operatorname{diag}(\Phi_{x_1}(x)I_{r_{ol1}},\ldots,\Phi_{x_{\mathsf{N}_x}}(x)I_{r_{ol\mathsf{N}_x}}),$$

[‖] The definition must be somewhat looser than in [18] or [13], for an important reason to be explained in § 6, page 43.

$r_{ol} = (r_{ol1}, \ldots, r_{ol\mathsf{N}_x})'$ *being an adequate vector in* $\mathbb{N}^{\mathsf{N}_x}$*, and* $B_u^\sharp$, $C_y^\sharp$, $B_p^\sharp$, $D_{yp}^\sharp$, $C_q^\sharp$, $D_{qu}^\sharp$, $D_{qp}^\sharp$ *some appropriate constant matrices. Moreover, for all values of* x *such that* $\det(I - D_{qp}^\sharp \Delta_{ol}(\Phi_x(x))) \neq 0$, (8) *is said* well-posed *and can be equivalently represented by*

$$\begin{pmatrix} \dot{x} \\ y \\ q^\sharp \end{pmatrix} = \begin{pmatrix} 0 & B_u^\sharp & B_p^\sharp \\ C_y^\sharp & 0 & D_{yp}^\sharp \\ C_q^\sharp & D_{qu}^\sharp & D_{qp}^\sharp \end{pmatrix} \begin{pmatrix} x \\ u \\ p^\sharp \end{pmatrix}, \; p^\sharp = \Delta_{ol}(\Phi_x(x))\, q^\sharp, \tag{9}$$

which is the interconnection of an LTI system of state vector x*, input vector* $(u', p^{\sharp\prime})'$*, and output vector* $(y', q^{\sharp\prime})'$*, with a* $n_p(r_{ol}) \times n_p(r_{ol})$ *state-dependent matrix gain* $\Delta_{ol}(\Phi_x(x))$ *joining* $q^\sharp$ *and* $p^\sharp$*. With a slight word misuse,* (8) *and* (9)*, which are equivalent under the well-posedness assumption, will henceforth be termed* Linear Fractional Transform (LFT) *of* (5)*, see [44].*

The LFT (9) satisfies the relationships $\{B_p^\sharp \Delta_{ol}(\Phi_x(x))(I - D_{qp}^\sharp \Delta_{ol}(\Phi_x(x)))^{-1} C_q^\sharp = 0$, $D_{yp}^\sharp \Delta_{ol}(\Phi_x(x))(I - D_{qp}^\sharp \Delta_{ol}(\Phi_x(x)))^{-1} D_{qu}^\sharp = 0\}$, which specialize into $\{C_y^\sharp = I, \;\; D_{yp}^\sharp = 0, \;\; C_q^\sharp = 0\}$ when $y = x$. Some systematic rules shown in [44] and [13] can be used in order to build an LFT of a rational system, this representation being nonunique.

As expected, similar arguments hold for the closed-loop system, namely, there exist constant matrices $\tilde{A}^\sharp$, $\tilde{B}_p^\sharp$, $\tilde{C}_q^\sharp$, $\tilde{D}_{qp}^\sharp$ such that (7) is equivalent to the LFT

$$\begin{pmatrix} \dot{\tilde{x}} \\ \tilde{q}^\sharp \end{pmatrix} = \begin{pmatrix} \tilde{A}^\sharp & \tilde{B}_p^\sharp \\ \tilde{C}_q^\sharp & \tilde{D}_{qp}^\sharp \end{pmatrix} \begin{pmatrix} \tilde{x} \\ \tilde{p}^\sharp \end{pmatrix}, \; \tilde{p}^\sharp = \Delta(\Phi(x))\, \tilde{q}^\sharp \tag{10}$$

$$\text{with } \Delta(\Phi(x)) = \operatorname{diag}(\Phi_1(x) I_{r_1}, \ldots, \Phi_{\mathsf{N}}(x) I_{r_{\mathsf{N}}}), \; r = (r_1 \ldots r_{\mathsf{N}})' \in \mathbb{N}^{\mathsf{N}},$$

under the well-posedness assumption $x \in \{\xi : \det(I - \tilde{D}_{qp}^\sharp \Delta(\Phi(\xi))) \neq 0\}$.

This section ends with the definition of the minimality of an LFT, which will turn to be an important notion in the sequel.

Definition 3.3 (Minimality of an LFT) *An LFT is said* minimal *if the vector* r *is such that* $n_p(r) \stackrel{\Delta}{=} \sum_{i=1}^{\mathsf{N}} r_i$ *has the least possible value.*

From [17], any rational system entailing monomials of maximum degree m_i in Φ_i can be turned into an LFT whose feedback matrix $\Delta(\Phi) = \operatorname{diag}(\Phi_1 I_{r_1}, \Phi_2 I_{r_2}, \ldots)$ satisfies $r_i \geq m_i$ for every i. Yet, to our knowledge, there is no analytical technique enabling the computation of the minimal LFT of a rational system. Nevertheless, *ad hoc* arguments can sometimes be used in conjunction with the systematic building rules mentioned above. Several numerical approaches to the reduction of LFTs are also referenced in [13].

3.3 Global linearization

Assume that the following assumption holds:

Hypothesis 3.4 (Boundedness & Well-posedness) *The vector* $\Phi = \Phi(x) \in \mathbb{R}^{\mathsf{N}}$ *involved in* (7) *takes its values in a parallelotope* $\Xi \stackrel{\Delta}{=} \prod_{i=1}^{\mathsf{N}} [\underline{\Phi}_i; \overline{\Phi}_i]$ *defined* a priori, *viz.*

$$x \in \Xi_f \stackrel{\Delta}{=} \{\xi \in \mathbb{R}^n \,:\, \Phi(x) \in \Xi, \text{ with } \Xi \stackrel{\Delta}{=} \prod_{i=1}^{\mathsf{N}} [\underline{\Phi}_i; \overline{\Phi}_i]\}, \tag{11}$$

onto which the closed-loop LFT (10) *is* well-posed, *i.e.*

$$\forall \Phi \in \Xi \stackrel{\Delta}{=} \prod_{i=1}^{\mathsf{N}} [\underline{\Phi}_i; \overline{\Phi}_i], \ \det\left(I - \tilde{D}_{qp}^{\sharp} \Delta(\Phi)\right) \neq 0. \tag{12}$$

Consider the uncertain linear system

$$\dot{\tilde{x}} = \tilde{\mathbf{A}}(\delta^{\sharp})\tilde{x} \tag{13}$$

with $\delta^{\sharp}$ a time-varying uncertain parameters vector taking any value in the parallelotope Ξ. An elementary reasoning shows that a state trajectory of the genuine nonlinear closed-loop system (7) also satisfies (13) if and only if the boundedness condition (11) is satisfied all along this trajectory. As aforementioned, the embedding of the genuine nonlinear system (7) into the uncertain linear system (13) will be referred to as "global linearization".

Definition 3.5 (SLNDI) *Under Hypothesis 3.4, the uncertain linear system* (13) *can be put into the form of the LFT*

$$\begin{pmatrix} \dot{\tilde{x}} \\ \tilde{q}^{\sharp} \end{pmatrix} = \begin{pmatrix} \tilde{A}^{\sharp} & \tilde{B}_p^{\sharp} \\ \tilde{C}_q^{\sharp} & \tilde{D}_{qp}^{\sharp} \end{pmatrix} \begin{pmatrix} \tilde{x} \\ \tilde{p}^{\sharp} \end{pmatrix}, \ \tilde{p}^{\sharp} = \Delta(\delta^{\sharp})\,\tilde{q}^{\sharp} \tag{14}$$

$$\text{with } \Delta(\delta^{\sharp}) = \mathrm{diag}\left(\delta_1^{\sharp} I_{r_1}, \ldots, \delta_{\mathsf{N}}^{\sharp} I_{r_{\mathsf{N}}}\right),\ r = (r_1 \ldots r_{\mathsf{N}})' \in \mathbb{N}^{\mathsf{N}},\ \text{and } \forall i = 1, \ldots, \mathsf{N},\ \delta_i^{\sharp} \in [\underline{\Phi}_i; \overline{\Phi}_i],$$

which can be considered as the connection of an LTI system with a time-varying uncertain matrix gain $\Delta(\delta^{\sharp})$.

Through a normalization —*or* loop-shifting— *step, thoroughly described in [13, 1],* (14) *can be turned to the simplified form —in which the bounds* $\overline{\Phi}_i$ *and* $\underline{\Phi}_i$ *implicitly appear in the definition of the matrices* $\tilde{A}$, $\tilde{B}_p$, $\tilde{C}_q$, $\tilde{D}_{qp}$—

$$\begin{pmatrix} \dot{\tilde{x}} \\ \tilde{q} \end{pmatrix} = \begin{pmatrix} \tilde{A} & \tilde{B}_p \\ \tilde{C}_q & \tilde{D}_{qp} \end{pmatrix} \begin{pmatrix} \tilde{x} \\ \tilde{p} \end{pmatrix}, \ \tilde{p} = \Delta\,\tilde{q} \tag{15}$$

$$\text{with } \Delta \stackrel{\Delta}{=} \Delta(\delta) = \mathrm{diag}\left(\delta_1 I_{r_1}, \ldots, \delta_{\mathsf{N}} I_{r_{\mathsf{N}}}\right),\ r = (r_1 \ldots r_{\mathsf{N}})' \in \mathbb{N}^{\mathsf{N}},\ \text{and } \forall i = 1, \ldots, \mathsf{N},\ \delta_i \in [-1; +1].$$

Notice that Δ *with no argument henceforth represents a time-varying uncertain matrix gain of* $\blacktriangle(r)$ *with no memory, instead of a matrix function. The representations* (14) *and* (15) *are respectively termed an unnormalized and normalized* Structured Norm-Bounded Linear Differential Inclusion (SNLDI).

3.4 Comments

Rational systems look fairly well suited to visual servoing. On the one hand, the controllers (6) encompass many usual 2D or 3D strategies. For instance, the inverse Jacobian 3D schemes mentioned by Martinet in [32], whose equations are $u = -\lambda \mathbf{B}^{+}(0)\,x$ and $u = -\lambda \mathbf{B}^{+}(x)\,x$, respectively correspond to a linear static state feedback $u = K\,x$ and to a nonlinear rational static state feedback $u = K(\Phi_{cx}(x))\,x$. Similarly, the inverse Jacobian 2D controllers $u = -\lambda\,[J(s^*,z^*)]^{+}\,(s-s^*)$ and $u = -\lambda\,[J(s,z)]^{+}\,(s-s^*)$, proposed in Espiau *et al.* [19] and thoroughly studied in [6], can also be dealt with. Indeed, the so-called image Jacobian $J(.,.)$ —defined from $\dot{s} = J(s,z)u$— is a rational function of s and of the vector z made up with the depths $z_i = \overrightarrow{ST_i}.\overrightarrow{z_S}$, so that these 2D servos respectively correspond to a linear static output feedback $u = K\,(s-s^*)$ and a static gain-scheduled output feedback $u = K(\Phi_{cx}(x))\,(s-s^*)$. The proposed method can also handle dynamic output feedbacks by associating constant matrices to $\mathbf{K_c}(.)$, $\mathbf{K_{cy}}(.)$, $\mathbf{K_u}(.)$, $\mathbf{K}(.)$. The general case (6) corresponds to a dynamic gain-scheduled output feedback [**].

On the other hand, the aforementioned additional variables $\zeta_j = \zeta_j(\tilde{x}),\ j = 1,\ldots,n_\zeta$, are rational. For controllers like (6), they can be written, with $Z_{\zeta_j}(.)$ a rational function well-defined at 0,

$$\zeta_j = Z_{\zeta_j}(\Phi_{\zeta_j}(x))\tilde{x},\ \Phi_{\zeta_j}(x) \in \mathbb{R}^{\mathsf{N}_{\zeta_j}}. \tag{16}$$

As outlined in the introduction to this section, the multicriteria analysis or synthesis is performed on the whole set of the trajectories of the SNLDI (15) embedding the original nonlinear closed-loop system (7). Care must be taken to limit as much as possible the conservatism of this strategy. First, the choice of the bounds $\overline{\Phi}_i$ and $\underline{\Phi}_i$ come from a compromize: the parallelotope Ξ must be wide enough to handle relevant trajectories of the closed-loop system (7), while sufficiently restricted to limit the number of spurious trajectories. Next, as the entries of the uncertain vector $\delta^\sharp$ in (13) are implicitly assumed independent with each other, no instantaneous relationship should exist between the components of Φ before the global linearization process. Lastly, other sources of conservatism will appear in the next section, coming from the underlying robust control methods. One of these lies in the use of an outer approximation of the SNLDI (15), rather than (15) itself, which is all the more conservative as the size of the uncertain matrix Δ is high. So, minimal LFTs must be determined when possible.

Some important points on the well-posedness issue in Hypothesis 3.4 are also of concern. The well-posedness of the LFT of a rational system on a set $\mathscr{X}$ requires that the rational matrix functions involved in this system be well-defined on $\mathscr{X}$. In addition, the references [13, 1] show that the well-posedness of the unnormalized SNLDI (14) on Ξ is equivalent to assuming that (14) is well-posed at the center of Ξ and the normalized form (15) is well-posed on $[-1;+1]^{\mathsf{N}}$. Yet, the well-posedness of (14) at the center of Ξ is

[**] Notice however that $2\frac{1}{2}$D controllers as these of Malis *et al.* [30] may not straightly fit in this framework.

a necessary condition for the computation of the matrices $\tilde{A}$, $\tilde{B}_p$, $\tilde{C}_q$, $\tilde{D}_{qp}$ involved in (15). So, once these matrices are given, to ensure the well-posedness of the unnormalized SNLDI (14) on Ξ, it just remains to verify that $\det(I-\tilde{D}_{qp}\Delta)$ is nonzero for all Δ in $\blacktriangle(r)$ —viz. that the normalized SNLDI (15) is well-posed on $[-1;+1]^{\mathsf{N}}$. This is why, unless explicitely mentioned, only normalized SNLDIs will be considered.

At last, it may be noticed that even though the function $\tilde{\mathbf{A}}(\Phi(\xi))$ in the closed-loop equation (7) is well-defined on a set $\mathscr{X}$ when $\det(I-\tilde{D}^{\sharp}_{qp}\Delta(\Phi(\xi)))$ is nonzero on $\mathscr{X}$, it is not necessarily the case for all the matrix functions appearing in (5)–(6), e.g. because of internal simplifications. In the same vein as a remark in § 2.3, a way to avoid this potential problem is to ensure the boundedness of u and $s-s^*$ by introducing them as additional variables.

This paper henceforth assumes that $\Phi_x(x)$ is equal to x and $\Phi_{cx}(x)$ is made with a subset of the entries of x, so that $\Phi(x)=x$ which is the most immediate choice whatever the considered visual servo. Quite often, $\Phi_{\zeta_j}(x)=x$ can be assumed as well. Then, necessary conditions for the well-posedness of some LFTs can be established from the following notes.

In the 6DOF case, the matrix function $\mathbf{B}(x)$ involved in the open-loop equation (5) can be shown to be well-defined as soon as $M=\tan(\frac{\mu}{2})$ belongs to the open interval $]-1;+1[$, which is always true. In addition, if a 2D servo is considered, y is set to the difference $s-s^*$, and the matrix $\mathbf{C}(x)$ comes to be not well-defined as soon as x is such that at least one target spot, say T_i, admits a null depth along the $\overrightarrow{z_S}$ axis of frame F_S, i.e. when the value of x implies that $\exists i\in\{1,\ldots,\mathsf{M}\} : z_i=\overrightarrow{ST_i}.\overrightarrow{z_S}=0$. Such a sensor-target situation does not occur in a problem formulation taking into account image constraints, since it implies that some target points would belong to a plane including the camera optical center S and orthogonal to the optical axis. In fact, the z_i's are all strictly positive.

The same obviously holds on the matrix function $Z_{\zeta_j}(x)$ in equation (16) when the additional variable ζ_j is defined as the difference $X_j-X_j^*$ or $Y_j-Y_j^*$ in order to handle image constraints. The reference [1] shows that $Z_{\zeta_j}(x)$ in (16) is well-defined whatever the value of x when ζ_j terms the 3D distance $d_{3\mathrm{D}_j}$ from the center S of frame F_S to a wall. These conclusions are useful if $Z_{\zeta_j}(x)$ is also written as an LFT, see § 4.2.4-A.

The reader is referred to [1] for a discussion on cases in which λ, μ and ν lie in wider intervals and/or uncertainties affect (7). Controllers showing a rational dependence on $\Phi_{cx}(\tilde{x})$ instead of $\Phi_{cx}(x)$, which lead to $\Phi(\tilde{x})$ (resp. $\Phi_{\zeta_j}(\tilde{x})$) as argument of (7) (resp. of (16)), are also briefly outlined therein. In this paper, results concerning additional variables will be presented under the assumption $\Phi_{\zeta_j}(\tilde{x})=\tilde{x}$ instead of $\Phi_{\zeta_j}(x)=x$, which leads to a simplified formulation.

4 First step to the satisfaction of the criteria

In this section, conditions are given guaranteeing some specifications of the standard visual servocontrol problem stated in § 2.3. As $\Phi(x)$ has been set to x, Ξ_f and Ξ are equal. The bounds $\overline{\Phi_i}$ and $\underline{\Phi_i}$ correspond to the i^{th} entry x_i of x and will thus be respectively denoted $\overline{x}_i$ and $\underline{x}_i$.

4.1 Basics

4.1.1 Convergence of the camera to the reference situation

As aforementioned, the asymptotic stability of the equilibrium state 0 of the closed-loop system (7) is a sufficient condition for the correct positioning of the camera at the reference final situation.

By § 3.3, as soon as Hypothesis 3.4 on boundedness and well-posedness is satisfied, the set of the state trajectories of the SNLDI (15) contains all the trajectories of the genuine closed-loop system that belong to $\tilde{\Xi}_f \stackrel{\Delta}{=} \Xi_f \times \mathbb{R}^m = \{\xi \in \mathbb{R}^{(n+m)} : (\xi_1, \ldots, \xi_n)' \in \Xi_f\}$. So, if (15) is well-posed for all the admissible values of Δ, ensuring the asymptotic stability of this SNLDI is sufficient for the convergence to 0 of all the trajectories of (7) that wholly lie in $\tilde{\Xi}_f$[††]. Yet, it is important to notice that though the asymptotic stability of the SNLDI (15) is global, nothing can be said about the convergence of these responses of the nonlinear closed-loop system (7) that do not completely remain in $\tilde{\Xi}_f$. For instance, if the responses of (7) can just be surrounded by a set $\tilde{\overline{\Xi}}_f \stackrel{\Delta}{=} \overline{\Xi}_f \times \mathbb{R}^m$ such that $\Xi_f \subset \overline{\Xi}_f$, the asymptotic stability of the "broader" inclusion $\dot{\tilde{x}} = \tilde{\mathbf{A}}(\delta^\sharp)\tilde{x}$, with $\delta^\sharp \in \overline{\Xi}_f$, should be studied instead.

The global asymptotic stability of the SNLDI (15) is proved by finding a matrix $P > 0$ such that the quadratic Lyapunov function $V(\xi) = \xi' P \xi$ decreases along all the state trajectories of this inclusion, i.e. such that $\frac{dV(\tilde{x}(t))}{dt} < 0$ for all the admissible realizations of Δ. As an immediate consequence, each of the nested ellipsoids centered at the origin 0 and corresponding to a constant value of the Lyapunov function V is an invariant set, in that it encloses all the inclusion's trajectories beginning in it. The focus will be often put on $\mathscr{E}_P \stackrel{\Delta}{=} \{\xi \in \mathbb{R}^{(n+m)} : \xi' P \xi \leq 1\}$. Further, the closed-loop decay rate[‡‡] —or largest Lyapunov exponent— is at least α when the inequality $\frac{dV(\tilde{x}(t))}{dt} < -2\alpha V(\tilde{x}(t))$ is satisfied. Then, the relationship $\tilde{x}(t_0) \in \mathscr{E}_P$ implies that for all subsequent time t, $\tilde{x}(t)$ lies in the Shunken ellipsoid $e^{-\alpha(t-t_0)}\mathscr{E}_P \subset \mathscr{E}_P$.

From the above arguments, the ellipsoid $\mathscr{E}_P$ can be made an inner approximation to the attraction basin of the equilibrium 0 of the closed-loop system (7) by ensuring the well-posedness of the embedding SNLDI (15) for all the admissible values of Δ, and by putting additional constraints on P so that the set relationship $\mathscr{E}_P \subset \tilde{\Xi}_f$ holds. As $0_{(n+m;1)}$ belongs to $\mathscr{E}_P$, the constraint $\mathscr{E}_P \subset \tilde{\Xi}_f$ requires that $0_{(n;1)} \in \Xi_f$. Moreover, $\mathscr{E}_P$ is symmetric w.r.t. the origin, so that the relationship $\mathscr{E}_P \subset \tilde{\Xi}_f$ is equivalent to $\mathscr{E}_P \subset \square_f \subset \tilde{\Xi}_f$

[††] No boundedness assumption is made on x_c as no output feedback is considered showing a rational dependence on x_c.

[‡‡] The decay rate is the largest $\beta > 0$ such that $\lim_{t \to +\infty} e^{\beta t} ||\tilde{x}(t)|| = 0$.

with $\square_f \triangleq \{\xi \in \mathbb{R}^{(n+m)} : {\xi_i}^2 \leq \underline{x}_i^2 \text{ and } {\xi_i}^2 \leq \overline{x}_i^2,\ i=1,\ldots,n\}$ the widest symmetric parallelotope enclosed by $\tilde{\Xi}_f$. So, in the case of an asymmetric Ξ_f, to take into account some values of $\tilde{x}$ in $\tilde{\Xi}_f \backslash \square_f$, the global linearization step must be performed by replacing Ξ_f by its smallest symmetric outer parallelotope. This modification of course induces some conservatism, in that the obtained SNLDI concerns a broader set of uncertain parameters.

4.1.2 *A priori* knowledge about the initial sensor-target relative situation

Many visual servoing problems involve some knowledge of the initial sensor-target relative situation. For instance, in an analysis context, one may want to check if a given control can steer the camera from a relative situation x_0 to the reference pose, without willing to compute a fine approximation of the whole convergence basin. Similarly, when synthesizing a visual-based control law, this initial situation, though unknown, may be supposed to belong to a predefined set $\mathscr{E}_0$.

Such cases can be dealt with by making $\mathscr{E}_P$ enclose the closed-loop initial state vector $\tilde{x}_0 = (x_0', 0'_{(m;1)})' \in \mathbb{R}^{(n+m)}$ or the set $\tilde{\mathscr{E}}_0 = \{\xi = (\xi_0', 0'_{(m;1)})' \in \mathbb{R}^{(n+m)} : \xi_0 \in \mathscr{E}_0\}$, respectively.

4.1.3 Additional constraints

The actuators saturations are taken into account by keeping into predefined admissible symmetric limits the norm of some subvectors extracted from u, e.g. by requiring that $|u_j| = |W_j' u| \leq \overline{u}_j$ for each $j=1,\ldots,n_u$, where $W_j \triangleq \mathrm{col}_j(I_{n_u})$. Besides, the target is kept visible from the camera if and only if $X_j - X_j^* \in [\underline{X} - X_j^*; \overline{X} - X_j^*]$ and $Y_j - Y_j^* \in [\underline{Y} - Y_j^*; \overline{Y} - Y_j^*]$, $j=1,\ldots,\mathsf{M}$, with $\underline{X}$, $\overline{X}$, $\underline{Y}$ and $\overline{Y}$ the physical dimensions of the camera image plane. Similarly, the camera is kept in a corridor without hitting its walls if and only if a 3D distance d_{3D_j} is kept in the security interval $[\underline{d_{\mathrm{WALL}\,j}}; \overline{d_{\mathrm{WALL}\,j}}]$.

The expressions of ζ_j corresponding to all these specifications noticeably fall into two different classes.

A Case $\zeta_j = Z_{\zeta_j}\tilde{x} \in [-\overline{\zeta}_j; \overline{\zeta}_j]$ Such a constraint corresponds to the avoidance of the actuators saturations when a static state feedback $u = Kx$ is used, e.g. with $Z_{\zeta_j} = W_j' K$. It is satisfied if and only if $\tilde{x} \in \mathscr{A}_{\zeta_j}$, where $\mathscr{A}_{\zeta_j} \triangleq \{\xi \in \mathbb{R}^{n+m} : \xi' Z_{\zeta_j}' Z_{\zeta_j} \xi \leq \overline{\zeta}_j^2\}$. As in § 4.1.1 and § 4.1.2, $\tilde{x} \in \mathscr{A}_{\zeta_j}$ can be guaranteed by adding constraints on P so that $\mathscr{E}_P \subset \mathscr{A}_{\zeta_j}$. Notice that the set $\mathscr{A}_{\zeta_j}$ is convex and symmetric w.r.t. the origin.

B Case $\zeta_j = Z_{\zeta_j}(\tilde{x})\tilde{x} \in [\underline{\zeta}_j; \overline{\zeta}_j]$ Avoidance of actuators saturations when the controller is not a static state feedback, 2D constraints and 3D constraints involve an additional variable ζ_j in the form $\zeta_j = Z_{\zeta_j}(\tilde{x})\tilde{x}$. The set membership $\zeta_j \in [\underline{\zeta}_j; \overline{\zeta}_j]$ is then equivalent to $\tilde{x} \in \mathscr{A}_{\zeta_j}$, where $\mathscr{A}_{\zeta_j} \triangleq \{\xi \in \mathbb{R}^{n+m} : \left(Z_{\zeta_j}(\xi)\,\xi - \hat{\zeta}_j\right)^2 \leq \tilde{\zeta}_j^2\}$, with $\hat{\zeta}_j = \frac{\overline{\zeta}_j + \underline{\zeta}_j}{2}$ and $\tilde{\zeta}_j = \frac{\overline{\zeta}_j - \underline{\zeta}_j}{2}$. As was done before, $\tilde{x} \in \mathscr{A}_{\zeta_j}$

can be ensured by "sizing" P so that $\mathscr{E}_P$ lies into $\mathscr{A}_{\zeta_j}$. When the camera is at the reference pose, all the specifications are satisfied. In other words, $0 \in \mathscr{A}_{\zeta_j}$, which implies $\hat{\zeta}_j^2 \leq \tilde{\zeta}_j^2$.

It can be observed —e.g. for 2D and 3D specifications— that the set $\mathscr{A}_{\zeta_j}$ is generally asymmetric w.r.t. the origin. Because of the symmetry of the invariant ellipsoid $\mathscr{E}_P$, expecting $\mathscr{E}_P \subset \mathscr{A}_{\zeta_j}$ prevents the initial states $\check{x}_0 \in \mathscr{A}_{\zeta_j}$ such that $-\check{x}_0 \notin \mathscr{A}_{\zeta_j}$ from being handled. In addition, contrarily to the case $\zeta_j = Z_{\zeta_j}\tilde{x} \in [-\overline{\zeta}_j; \overline{\zeta}_j]$, $\mathscr{A}_{\zeta_j}$ is not necessarily convex. As $\mathscr{E}_P$ is convex, the initial states $\check{x}_0 \in \mathscr{A}_{\zeta_j}$ such that the line segment between $\check{x}_0$ and $-\check{x}_0$ does not wholly lie into $\mathscr{A}_{\zeta_j}$ cannot be considered either.

At last, let's remark that the functions $Z_{\zeta_j}(.)$ corresponding to 2D or 3D constraints are part of the problem data. The same holds for Z_{ζ_j} and/or $Z_{\zeta_j}(.)$ concerning actuators saturations in an analysis context. Nevertheless, when the aim is to avoid the actuators saturations in a synthesis context, the controller is an unknown of the problem, and so are Z_{ζ_j} and/or $Z_{\zeta_j}(.)$. Dealing with actuators saturations in a synthesis problem is thus the object of a special treatment.

4.1.4 Handling the constraints through Matrix Inequalities

All the specifications considered so far can be expressed as the negativeness of a quadratic function of x, p, q whenever other quadratic forms of these variables are negative. Sufficient conditions —which are sometimes nonconservative— can thus be obtained through the $\mathscr{S}$-procedure [5], leading to LMIs on P or $Q = P^{-1}$ and other variables.

Conditions on the SNLDI (15) must take into account the relationship $p = \Delta q$. In order to handle it through the $\mathscr{S}$-procedure, the following lemma, coming from [18, 13, 15], is used.

Lemma 4.1 *Let the sets $\mathscr{B}(r)$, $\mathscr{S}(r)$, $\mathscr{G}(r)$ be defined following § 0. Whatever the couple (S,G) in $\mathscr{S}(r) \times \mathscr{G}(r)$, the set $\mathscr{V}(r) \stackrel{\Delta}{=} \{(p,q) : \exists \Delta \in \blacktriangle(r),\ p = \Delta q\}$ in included into the set $\mathscr{W}(S,G) \stackrel{\Delta}{=} \left\{(p,q) : \binom{q}{p}' \begin{pmatrix} S & G \\ G' & -S \end{pmatrix} \binom{q}{p} \geq 0\right\}$.*

The conservatism of the quadratic outer approximation $\mathscr{W}(S,G)$ coming from this lemma is somewhat limited, in that the mathematical properties of the matrix Δ are taken into account, viz. its block-diagonal structure, the fact that $\delta_i \in \mathbb{R}$ and $|\delta_i| \leq 1$, $i = 1, \ldots, \mathsf{N}$. However, this outer approximation is all the more pessimistic as $n_p(r)$ grows, see for example the discussion in [1]. So, to limit the conservatism of the overall approach proposed in this paper, the SNLDI (15) should be obtained from a minimal LFT.

As $\mathscr{V}(r)$ is a subset of $\mathscr{W}(S,G)$ whatever the admissible matrices S and G, these matrices will henceforth be considered as decision variables, whose values are looked for so as to enable the most helpful handling of the various criteria.

4.1.5 From feasibility to optimization problems

The multicriteria analysis or synthesis has been turned into a feasibility problem concerning the matrix P or $Q = P^{-1}$ and other quantities. Several solutions generally exist, but all are not relevant to the visual servocontrol problem in hand. So, the search should be guided by a criterion to be minimized. Some hints are hereafter given, from which the definition of an optimization problem is left to the reader.

In order to get a good characterization of the multicriteria basin of convergence of the camera, or to make one controller ensure the positioning from many initial sensor-target situations, it is worth determining the maximum "size" invariant ellipsoid $\mathscr{E}_P$. As mentioned in [5], the volume of $\mathscr{E}_P$ is a decreasing function of $\log(\det(P))$. Likewise, the sum of squares of $\mathscr{E}_P$'s principal axes lengths is a decreasing function of $\mathrm{trace}\,(P)$[†]. The maximization of this last criterion through the minimization of $\mathrm{trace}\,(P)$ is a convex problem when the constraints involve LMIs on P. If LMIs on $Q = P^{-1}$ are used, the volume of $\mathscr{E}_P$ can be maximized by minimizing $\log(\det(Q^{-1}))$, which is also a convex problem.

The introduction of the closed-loop decay rate α into the study can show several practical advantages. On the one hand, the feasibility of the forthcoming matrix inequalities can be checked for a fixed value of α, e.g. to determine which initial camera situations can be steered to the reference pose within a given settling time while satisfying the various criteria. On the other hand, α can be introduced as a decision variable. The minimization of $(-\alpha)$ subject to the inequality $\alpha > 0$ together with the different constraints thus leads to the maximum closed-loop decay rate that can be ensured by this approach. If the matrix inequalities are linear when α is fixed, this optimization problem is a Generalized Eigenvalue Problem (GEVP), which is quasiconvex and can still be efficiently solved.

Unless explicitely mentioned —e.g. in § 4.2.4 and § 4.3.4, which is an original contribution [2] though using fairly classical arguments—, the forthcoming matrix inequalities have been established in the work of El Ghaoui *et al.* [18, 17, 14, 13] or can be straightly infered. Such standard results are thus given without proof, but these are gathered in [1]. Dynamic state feedbacks are not considered, as analyzing or synthesizing such controllers for the considered SNLDIs through quadratic Lyapunov functions leads to no enhancement compared to static state feedbacks. The synthesis of output feedbacks, though essential in practice, is not dealt with for space reasons and because —except for some full-rank gain-scheduled controllers— it leads to nonconvex problems, see [1] for details on their application.

[†]More precisely, the sum of squares of $\mathscr{E}_P$'s principal axes lengths is equal to $4\,\mathrm{trace}\,(P^{-1})$, which is indeed a decreasing function of $\mathrm{trace}\,(P)$.

4.2 Resulting conditions for multicriteria analysis

Recall that the closed-loop nonlinear system is embedded into the normalized SNLDI (15). In an analysis context, which is the topic of this section, the matrices $\tilde{A}$, $\tilde{B}_p$, $\tilde{C}_q$ and $\tilde{D}_{qp}$ defining this SNLDI are known. When possible, these matrices are determined so as to get a minimal LFT.

4.2.1 Convergence of the camera to the reference situation

A Global asymptotic stability of the SNLDI (15) Assume that a value of $\alpha \geq 0$ is presumably given. The quadratic stability of the SNLDI (15) as well as the decay rate α are ensured if the following LMI on P, S and G is feasible:

$$\exists\, P>0,\ S\in\mathscr{S}(r),\ G\in\mathscr{G}(r),\ \begin{pmatrix} \tilde{A}'P+P\tilde{A}+\tilde{C}_q'S\tilde{C}_q+2\alpha P & P\tilde{B}_p+\tilde{C}_q'S\tilde{D}_{qp}+\tilde{C}_q'G \\ \star & \tilde{D}_{qp}'S\tilde{D}_{qp}-S+\tilde{D}_{qp}'G+G'\tilde{D}_{qp} \end{pmatrix}<0. \qquad (17)$$

B Satisfaction of the Hypothesis 3.4 The references [18, 20] give the following sufficient condition for the well-posedness of the normalized SNLDI (15):

$$\exists\, S\in\mathscr{S}(r),\ G\in\mathscr{G}(r),\ \text{such that } \tilde{D}_{qp}'S\tilde{D}_{qp}-S+\tilde{D}_{qp}'G+G'\tilde{D}_{qp}<0. \qquad (18)$$

Yet, the matrix inequality (18) is satisfied as soon as (17) holds, so that (17) does ensure the well-posedness of the SNLDI used to embed the genuine nonlinear closed-loop system.

For $i=1,\ldots,n$, let $W_i \stackrel{\Delta}{=} \mathrm{col}_i(I_{(n+m)})$ and $\rho_i \stackrel{\Delta}{=} \min(|\underline{x}_i|;|\overline{x}_i|)$. The constraint $\mathscr{E}_P \subset \tilde{\Xi}_f \stackrel{\Delta}{=} \Xi_f \times \mathbb{R}^m$, which ensures the boundedness assumption during the building of the SNLDI, is satisfied if and only if the following $2n$ LMIs on P and τ_i, $i=1,\ldots,n$, are feasible:[‡]

$$\exists\, \tau_1\in\mathbb{R}^{+*},\ldots,\tau_n\in\mathbb{R}^{+*},\ \forall i=1,\ldots,n,\ -\tau_i\rho_i^2+1\leq 0 \text{ and } \tau_i W_i W_i'-P\leq 0. \qquad (19)$$

The problems (19) and (17) are simultaneously solved.

4.2.2 *A priori* knowledge about the initial sensor-target relative situation

Assume that the initial sensor-target situation x_0 is perfectly known. The initial closed-loop state vector $\tilde{x}_0 = (x_0', 0'_{(m;1)})' \in \mathbb{R}^{(n+m)}$ belongs to the ellipsoid $\mathscr{E}_P$ if and only if the following trivial LMI on P is satisfied:

$$\tilde{x}_0' P \tilde{x}_0 - 1 \leq 0. \qquad (20)$$

[‡]The LMIs (19), (22), (28), (30) concern boundedness constraints of the form $||C\tilde{x}|^{\rho}| \leq \frac{1}{\upsilon},\ \forall \tilde{x} : \tilde{x}'P\tilde{x}\leq 1$, with $\upsilon>0$. They are obtained by a straight application of the $\mathscr{S}$-procedure, but can be shown to be equivalent to the simpler LMIs developed in [18, 13], see § B.1.

In order to analyze the convergence from every initial sensor-target relative situation in the ellipsoid $\mathscr{E}_0 \triangleq \{\xi \in \mathbb{R}^n : \xi = x_0 + Ez,\ z'z \leq 1\}$ centered on x_0, it is sufficient to make $\mathscr{E}_P$ enclose $\tilde{\mathscr{E}}_0 \triangleq \{\xi = (\xi_0', 0'_{(m;1)})' \in \mathbb{R}^{(n+m)} : \xi_0 \in \mathscr{E}_0\} = \{\xi \in \mathbb{R}^{(n+m)} : \xi = \tilde{x}_0 + \tilde{E}z,\ z'z \leq 1\}$, with $\tilde{E} \triangleq \begin{pmatrix} E & 0_{(n;m)} \\ 0_{(m;n)} & 0_{(m;m)} \end{pmatrix}$. A necessary and sufficient condition is the feasibility of the LMI on τ_0 and P,

$$\exists\ \tau_0 \in \mathbb{R}^+,\ \begin{pmatrix} \tilde{E}'P\tilde{E} - \tau_0 I_{n+m} & \tilde{E}'P\tilde{x}_0 \\ \star & \tilde{x}_0'P\tilde{x}_0 - 1 + \tau_0 \end{pmatrix} \leq 0. \tag{21}$$

Note that the above equations return to enclose x_0 or $\mathscr{E}_0$ by the ellipsoid $\mathscr{E}_{P_x}$ which is the intersection of $\mathscr{E}_P$ with the x-space. Of course, a common solution is looked for the problems (20)/(21), (19) and (17).

4.2.3 Constraints of the type $\zeta_j = Z_{\zeta_j}\tilde{x} \in [-\overline{\zeta}_j; \overline{\zeta}_j]$

The condition $\mathscr{E}_P \subset \mathscr{A}_{\zeta_j}$, with $\mathscr{A}_{\zeta_j} \triangleq \{\xi \in \mathbb{R}^{n+m} : \xi' Z'_{\zeta_j} Z_{\zeta_j} \xi \leq \overline{\zeta}_j^2\}$, is satisfied if and only if the following LMI on P and τ_{ζ_j}, to be added to the problem $\{(19), (17)\}$, is feasible:

$$\exists\ \tau_{\zeta_j} \in \mathbb{R}^{+*},\ -\tau_{\zeta_j}\overline{\zeta}_j^2 + 1 \leq 0 \text{ and } \tau_{\zeta_j} Z'_{\zeta_j} Z_{\zeta_j} - P \leq 0. \tag{22}$$

4.2.4 Constraints of the type $\zeta_j = Z_{\zeta_j}(\tilde{x})\tilde{x} \in [\underline{\zeta}_j; \overline{\zeta}_j]$

As mentioned in § 4.1.3-B, the aim is to guarantee the set inclusion $\mathscr{E}_P \subset \mathscr{A}_{\zeta_j}$, with $\mathscr{A}_{\zeta_j} \triangleq \{\xi \in \mathbb{R}^{n+m} : (Z_{\zeta_j}(\xi)\xi - \hat{\zeta}_j)^2 \leq \tilde{\zeta}_j^2\}$. Two different methods are hereafter given to solve this problem. Though, to our knowledge, these are original —for this problem seems not to have been considered in the literature— they rely on fairly classical arguments. Their proof is given in Appendix B.2.

Both methods rely on the definition of a set $\mathscr{B}_{\zeta_j}$ such that $\mathscr{B}_{\zeta_j} \subset \mathscr{A}_{\zeta_j}$, and ensure the relationship $\mathscr{E}_P \subset \mathscr{B}_{\zeta_j}$. In the first one, $\mathscr{B}_{\zeta_j}$ is determined through the global linearization of $\zeta_j = Z_{\zeta_j}(\tilde{x})\tilde{x}$, while the second approach defines $\mathscr{B}_{\zeta_j}$ as the intersection of some quadratic functions determined *ad hoc*.

A Global linearization of $\zeta_j = Z_{\zeta_j}(\tilde{x})\tilde{x}$ The paragraphs § 3.2–§ 3.3 led to the global linearization of the rational closed-loop system (7). As $Z_{\zeta_j}(.)$ is a rational function well-defined at 0, a similar process can be performed on the expression $\zeta_j = Z_{\zeta_j}(\tilde{x})\tilde{x}$ assuming that $x \in \Xi_f$, i.e. $\tilde{x} = (x', x_c')' \in \tilde{\Xi}_f$, and under a well-posedness assumption. After normalization, one gets an embedding static inclusion $\zeta_j(\tilde{x}, \Delta_\zeta)$ in the form of the following LFT:

$$\begin{pmatrix} \zeta_j(\tilde{x}, \Delta_\zeta) \\ q_\zeta \end{pmatrix} = \begin{pmatrix} \tilde{C}_\zeta & \tilde{D}_{p_\zeta} \\ \tilde{C}_{q_\zeta} & \tilde{D}_{qp_\zeta} \end{pmatrix} \begin{pmatrix} \tilde{x} \\ p_\zeta \end{pmatrix},\ p_\zeta = \Delta_\zeta q_\zeta,\ \text{with } \Delta_\zeta \in \blacktriangle(r_\zeta),\ r_\zeta = (r_{\zeta_1}, \ldots, r_{\zeta_{N_\zeta}})'. \tag{23}$$

Here also, according to a remark in § 3.4, if the matrices $\tilde{C}_\zeta$, $\tilde{D}_{p_\zeta}$, $\tilde{C}_{q_\zeta}$, $\tilde{D}_{qp_\zeta}$ can be computed, it remains to verify that for all Δ_ζ in $\blacktriangle(r_\zeta)$, the determinant $\det(I-\tilde{D}_{qp_\zeta}\Delta_\zeta)$ is nonzero to ensure the well-posedness of (23). Then, whatever the vector $\tilde{x}$ in $\tilde{\Xi}_f$, there exists a realization of the uncertain matrix Δ_ζ in $\blacktriangle(r_\zeta)$ such that the equality $Z_{\zeta_j}(\tilde{x})\tilde{x}=\zeta_j(\tilde{x},\Delta_\zeta)$ holds.

Let $\mathscr{C}_{\zeta_j}\triangleq\{\xi\in\mathbb{R}^{(n+m)}$: the inequality $(\zeta_j(\xi,\Delta_\zeta)-\hat{\zeta}_j)^2\le\tilde{\zeta}_j^2$ holds *for all* $\Delta_\zeta\in\blacktriangle(r_\zeta)\}$. Returning briefly to the unnormalized form of (23) readily shows that, under the well-posedness assumption, the set $\mathscr{B}_{\zeta_j}\triangleq\mathscr{C}_{\zeta_j}\cap\tilde{\Xi}_f=\{\xi\in\tilde{\Xi}_f:\forall\tilde{\delta}^\sharp\in\tilde{\Xi}_f,\,(Z_{\zeta_j}(\tilde{\delta}^\sharp)\xi-\hat{\zeta}_j)^2\le\tilde{\zeta}_j^2\}$ is included into the set $\mathscr{A}_{\zeta_j}\cap\tilde{\Xi}_f=\{\xi\in\tilde{\Xi}_f:(Z_{\zeta_j}(\xi)\xi-\hat{\zeta}_j)^2\le\tilde{\zeta}_j^2\}$. So, the constraint $\mathscr{E}_P\subset\mathscr{B}_{\zeta_j}\triangleq(\mathscr{C}_{\zeta_j}\cap\tilde{\Xi}_f)$ is a sufficient condition for $\mathscr{E}_P\subset\mathscr{A}_{\zeta_j}$. The set inclusion $\mathscr{E}_P\subset\tilde{\Xi}_f$ is ensured by the LMIs (19). Thus, to make $\mathscr{E}_P\subset\mathscr{A}_{\zeta_j}$ hold, it is sufficient to add some constraints guaranteeing the relationship $\mathscr{E}_P\subset\mathscr{C}_{\zeta_j}$ and the well-posedness of (23).

Theorem 4.2 *The feasibility of the following LMI on P,* τ_ζ, S_ζ *and* G_ζ *is a sufficient condition for the well-posedness of* (23) *and the set relationship* $\mathscr{E}_P\subset\mathscr{C}_{\zeta_j}$ *—which, if* $\mathscr{E}_P\subset\tilde{\Xi}_f$ *holds, then ensures that* $\mathscr{E}_P\subset\mathscr{B}_{\zeta_j}\triangleq(\mathscr{C}_{\zeta_j}\cap\tilde{\Xi}_f)\subset\mathscr{A}_{\zeta_j}$*—:*

$$\exists\,\tau_\zeta\in\mathbb{R}^{+*},\,S_\zeta\in\mathscr{S}(r_\zeta),\,G_\zeta\in\mathscr{G}(r_\zeta),\,\tau_\zeta M_1+M_2-M_0<0, \tag{24}$$

$$\textit{with}\quad M_0=\begin{pmatrix}P&0&0\\ \star&0&0\\ \star&\star&-1\end{pmatrix},\ M_1=\begin{pmatrix}\tilde{C}_\zeta'\tilde{C}_\zeta&\tilde{C}_\zeta'\tilde{D}_{p_\zeta}&-\tilde{C}_\zeta'\hat{\zeta}_j\\ \star&\tilde{D}_{p_\zeta}'\tilde{D}_{p_\zeta}&-\tilde{D}_{p_\zeta}'\hat{\zeta}_j\\ \star&\star&\hat{\zeta}_j^2-\tilde{\zeta}_j^2\end{pmatrix},$$

$$M_2=\begin{pmatrix}\tilde{C}_{q_\zeta}'S_\zeta\tilde{C}_{q_\zeta}&\tilde{C}_{q_\zeta}'S_\zeta\tilde{D}_{qp_\zeta}+\tilde{C}_{q_\zeta}'G_\zeta&0\\ \star&\tilde{D}_{qp_\zeta}'S_\zeta\tilde{D}_{qp_\zeta}-S_\zeta+\tilde{D}_{qp_\zeta}'G_\zeta+G_\zeta'\tilde{D}_{qp_\zeta}&0\\ \star&\star&0\end{pmatrix}.$$

The problems (24), (19), (17) *are jointly solved.*

Note that a set of decision variables $\{\tau_{\zeta_j},S_{\zeta_j},G_{\zeta_j}\}$ and of vector/matrices $\{r_{\zeta_j},\tilde{C}_{\zeta_j},\tilde{D}_{p_{\zeta_j}},\tilde{C}_{q_{\zeta_j}},\tilde{D}_{qp_{\zeta_j}}\}$ must be defined for each additional variable ζ_j. The index j has not been made explicit in order to simplify the notations.

B Inner approximation of $\mathscr{A}_{\zeta_j}$ by the intersection of quadratic functions Assume that a set of $l_{\zeta_j}\ge1$ scalar numbers $\beta_{\zeta_j}^k<0$ and matrices $\tilde{F}_{\zeta_j}^k\in\mathbb{R}^{1\times(n+m)}$, $\tilde{V}_{\zeta_j}^k=\tilde{V}_{\zeta_j}^{k\,\prime}\in\mathbb{R}^{(n+m)\times(n+m)}$, $k=1,\ldots,l_{\zeta_j}$, has been predetermined in an *ad hoc* way so that $\mathscr{B}_{\zeta_j}\triangleq\bigcap_{k=1}^{l_{\zeta_j}}\mathscr{B}_{\zeta_j}^k\subset\mathscr{A}_{\zeta_j}$ where $\mathscr{B}_{\zeta_j}^k\triangleq\{\xi\in\mathbb{R}^{(n+m)}:\begin{pmatrix}\xi\\1\end{pmatrix}'\tilde{N}_{\zeta_j}^k\begin{pmatrix}\xi\\1\end{pmatrix}\le0\}$ and $\tilde{N}_{\zeta_j}^k\triangleq\begin{pmatrix}\tilde{V}_{\zeta_j}^k&\tilde{F}_{\zeta_j}^{k\,\prime}\\ \star&\beta_{\zeta_j}^k\end{pmatrix}$. Making $\mathscr{E}_P$ lie into each set $\mathscr{B}_{\zeta_j}^k$ thus ensures that $\mathscr{E}_P\subset\mathscr{B}_{\zeta_j}$, and consequently that $\mathscr{E}_P\subset\mathscr{A}_{\zeta_j}$.

Theorem 4.3 *The relationship* $\mathscr{E}_P \subset \mathscr{B}_{\zeta_j} = \bigcap_{k=1}^{l_{\zeta_j}} \mathscr{B}^k_{\zeta_j}$ *holds if and only if the following* l_{ζ_j} *LMIs on P and* $\tau^k_{\zeta_j}$, $k = 1,\ldots,l_{\zeta_j}$, *are satisfied:*

$$\exists\ \tau^1_{\zeta_j} \in \mathbb{R}^{+*},\ldots,\tau^{l_{\zeta_j}}_{\zeta_j} \in \mathbb{R}^{+*},\ \forall k = 1,\ldots,l_{\zeta_j},\ \tau^k_{\zeta_j}\tilde{N}^k_{\zeta_j} - \begin{pmatrix} P & 0 \\ \star & -1 \end{pmatrix} \leq 0. \tag{25}$$

The problems (25)*,* (19)*,* (17) *are jointly solved.*

4.3 Conditions for the synthesis of a linear static state feedback $u = Kx$

When the aim is to synthesize a linear static state feedback $u = Kx$, the normalized SNLDI (15) into which the nonlinear closed-loop system is embedded has the form

$$\begin{pmatrix} \dot{x} \\ q \end{pmatrix} = \begin{pmatrix} B_uK & B_p \\ D_{qu}K & D_{qp} \end{pmatrix} \begin{pmatrix} x \\ p \end{pmatrix},\ p = \Delta q,\ \text{with } \Delta \in \blacktriangle(r),\ r = (r_1,\ldots,r_{\mathsf{N}})'. \tag{26}$$

Notice that in this whole section, the closed-loop state vector $\tilde{x}$ is equal to the open-loop state vector x so that Ξ_f and $\tilde{\Xi}_f$ defined in Hypothesis 3.4 and § 4.2.1 match. The matrices B_u, B_p, D_{qu} and D_{qp}, as well as the virtual signals p and q and the matrix gain Δ, are involved in the normalized SNLDI that would be obtained by globally linearizing the open-loop LFT (9) in the case when $y = x$, see the remarks following Definition 3.2. When possible, a minimal form of the open-loop LFT (9) would be looked for.

4.3.1 Convergence of the camera to the reference situation

A Global asymptotic stability of the SNLDI (26) **and satisfaction of the well-posedness assumption** (12) Consider a fixed $\alpha \geq 0$. The quadratic stability and the well-posedness of the SNLDI (26) as well as the decay rate α are ensured if the following LMI on Q, Y, T and H is feasible:

$$\exists\ Q > 0,\ Y \in \mathbb{R}^{n_u \times n},\ T \in \mathscr{S}(r),\ H \in \mathscr{G}(r),\ \begin{pmatrix} B_pTB_p' + B_uY + Y'B_u' + 2\alpha Q & B_pTD_{qp}' + Y'D_{qu}' + B_pH \\ \star & D_{qp}TD_{qp}' - T + D_{qp}H + H'D_{qp}' \end{pmatrix} < 0. \tag{27}$$

The value of K is then computed from the solution of (27) by $K = YQ^{-1}$.

B Satisfaction of the boundedness assumption (11) When a static state feedback is considered, the boundedness assumption which underlies the definition of the SNLDI (26) returns to the constraint $\mathscr{E}_P \subset \Xi_f$. Though the matrix inequalities (19) obtained in an analysis context can be adapted to guarantee this property, they involve a matrix P related to the matrix Q in (27) by the bilinear equality $PQ = I$. To keep the whole feasibility/optimization problem convex, the constraint $\mathscr{E}_P \subset \Xi_f$ should be reformulated if possible as an LMI which does not involve the matrix P.

For $i=1,\ldots,n$, let $W_i \stackrel{\Delta}{=} \mathrm{col}_i(I_n)$ and $\rho_i \stackrel{\Delta}{=} \min(|\underline{x}_i|;|\overline{x}_i|)$. The constraint $\mathscr{E}_P \subset \Xi_f$ is satisfied if and only if the following $2n$ LMIs on Q and σ_i, $i=1,\ldots,n$, are feasible:

$$\exists\ \sigma_1 \in \mathbb{R}^{+*},\ldots,\sigma_n \in \mathbb{R}^{+*},\ \forall i=1,\ldots,n,\ -\rho_i^2+\sigma_i \leq 0,\ \text{and}\ \begin{pmatrix} -Q & QW_i \\ \star & -\sigma_i \end{pmatrix} \leq 0. \tag{28}$$

The problems (28) and (27) are simultaneously solved.

4.3.2 *A priori* knowledge about the initial sensor-target relative situation

For the reasons mentioned in § 4.3.1-B, the constraints (20) and (21) obtained in the analysis context are replaced by LMIs which do not explicitely involve the variable P.

The following LMI on Q (resp. on Q and σ_0) is equivalent to (20) (resp. (21)) when m is set to 0, and is thus necessary and sufficient for $x_0 \in \mathscr{E}_P$ (resp. $\mathscr{E}_0 \stackrel{\Delta}{=} \{\xi \in \mathbb{R}^n : \xi = x_0 + Ez,\ z'z \leq 1\} \subset \mathscr{E}_P$:)

$$\begin{pmatrix} -1 & x_0' \\ \star & -Q \end{pmatrix} \leq 0. \quad \left(\text{resp. } \exists\ \sigma_0 \in \mathbb{R}^+,\ \begin{pmatrix} -\sigma_0 I_n & 0_{(n;1)} & E' \\ \star & \sigma_0 - 1 & x_0' \\ \star & \star & -Q \end{pmatrix} \leq 0.\right) \tag{29}$$

A common solution is looked for the problems (29), (28) and (27).

4.3.3 Avoidance of the actuators saturations

The j^{th} constraint on the actuators is satisfied if and only if $W_j'Kx \in [-\overline{u}_j;\overline{u}_j]$ with $W_j \stackrel{\Delta}{=} \mathrm{col}_j(I_{n_u})$. A necessary and sufficient condition for $\mathscr{E}_P \subset \mathscr{A}_{u_j}$ with $\mathscr{A}_{u_j} \stackrel{\Delta}{=} \{\xi \in \mathbb{R}^n : \xi' K' W_j W_j' K \xi \leq \overline{u}_j^2\}$ is the feasibility of the LMIs on Q, Y and σ_{u_j},

$$\exists\ \sigma_{u_j} \in \mathbb{R}^{+*},\ -\overline{u}_j^2+\sigma_{u_j} \leq 0 \text{ and } \begin{pmatrix} -Q & Y'W_j \\ \star & -\sigma_{u_j} \end{pmatrix} \leq 0. \tag{30}$$

The problems (30), (28) and (27) are simultaneously solved.

4.3.4 Constraints of the type $\zeta_j = Z_{\zeta_j}(\tilde{x})\tilde{x} \in [\underline{\zeta}_j;\overline{\zeta}_j]$

This section shows how the LMIs in Theorems 4.2 and 4.3 —which were developed in § 4.2.4— can be turned into LMIs which do not explicitely involve the matrix P.

A Global linearization of $\zeta_j = Z_{\zeta_j}(\tilde{x})\tilde{x}$

Theorem 4.4 *The following LMI on Q, σ_ζ, T_ζ and H_ζ, which is equivalent to* (24)*, is a sufficient condition to $\mathscr{E}_P \subset \mathscr{C}_{\zeta_j}$ —which, if $\mathscr{E}_P \subset \tilde{\Xi}_f$ holds, then ensures that $\mathscr{E}_P \subset \mathscr{B}_{\zeta_j} \stackrel{\Delta}{=} (\mathscr{C}_{\zeta_j} \cap \tilde{\Xi}_f) \subset \mathscr{A}_{\zeta_j}$—:*

$$\exists\, \sigma_\zeta \in \mathbb{R}^{+*},\ T_\zeta \in \mathscr{S}(r_\zeta),\ H_\zeta \in \mathscr{G}(r_\zeta),\ \begin{pmatrix} R_1 & 0 & R_2 & 0 \\ \star & -\sigma_\zeta \tilde{\zeta}_j^2 & -\sigma_\zeta \hat{\zeta} & \sigma_\zeta \\ \star & \star & R_3 & 0 \\ \star & \star & \star & -1 \end{pmatrix} < 0, \tag{31}$$

$$\text{with } R_1 = \tilde{D}_{qp_\zeta} T_\zeta \tilde{D}'_{qp_\zeta} - T_\zeta + \tilde{C}_{q_\zeta} Q \tilde{C}'_{q_\zeta} + \tilde{D}_{qp_\zeta} H_\zeta - H_\zeta \tilde{D}_{qp_\zeta},\ R_2 = \tilde{D}_{qp_\zeta} T_\zeta \tilde{D}'_{p_\zeta} + \tilde{C}_{q_\zeta} Q \tilde{C}'_\zeta + H'_\zeta \tilde{D}'_{p_\zeta},$$
$$R_3 = \tilde{D}_{p_\zeta} T_\zeta \tilde{D}'_{p_\zeta} - \sigma_\zeta + \tilde{C}_\zeta Q \tilde{C}'_\zeta.$$

The problems (31)*,* (28) *and* (27) *are jointly solved.*

As was the case for the analysis conditions, the variables σ_ζ, T_ζ and H_ζ, as well as the quantities r_ζ, $\tilde{C}_\zeta$, $\tilde{D}_{p_\zeta}$, $\tilde{C}_{q_\zeta}$, $\tilde{D}_{qp_\zeta}$, should have been indexed by j, which was ommited to alleviate the notations. The proof is given in Appendix B.3.

B Inner approximation of $\mathscr{A}_{\zeta_j}$ by the intersection of quadratic functions The notations are these of § 4.2.4-B, but the matrices $\tilde{V}^k_{\zeta_j}$ are assumed positive semidefinite so that they can be expressed as $\tilde{V}^k_{\zeta_j} = \tilde{R}^{k'}_{\zeta_j} \tilde{R}^k_{\zeta_j}$. Recall that $m = 0$ as the controller is static.

Theorem 4.5 *The following set of l_{ζ_j} LMIs on Q and $\sigma^k_{\zeta_j}$, which is necessary and sufficient for $\mathscr{E}_P \subset \mathscr{B}_{\zeta_j} = \bigcap_{k=1}^{l_{\zeta_j}} \mathscr{B}^k_{\zeta_j}$, can be obtained from* (25)*:*

$$\exists\, \sigma^1_{\zeta_j} \in \mathbb{R}^{+*}, \ldots, \sigma^{l_{\zeta_j}}_{\zeta_j} \in \mathbb{R}^{+*},\ \forall k = 1, \ldots, l_{\zeta_j},\ \begin{pmatrix} \sigma^k_{\zeta_j} \beta^k_{\zeta_j} + \tilde{F}^k_{\zeta_j} Q \tilde{F}^{k'}_{\zeta_j} & \sigma^k_{\zeta_j} & \tilde{F}^k_{\zeta_j} Q \tilde{R}^{k'}_{\zeta_j} \\ \star & -1 & 0 \\ \star & \star & -\sigma^k_{\zeta_j} I_{(n+m)} + \tilde{R}^k_{\zeta_j} Q \tilde{R}^{k'}_{\zeta_j} \end{pmatrix} \leq 0. \tag{32}$$

The problems (32)*,* (28) *and* (27) *are jointly solved.*

4.4 Conditions for the synthesis of a nonlinear static state feedback

This section aims at synthesizing the parameters K and K_p of a nonlinear rational static state feedback having the form

$$u = \left(K + K_p \Delta(x) \left(I - (D_{qp} + D_{qu} K_p) \Delta(x) \right)^{-1} D_{qu} K \right) x. \tag{33}$$

As explained in [1], the use of such a controller enables to keep the same Δ matrix in the LFTs of the open-loop system and in closed-loop, thus making easier the determination of a minimal closed-loop LFT.

The normalized SNLDI (15) representing the uncertain linear system into which the nonlinear closed-loop system is embedded has the form

$$\begin{pmatrix} \dot{x} \\ q \end{pmatrix} = \begin{pmatrix} B_u K & (B_p + B_u K_p) \\ D_{qu} K & (D_{qp} + D_{qu} K_p) \end{pmatrix} \begin{pmatrix} x \\ p \end{pmatrix}, \; p = \Delta q, \text{ with } \Delta \in \blacktriangle(r). \tag{34}$$

The remarks made at the beginning of § 4.3 concerning the open-loop still hold.

Similarly to the global linearization process that was performed in § 4.2.4-A so as to get the embedding static inclusion $\zeta_j(\tilde{x}, \Delta_\zeta)$ in the form of the LFT (23) for the rational expression $\zeta_j = Z_{\zeta_j}(\tilde{x})\tilde{x}$ assuming that $\tilde{x} \in \tilde{\Xi}_f$ and under a well-posedness assumption, the global linearization of the rational static state feedback control (33) leads to the normalized static inclusion

$$\begin{pmatrix} u(x,\Delta) \\ q \end{pmatrix} = \begin{pmatrix} K & K_p \\ D_{qu} K & (D_{qp} + D_{qu} K_p) \end{pmatrix} \begin{pmatrix} x \\ p \end{pmatrix}, \; p = \Delta q, \text{ with } \Delta \in \blacktriangle(r). \tag{35}$$

Though the results of this section are not explicitely mentioned in the robust control literature, they can be obtained through fairly classical arguments.

4.4.1 Convergence of the camera to the reference situation

A Global asymptotic stability of (34) **and satisfaction of the well-posedness assumption** (12)

Theorem 4.6 *Consider a fixed $\alpha \geq 0$. The quadratic stability of the SNLDI* (34)*, the well-posedness of the inclusions* (34) *and* (35)*, as well as the decay rate α are ensured if the following LMI on Q, Y, Y_2 and T is feasible:*

$$\exists\, Q > 0,\, Y \in \mathbb{R}^{n_u \times n},\, Y_2 \in \mathbb{R}^{n_u \times n_p(r)},\, T \in \mathscr{S}(r), \begin{pmatrix} Y' B_u' + B_u Y + 2\alpha Q & B_p T + B_u Y_2 & Y' D_{qu}' \\ \star & -T & T D_{qp}' + Y_2' D_{qu}' \\ \star & \star & -T \end{pmatrix} < 0. \tag{36}$$

The values of K and K_p are then computed from the solution of (36) *by $K = YQ^{-1}$ and $K_p = Y_2 T^{-1}$.*

The proof is given in Appendix B.4.

B Satisfaction of the boundedness assumption (11) As was the case for the synthesis of a linear static state feedback in § 4.3.1-B, this hypothesis is ensured by joining the $2n$ LMIs (28) on Q and σ_i, $i = 1, \ldots, n$, to the problem (36).

4.4.2 *A priori* knowledge about the initial sensor-target relative situation

Similarly to the synthesis of a linear static state feedback, the constraint $x_0 \in \mathscr{E}_P$ or $\mathscr{E}_0 \subset \mathscr{E}_P$ is ensured by uniting to the problem {(36),(28)} the LMI (29) on Q developed in § 4.3.2.

4.4.3 Avoidance of the actuators saturations

The j^{th} constraint on the actuators is satisfied by means of the condition $\mathscr{E}_P \subset \mathscr{A}_{u_j}$, with $\mathscr{A}_{u_j} \triangleq \{\xi \in \mathbb{R}^n : u' W_j W_j' u \leq \overline{u}_j^2,\ u \text{ being defined by (33)}\}$. Considering the inclusion (35) coming from the global linearization of the control law (33), and using the same reasoning as in § 4.2.4-A, the constraint $\mathscr{E}_P \subset \mathscr{B}_{u_j} \triangleq (\mathscr{C}_{u_j} \cap \Xi_f)$, with $\mathscr{C}_{u_j} \triangleq \{\xi \in \mathbb{R}^n : \forall \Delta \in \blacktriangle(r),\ (W_j' u(\xi, \Delta))^2 \leq \overline{u}_j^2\}$, turns to be sufficient to guarantee that $\mathscr{E}_P \subset \mathscr{A}_{u_j}$.

Theorem 4.7 *The condition $\mathscr{E}_P \subset \mathscr{C}_{u_j}$ —which, if $\mathscr{E}_P \subset \Xi_f$ holds, then ensures that $\mathscr{E}_P \subset \mathscr{B}_{u_j} \triangleq (\mathscr{C}_{u_j} \cap \Xi_f) \subset \mathscr{A}_{u_j}$— is satisfied if the following LMIs on Y, Y_2, Q, T and σ_{u_j} are feasible:*

$$\exists\, \sigma_{u_j} \in \mathbb{R}^{+*},\ -\overline{u}_j^2 + \sigma_{u_j} \leq 0 \text{ and } \begin{pmatrix} -Q & 0 & Y' W_j & Y' D_{qu}' \\ \star & -T & Y_2' W_j & T D_{qp}' + Y_2' D_{qu}' \\ \star & \star & -\sigma_{u_j} & 0 \\ \star & \star & \star & -T \end{pmatrix} \leq 0. \tag{37}$$

The problems (37)*,* (28)*,* (36) *are simultaneously solved.*

It must be kept in mind that the matrix T involved in the LMI (37) is the same as in the LMI (36) related to the stability of the SNLDI (34). One could replace T in Theorem 4.7 by another decision variable $T_{uj} \in \mathscr{S}(r)$ in order to reduce the conservatism of the approach. Yet, in this case, the change of variable $Y_2 = K_p T$ would be forbidden, so that the inequalities (37) and (36) should be replaced by Bilinear Matrix Inequalities (BMIs). The proof is given in Appendix B.4.

4.4.4 Constraints of the type $\zeta_j = Z_{\zeta_j}(\tilde{x})\tilde{x} \in [\underline{\zeta}_j; \overline{\zeta}_j]$

As was the case for the synthesis of a linear static state feedback, depending on whether the global linearization of $\zeta_j = Z_{\zeta_j}(\tilde{x})\tilde{x}$ (§ 4.3.4-A) or an inner approximation of $\mathscr{A}_{\zeta_j}$ by quadratic forms (§ 4.3.4-B) is used, such constraints are ensured by either Theorem 4.4 or Theorem 4.5, respectively.

4.5 Case studies

The above developments are applied to two case studies. The first one concerns the multicriteria synthesis of a 3D servo for the positioning of a 3DOF camera, while the second one concerns the analysis of a 2D servo on a 2DOF camera. The detailed computations can be found in [1] and are not reported here. The focus is only put on the most prominent properties.

4.5.1 Case study #1: multicriteria synthesis of 3-DOF position-based servo

The admissible movements of the considered camera are any translation in the plane $(T, \overrightarrow{y_T}, \overrightarrow{z_T})$ parallel to the ground and an azimuth rotation around the downward vertical axis $\overrightarrow{x_S} = \overrightarrow{x_T}$. This restricted problem is meaningful to us because it represents a pan-camera mounted on an holonomic robot NOMADIC XR4000, see Figure 3. In this case study, the control vector and the state vector are respectively set to

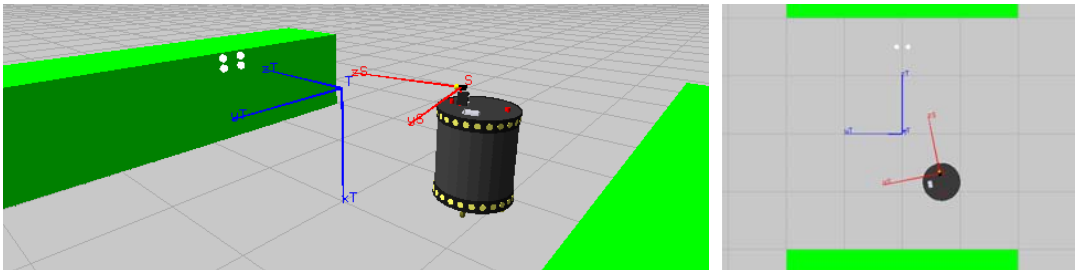

Figure 3: 3-DOF position-based control (perspective and upper orthogonal views)

$u = (V_y, V_z, \Omega_x)'$ and $x = (t_y, t_z, L \triangleq \tan(\frac{\lambda}{2}))'$ with λ the azimuth angle $\widehat{\overrightarrow{z_S}, \overrightarrow{z_T}}$ around $\overrightarrow{x_S} = \overrightarrow{x_T}$. The target is fitted with four spots T_i, $i = 1, \ldots, 4$, whose respective coordinates expressed in the frame F_T belong to the set $\{(0.05\varepsilon_1, 0.1\varepsilon_2, 1.5)', \varepsilon_1 = \pm 1, \varepsilon_2 = \pm 1\}$. The aim is to synthesize a static linear position-based servo —state feedback controller— such that the convergence is ensured with the maximum decay rate α. The control signal must satisfy the loose constraints $|V_y| \leq \overline{V}_y = 1.5\,\mathrm{m.s}^{-1}$, $|V_z| \leq \overline{V}_z = 1.5\,\mathrm{m.s}^{-1}$ and $|\Omega_x| \leq \overline{\Omega}_x = 1\,\mathrm{rad.s}^{-1}$. The reference situation is such that T lies in the axis of symmetry of a 4m wide corridor, with the axis $\overrightarrow{z_T}$ orthogonal to the walls. The 3D contraint on the camera motion is thus modeled by $|d_{3\mathrm{D}}| \leq \overline{d_{\mathrm{WALL}}} = 2\,\mathrm{m}$, where $d_{3\mathrm{D}} \triangleq \overrightarrow{z_T}.\overrightarrow{TS}$. Concerning the 2D constraints, a unity camera focal length $f = 1$ is assumed, and the virtual bounds corresponding to the physical limits of the image plane are termed $\underline{X} = -\overline{X}$ and $\underline{Y} = -\overline{Y}$. As the choice $\{\overline{X} = 0.3\,\mathrm{m}, \overline{Y} = 0.25\,\mathrm{m}\}$ leads to an unfeasible problem, $\overline{X} = 0.3\,\mathrm{m}$ and $\overline{Y} = 0.4\,\mathrm{m}$ are considered instead. The initial state vector is set to $x_0 = (0.5, 0.8, 0.1)'$, for a farther initial sensor-target situation would make the problem unfeasible.

The nonlinear closed-loop system is embedded into the normalized SNLDI (26), which is computed assuming that $\Xi_f = [-\overline{t_y}; \overline{t_y}] \times [-\overline{t_z}; \overline{t_z}] \times [-\overline{L}; \overline{L}]$, with $\overline{t_y} = 3\,\mathrm{m}$, $\overline{t_z} = 2\,\mathrm{m}$, $\overline{L} = 1$. This SNLDI is obtained from a minimal LFT, and turns to be well-posed whatever the value of x. 3D constraints are dealt with through the approach developed in § 4.3.4-A. The static inclusion used to embed the additional variable $d_{3\mathrm{D}}$ can be shown to come from a minimal ever well-posed LFT. A minimal LFT can also be defined for the additional variables $X_i - X_i^*$ and $Y_i - Y_i^*$, for which the well-posedness necessary condition $x \in \mathscr{O}_1 \triangleq \{(t_y, t_z, L) : \forall i \in \{1, \ldots, 4\},\ z_i = \overrightarrow{ST_i}.\overrightarrow{z_S} \neq 0\}$ outlined in § 3.4 turns to be sufficient in this case study. However, taking into account the 2D constraints by globally linearizing this LFT and applying the results of § 4.3.4-A leads to an unfeasible LMI problem. So, the 2D constraints are dealt with by approxi-

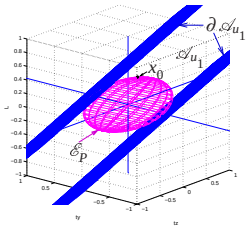

Fig. 4: $\mathscr{E}_P \subset \mathscr{A}_{u_1}$

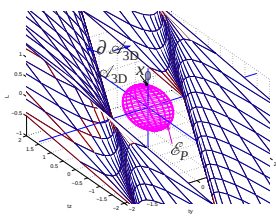

Fig. 5: $\mathscr{E}_P \subset \mathscr{A}_{3D}$

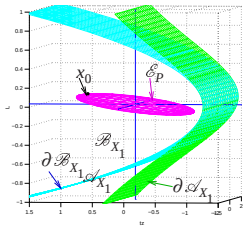

Fig. 6: $\mathscr{E}_P \subset \mathscr{B}_{X_1} \subset \mathscr{A}_{X_1}$

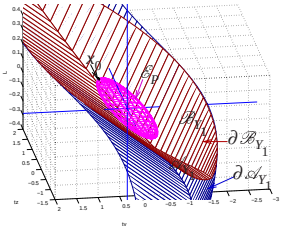

Fig. 7: $\mathscr{E}_P \subset \mathscr{B}_{Y_1} \subset \mathscr{A}_{Y_1}$

mating the target visibility domain through quadratic functions determined *ad hoc* [1].

The solution, with the MATLAB LMI Control Toolbox [21], of the GEVP problem consisting in the minimization of $-\alpha$ subject to the LMIs $\{(\alpha > 0)$,(27),(28),(29),(30),(31),(32)$\}$ leads to $K = \begin{pmatrix} 1.88 & -0.63 & 2.03 \\ -0.18 & 0.95 & 4.55 \\ -4.97 & -1.98 & 41.99 \end{pmatrix}$ and $\alpha = 0.3810$. To fix some ideas, the following relevant subsets of the state space are drawn in Figures 4,5,6,7: $\mathscr{E}_P \triangleq \{\xi : \xi' P \xi \leq 1\}$, $\mathscr{A}_{u_1} \triangleq \{\xi : |V_y| \leq \overline{V}_y\}$, $\partial\mathscr{A}_{u_1} \triangleq \{\xi : |V_y| = \overline{V}_y\}$, $\mathscr{A}_{3D} \triangleq \{\xi : |d_{3D}| \leq \overline{d_{\text{WALL}}}\}$, $\partial\mathscr{A}_{3D} \triangleq \{\xi : |d_{3D}| = \overline{d_{\text{WALL}}}\}$, $\mathscr{A}_{X_1} \triangleq \{\xi : |X_1| \leq \overline{X}\}$, $\partial\mathscr{A}_{X_1} \triangleq \{\xi : |X_1| = \overline{X}\}$, $\mathscr{A}_{Y_1} \triangleq \{\xi : |Y_1| \leq \overline{Y}\}$, $\partial\mathscr{A}_{Y_1} \triangleq \{\xi : |Y_1| = \overline{Y}\}$, and the boundaries $\partial\mathscr{B}_{X_1}$ (resp. $\partial\mathscr{B}_{Y_1}$) of the sets $\mathscr{B}_{X_1}$ (resp. $\mathscr{B}_{Y_1} \triangleq \mathscr{B}^1_{Y_1} \cap \mathscr{B}^2_{Y_1}$) resulting from the inner approximations of $\mathscr{A}_{X_1}$ (resp. $\mathscr{A}_{Y_1}$) by quadratic functions. Similar sets would be obtained for the other target spots and actuators. The fact that $\mathscr{E}_P$ belongs to the above sets confirms the satisfaction of the considered constraints. Simulation results would also corroborate this [1].

4.5.2 Case study #2: multicriteria analysis of 2-DOF image-based servo

A 2-DOF camera is considered whose possible displacements are made of translations and rotations along and around the optical axis $\overrightarrow{z_S} = \overrightarrow{z_T}$, so that $x = (t_z, N \triangleq \tan(\frac{\nu}{4}))'$ and $u = (V_z, \Omega_z)'$. A target fitted with 2 asymmetric spots T_1, T_2 is used, whose respective coordinates $(a_1, b_1, c)'$ and $(a_2, b_2, c)'$ expressed in frame F_T satisfy $a_1 = a_2 = 0$, $b_1 = 1$, $b_2 = -2$, $c = 1.5$, see Figure 8. The camera is moved by the image-based

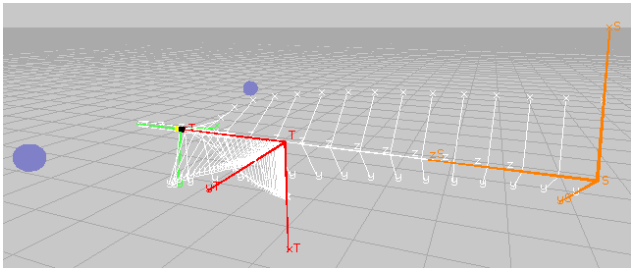

Figure 8: 2-DOF image-based control (perspective view)

control law $u = -\lambda [J(s^*, z^*)]^+ y$ described in [6], with $y = s - s^*$ as before, $z^* = (c, c)'$, $\lambda = 0.1$ and $J(s^*, z^*)$ the image Jacobian $J(s, z)$ —defined by $\dot{s} = J(s, z)u$— computed at the reference situation. No 3D constraint is imposed on the motion. The actuators limits are $|V_z| \leq \overline{V}_z = 1.5\,\text{m.s}^{-1}$ and $|\Omega_z| \leq \overline{\Omega}_z = 1\,\text{rad.s}^{-1}$. The camera focal length is selected to be $f = 1$, and the virtual limits of the image plane are set to

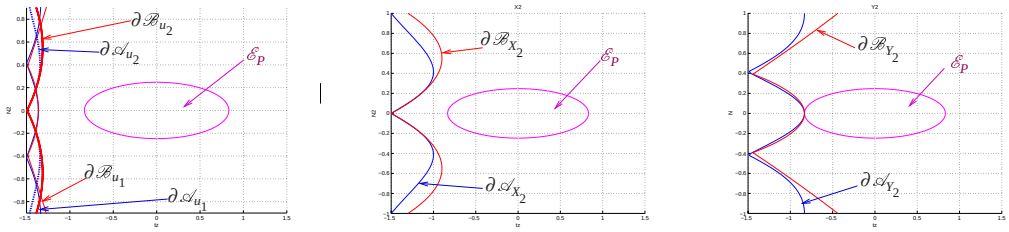

Figure 9: Static output feedback multicriteria analysis

$-\underline{X} = \overline{X} = 4\text{m}$ and $-\underline{Y} = \overline{Y} = 3\text{m}$. The aim is to determine the maximum size multicriteria basin of attraction, viz. the "widest" subset of the state space into which the convergence as well as the other criteria are ensured.

A closed-loop minimal LFT (10) can be straightly computed from the closed-loop state equation. The necessary condition $x \in \mathscr{O}_2 \stackrel{\Delta}{=} \{(t_z, N) : z_i = \overrightarrow{ST_i}.\overrightarrow{z_S} \neq 0,\ i = 1,2\}$ mentioned in § 3.4, i.e. $x \in \mathscr{O}_2 \stackrel{\Delta}{=} \{(t_z, N) : t_z \neq -c\}$, turns out to be sufficient for its well-posedness. So, the normalized closed-loop SNLDI (15) is computed assuming that x lies in the parallelotope $\Xi_f = [-\overline{t_z}; \overline{t_z}] \times [-\overline{N}; \overline{N}]$, $\overline{t_z} = 1\text{m}$, $\overline{N} = 0.8$, which is included into $\mathscr{O}_2^+ \stackrel{\Delta}{=} \{(t_z, N) : t_z > -c\} \subset \mathscr{O}_2$. The image and actuators constaints are taken into account through inner approximations by quadratic functions of the admissible sets they define, following the approach developed in § 4.3.4-B.

An ellipsoid $\mathscr{E}_P$ is looked for such that the sum of squares of its principal axes lengths is maximum. The solution, with the MATLAB LMI Control Toolbox [21], of the LMI problem consisting in the minimization of trace (P) under the LMIs $\{(17),(19),(25)\}$ leads to $P = \begin{pmatrix} 1.44 & \varepsilon \\ \star & 16.37 \end{pmatrix}$, with $\varepsilon \approx 0$. The results are illustrated in Figure 9. The left part of each plot shows the boundaries of the admissible subspace. $\partial\mathscr{A}_{u_i}$ terms the frontier of the set $\mathscr{A}_{u_i}$ into which the i^{th} actuator does not saturate, and $\partial\mathscr{B}_{u_i}$ is the boundary of the quadratic approximation $\mathscr{B}_{u_i}$ of $\mathscr{A}_{u_i}$. Likewise, the limits $\partial\mathscr{A}_{X_2}/\partial\mathscr{B}_{X_2}$ and $\partial\mathscr{A}_{Y_2}/\partial\mathscr{B}_{Y_2}$ of the sets $\mathscr{A}_{X_2}/\mathscr{B}_{X_2}$ and $\mathscr{A}_{Y_2}/\mathscr{B}_{Y_2}$ express the fact that the projection of T_2 must be kept into the camera image plane. Similar curves would be obtained for the spot T_1. The details are thoroughly developed in [1].

4.6 Conclusion

At this point, thanks to the insight gained by the solution to the two case studies, a conclusion can be made concerning the application to visual servoing of the above classical LMI control techniques.

As mentioned in § 4.1.4, a particular effort is necessary right at the modeling stage to determine a minimal closed-loop LFT. For instance in Case Study #2, the matrix Δ entailed in the closed-loop LFT (10) and in the open-loop LFT (9) would have been of higher size if (9) had been determined by separately computing the LFTs related to the open-loop state equation and to the open-loop output equation prior to their "stacking" via the standard rules mentioned in [44, 13]. Note that the spatial arrangement of the target

spots may also be adapted to get minimality, e.g. laying them on a plane orthogonal to the $\overrightarrow{z_T}$-axis may make it easier.

Other degrees of freedom which can limit the conservatism coming from global linearization are the selection of the vector function $\Phi(.)$ and of the parallelotope Ξ, see § 3.4. The fact that both scaling matrices S and G are free also turns to be extremely important in the outer approximation of the SNLDI embedding the closed-loop system. Indeed, even with a minimal closed-loop LFT, the first results that were obtained in [3] for Case Study #1 by selecting $G = 0_{(n_p(r);n_p(r))}$ —which amounts not to take into account the realness of Δ— led to very small coefficients in the third row of the state feedback gain K and thus a prohibitive decay rate.

A last source of conservatism due to the underlying Automatic Control techniques basically lies into the use of a unique quadratic Lyapunov function to check/ensure all the criteria for all the realizations of the outer approximation of the closed-loop SNLDI.

As foreboded, the geometric properties of the consequent invariant sets turn to be extremely penalizing in this robotics context. First, as explained at the end of § 4.1.1, they may require the definition of an unduly wide Ξ_f. More importantly, as is the case in the above case studies, they often lead to an extremely conservative solution, in that a synthesis problem may be feasible only if the initial and reference sensor-target situation are very close to each other, and the conclusions concerning an analysis may be poor. The Figures 5,6,7 confirm that the asymmetry w.r.t. 0 of the admissible sets $\mathscr{A}_{X_i}$ and $\mathscr{A}_{Y_i}$ —in which the invariant ellipsoid $\mathscr{E}_P$ is expected to lie— is a source of pessimism coming from the robotics problem itself, as is the nonconvexity of the region $\mathscr{A}_{3D}$ into which the 3D constraints are fulfilled, see the discussion in §4.1.3.B. Similarly, for Case Study #2, the asymmetry of $\mathscr{A}_{Y_i}$, $\mathscr{A}_{X_i}$ and $\mathscr{A}_{u_i}$ prevents any conclusion for some initial conditions from which the convergence is trivially ensured, e.g. $x_0 = (t_{z_0}, 0)'$ with $t_{z_0} > 0.9\,\mathrm{m}$.

Lastly, subtler well-posedness issues can explain some failures of the method. In the last case study mentioned, the well-posedness assumption implies that $\mathscr{E}_P \subset \Xi_f \subset \mathscr{O}_2^+ \stackrel{\Delta}{=} \{(t_z, N) : t_z > -c\}$, so initial states $x_0 = (t_{z_0}, 0)'$ with $t_{z_0} > c$ cannot be considered either. A similar cause can be given for the inability of the approach developed in § 4.3.4-A to take into account the 2D constraints in Case Study #1. Indeed, in order to ensure the well-posedness of the inclusion (23) related to image constraints, the parallelotope $\Xi_f = \Xi$ involved in the global linearization process is selected to lie into $\mathscr{O}_1^+ \stackrel{\Delta}{=} \{(t_y, t_z, L) : \forall i \in \{1,\ldots,4\},\ z_i = \overrightarrow{ST_i}.\overrightarrow{z_S} > 0\} \subset \mathscr{O}_1$. As the boundary of $\mathscr{O}_1^+$ is "V-shaped", strong conditions follow on Ξ_f, which prevent many meaningful cases from being considered.

To deal with the last sources of conservatism coming from the robotics problem itself, two extensions are hereafter presented. These were formerly developed in [1]. First, an analysis method is outlined and then applied to the Case Study #2. Next, a second method is proposed for analysis as well as for synthesis,

and its results on the Case Study #1 are shown.

5 Reduction of the conservatism

5.1 An analysis method

This section proposes some guidelines to get a better inner approximation of the multicriteria basin of convergence of a visual-based feedback system, while still using the quadratic approach outlined in § 4. It is still assumed that $\Phi(x)$ has been set to x, and only static controllers are considered —so that $\tilde{\Xi}_f = \Xi_f = \Xi$— but the results can be straightly extended. The main ideas are first exposed, and then applied to Case Study #2.

5.1.1 "Directed" ellipsoidal invariant sets

It may be worth selecting among the invariant ellipsoids $\mathscr{E}_P$ that verify all the constraints of the problem, the one —henceforth denoted by $\mathscr{E}_\theta$— having the maximum extent along a polar line crossing 0 and parametrized by a vector θ. The computation of $\mathscr{E}_\theta$ can merely be performed through an optimization problem subject to the LMI constraints developed in § 4.2. Notice that the large axis of $\mathscr{E}_\theta$ is not necessarily supported by the direction θ. Then, a better inner approximation of the whole basin of attraction of 0 can be got by making the union $\cup_{\{\theta\}} \mathscr{E}_\theta$ of such ellipsoids.

5.1.2 Optimization process on the parallelotope Ξ_f

The parallelotope Ξ_f involved in the global linearization of the closed-loop state equation (7) stands for a coarse a priori knowledge of the possible state vector values, rather than for a set of constraints to be satisfied by this vector. Clearly, getting the "maximum size" invariant ellipsoid $\mathscr{E}_P$ —*e.g.* the most extended along a direction θ, or the one having the largest volume— requires the selection of a sufficiently wide Ξ_f. When Ξ_f is "small enough", the converse is also true, viz. the larger the extent of Ξ_f, the greater $\mathscr{E}_P$. However, when Ξ_f is "too big", the set of trajectories of the SNLDI coming from the global linearization of the closed-loop equation is very rich, so that the LMIs defining $\mathscr{E}_P$ may not be feasible or at best may lead to a "small" $\mathscr{E}_P$. These effects of Ξ_f onto $\mathscr{E}_P$ can be observed by doing some simulations.

It thus sounds interesting to maximize the "size" of the ellipsoid $\mathscr{E}_P$ over all the possible parallelotopes Ξ_f, whose bounds $\underline{x}_i$ and $\overline{x}_i$ are considered as decision variables. To carry out this extension, one can rewrite all the matrix inequalities of §4.2 starting from the unnormalized form (14) of the closed-loop embedding inclusion. Yet, though the consequent matrix inequalities entail the parameters $\underline{x}_i$ and $\overline{x}_i$, $i = 1, \ldots, n$, they are nonlinear in the unknowns. For instance, when $\underline{x}_i = -\overline{x}_i$, stating $\overline{\overline{x}}_i \stackrel{\Delta}{=} \frac{1}{\overline{x}_i^2}$, the LMI conditions (17)–(19)

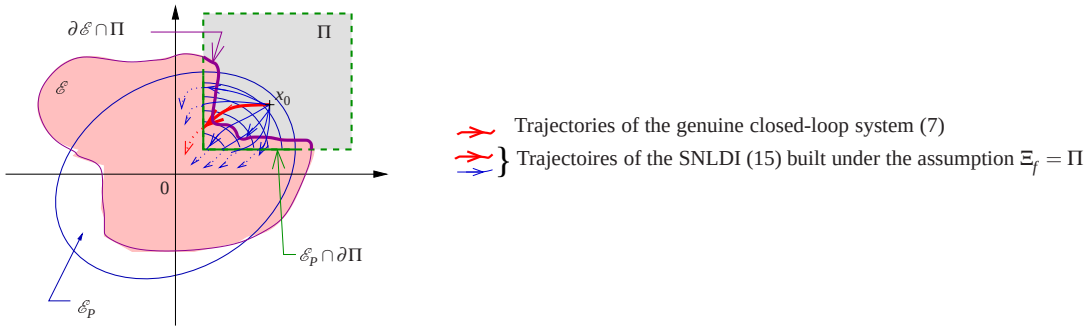

Figure 10: Reduction of the conservatism in an analysis context

ensuring the camera convergence are replaced by the following BMI on P, S, G, $\overline{\overline{x}}_i$ and τ_i, $i=1,\ldots,n$ [1]:

$$\exists\, P>0,\ S\in\mathscr{S}(r),\ G\in\mathscr{G}(r),\ \overline{\overline{x}}_1\in\mathbb{R}^{+*},\ldots,\overline{\overline{x}}_n\in\mathbb{R}^{+*},\ \tau_1\in\mathbb{R}^{+*},\ldots,\tau_n\in\mathbb{R}^{+*},$$
$$\begin{pmatrix}\tilde{A}^{\sharp'}P+P\tilde{A}^{\sharp}+\tilde{C}_q^{\sharp'}S\tilde{C}_q^{\sharp}+2\alpha P & P\tilde{B}_p^{\sharp}+\tilde{C}_q^{\sharp'}S\tilde{D}_{qp}^{\sharp}+\tilde{C}_q^{\sharp'}G\\ \star & \tilde{D}_{qp}^{\sharp'}S\tilde{D}_{qp}^{\sharp}-\overline{\overline{\Delta}}S+\tilde{D}_{qp}^{\sharp'}G+G'\tilde{D}_{qp}^{\sharp}\end{pmatrix}<0, \tag{38}$$
$$\tau_i W_i W_i^{'}-P\leq 0 \text{ and } -\tau_i+\overline{\overline{x}}_i\leq 0, \text{ with } \overline{\overline{\Delta}}\stackrel{\Delta}{=}\text{diag}\,(\overline{\overline{x}}_1 I_{r1},\ldots,\overline{\overline{x}}_n I_{rn}). \tag{39}$$

Consequently, the size of $\mathscr{E}_P$ over the BMI set defined by (38)–(39) can experience several local maxima, and the global maximization problem may be computationally untractable.

Fortunately, the "biggest" invariant ellipsoid needs not be accurately computed. Methods developed in the literature or even less involved calculations can be used as soon as they lead to a lower bound of the maximum size. For example, as in [18], a finite set of parallelotopes Ξ_f can be selected, onto which the "maximum size" ellipsoid is looked for, under the LMI constraints of §4.2. Of course, the inner approximation $\cup_{\{\theta\}}\mathscr{E}_\theta$ proposed above for the basin of attraction of 0 can be tightened by computing each ellipsoid $\mathscr{E}_\theta$ as suggested in this section from a "most helpful" parallelotope Ξ_θ.

5.1.3 Further reduction of the conservatism

Let $\mathscr{E}$ be an inner numerical approximation of the multicriteria basin of convergence of the visual servo. For instance, $\mathscr{E}$ can be computed as it has just been mentioned at the end of the above paragraph. This section shows how $\mathscr{E}$ can be expanded to a subset of a given parallelotope Π such that $\mathscr{E}\cap\Pi\neq\emptyset$ and $\mathscr{E}\cap\Pi\neq\mathscr{E}$. In addition, it is assumed that $\mathscr{E}\cap\Pi\neq\Pi$ lest the expansion would be already done. As is often the case in practice, it is assumed that 0 belongs to $\mathscr{E}$ and is outside Π. To simplify, the part $\partial\mathscr{E}\cap\Pi$ of the frontier $\partial\mathscr{E}$ of $\mathscr{E}$ which is inside Π is supposed to be connected, see Figure 10.

Let the global linearization of the closed-loop system (7) be henceforth performed under the assumption $\Xi_f=\Pi$. The quadratic stability of the SNLDI (15) —with $\Xi_f=\Pi$ therein— can be studied through the LMI (17), and an invariant ellipsoid $\mathscr{E}_P\stackrel{\Delta}{=}\{\xi\ :\ \xi' P\xi\leq 1\}$ can be defined as well. However, the only

conclusion which can be established is that the trajectories of the so-computed SNLDI just recover these parts of the trajectories of the genuine closed-loop system which lie in Π.

Assume that P is such that the ellipsoid $\mathscr{E}_P$ crosses the frontier $\partial\Pi$ of Π only once, that is, the intersection $\mathscr{E}_P \cap \partial\Pi$ is connected. A reasoning similar to § 4.1.1 shows that, as time progresses, the parts of the trajectories of the genuine nonlinear closed-loop system (7) which stay in Π intersect nested ellipsoids that correspond to decreasing values of the Lyapunov function used to establish the stability of the SNLDI. So, every trajectory of the genuine nonlinear closed-loop system which begins in $\mathscr{E}_P \cap \Pi$ crosses $\mathscr{E}_P \cap \partial\Pi$. Consequently, if $\mathscr{E}_P \cap \partial\Pi$ is a subset of $\mathscr{E}$, then every trajectory of the nonlinear system starting in $\mathscr{E}_P \cap \Pi$ converges to 0. If the other specifications are ensured over $\mathscr{E}_P \cap \Pi$, then the inner approximation $\mathscr{E}$ of the multicriteria basin of convergence can be supplemented with $(\mathscr{E}_P \cap \Pi) \setminus ((\mathscr{E}_P \cap \Pi) \cap \mathscr{E})$.

Though this extension still uses quadratic stability arguments, it doesn't suffer from all the limitations mentioned in § 4.6. For instance, when constraints on additional variables confine the closed-loop state vector to an asymmetric set $\mathscr{B}$, the inner approximation $\mathscr{E}$ is expanded if and only if $(\mathscr{E}_P \cap \Pi)$ is included in $\mathscr{B}$. It is readily seen that it is in no way required that the symmetric of $(\mathscr{E}_P \cap \Pi)$ with respect to 0 also lies in $\mathscr{B}$. In the same vein, the well-posedness of the SNLDI (15) built under the assumption $\Xi_f = \Pi$ may not be too strong a requirement.

All the above considerations are turned into LMIs on P and other variables. The first one takes account of $\mathscr{E}_P \cap \Pi \neq \emptyset$. Then, some edges $\partial_1\Pi, \partial_2\Pi, \ldots$ of the parallelotope Π are selected so that they must intersect $\mathscr{E}_P$ while keeping connected the union $\cup_{i\in\{1,2,\ldots\}}(\mathscr{E}_P \cap \partial_i\Pi)$. For each such edge $\partial_i\Pi$, the fact that $(\mathscr{E}_P \cap \partial_i\Pi) \subset \mathscr{E}$ is expressed. Further, some matrix inequalities must theorize that $\mathscr{E}_P$ must not go through the remaining edges of Π. These equations depend upon some coordinates of the vertices of Π that are not crossed by $\mathscr{E}_P$. Finally, the constraints to be put on $(\mathscr{E}_P \cap \Pi)$ are described in order to handle criteria other than stability. The $\mathscr{S}$-procedure is the cornerstone throughout this process.

Assume that a set of polar lines is selected starting from 0 and intersecting Π, each line being parametrized by a vector θ. For each such θ, $\mathscr{E}$ can be best enriched if the above ellipsoid $\mathscr{E}_P$ —whose part is merged with $\mathscr{E}$— is looked for so as to have the maximum extent along θ. The whole analysis method is summarized in Algorithm 1.

5.1.4 Application to the Case Study #2

This section is meant to illustrate the method on the multicriteria analysis problem of the image-based 2DOF servo already considered in § 4.5.2.

A STEP 1 of Algorithm 1 In this 2DOF case, the vector θ parametrizing any polar line along which the extent l of the invariant ellipsoid $\mathscr{E}_P \stackrel{\Delta}{=} \{\xi : \xi' P \xi \leq 1\}$ is maximized, is merely a scalar. Because of

Algorithm 1 Summary of the analysis method

STEP 1

1: Select n_θ directions $\theta_1,\ldots,\theta_{n_\theta}$
2: **FOR** $j=1\ldots n_\theta$ **DO**
3: $\theta=\theta_j$
4: Select n_Ξ (symmetric) parallelotopes $\Xi_1,\ldots,\Xi_{n_\Xi}$
5: **FOR** $k=1\ldots n_\Xi$ **DO**
6: Compute the normalized SNLDI (15) with $\Xi_f=\Xi_k$ therein
7: Determine $\mathscr{E}_\theta$ having the maximum extent l along the direction θ while satisfying the LMI constraints defined in § 4.2
8: **IF** this problem is feasible **THEN**
9: $\mathscr{E}_k=\mathscr{E}_\theta$ and $l_k=l$
10: **END IF**
11: **END FOR**
12: Select $\mathscr{E}_{\theta_j}\triangleq\arg\max_{\mathscr{E}_k,\ k=1,\ldots,n_\Xi} l_k$
13: **END FOR**
14: Define $\mathscr{E}=\bigcup_{j=1}^{n_\theta}\mathscr{E}_{\theta_j}$

STEP 2

1: Select n_θ directions $\theta_1,\ldots,\theta_{n_\theta}$
2: **FOR** $j=1\ldots n_\theta$ **DO**
3: $\theta=\theta_j$
4: Select n_Π parallelotopes $\Pi_1,\ldots,\Pi_{n_\Pi}$
5: **FOR** $k=1\ldots n_\Pi$ **DO**
6: Compute the normalized SNLDI (15) with $\Xi_f=\Pi\triangleq\Pi_k$ therein
7: Determine $\mathscr{E}_P$ having the maximum extent l along the direction θ while satisfying the properties mentioned in § 5.1.3
8: **IF** this problem is feasible **THEN**
9: $\mathscr{E}=\mathscr{E}\cup\Big((\mathscr{E}_P\cap\Pi)\setminus((\mathscr{E}_P\cap\Pi)\cap\mathscr{E})\Big)$, i.e. $\mathscr{E}=\mathscr{E}\cup(\mathscr{E}_P\cap\Pi)$
10: **END IF**
11: **END FOR**
12: **END FOR**
13: Output $\mathscr{E}$

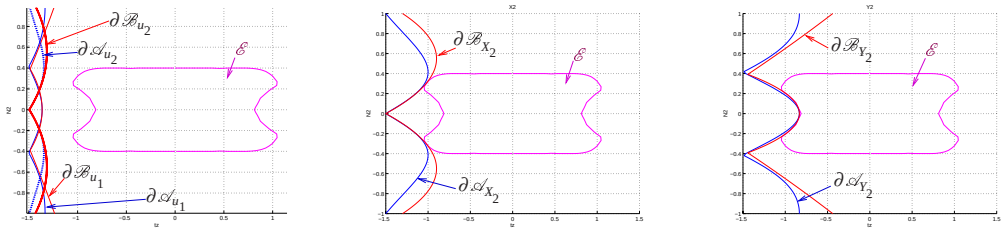

Figure 11: Static output feedback multicriteria analysis by STEP 1 of Algorithm 1

the symmetry of $\mathscr{E}_P$ —thus termed $\mathscr{E}_\theta$— w.r.t. the origin, $\mathscr{E}_\theta$ and $\mathscr{E}_{\theta+\pi}$ are equal, so that the n_θ directions $\theta_1,\ldots,\theta_{n_\theta}$ can be restricted to $[0;\pi]$. The analytic expression of the extent l is expressed as a decreasing function —which is parametrized by the angle θ— of a linear combination of the entries of the matrix P, see [1]. Then, for each θ, l is maximized under the LMIs $\{(17),(19)\}$ and other LMIs of the form (25), all the constraints being dealt with in the same way as in § 4.5.2. $n_\theta=100$ such optimizations are performed, corresponding to evenly spread directions. For each direction, n_Ξ parallelotopes $\Xi_k=[-\overline{t}_{z_k};\overline{t}_{z_k}]\times[-\overline{N_k};\overline{N_k}]$ are selected, with $\overline{t}_{z_k}>0$ and $\overline{N_k}>0$, $k=1,\ldots,n_\Xi$. In order to ensure the well-posedness of the embedding SNLDI (15) built with $\Xi_f=\Xi_k$, $-\overline{t}_{z_k}$ is selected so that $-\overline{t}_{z_k}>-c$. Figure 11 shows how the results of Figure 9 can be enhanced by defining the multicriteria basin of convergence $\mathscr{E}$ as $\mathscr{E}\triangleq\cup_{\{\theta\}}\mathscr{E}_\theta$.

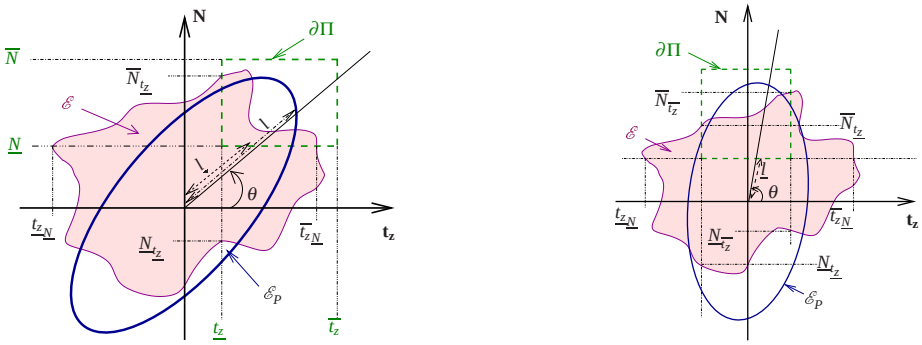

Case A *Case B*

Figure 12: Cases occuring during the finer multicriteria analysis of the image-based 2DOF servo, for $\theta \in [0; \frac{\pi}{2}]$

B Further reduction of the conservatism by STEP 2 of Algorithm 1 Given a direction θ and a parallelotope $\Pi = [\underline{t_z}; \overline{t_z}] \times [\underline{N}; \overline{N}]$, the ellipsoid $\mathscr{E}_P = \{\xi : \xi' P \xi \leq 1\}$ related to the SNLDI (15) computed with $\Xi_f = \Pi$ is sought for so that its extent l along the direction θ is maximum. The other constraints on $\mathscr{E}_P$ mentioned in § 5.1.3, which involve the multicriteria basin of convergence $\mathscr{E}$ determined above, are outlined in this section for $\theta \in [0; \frac{\pi}{2}]$, the extension to other angles intervals being straightforward.

Let *Case A* (resp. *Case B*) term the case when the point with coordinates $(\overline{t_z}, \underline{N})'$ lies outside (resp. inside) $\mathscr{E}$. Let $[\underline{N_{t_z}}; \overline{N_{t_z}}]$ be the widest interval such that $\underline{N} \in [\underline{N_{t_z}}; \overline{N_{t_z}}]$ and $[\underline{N_{t_z}}; \overline{N_{t_z}}] \subset \{\xi_2 \in \mathbb{R} : \xi = (\xi_1, \xi_2)' \in \mathscr{E}, \xi_1 = \underline{t_z}\}$, see Figure 12. $\underline{t_{z_N}}$, $\overline{t_{z_N}}$, $\underline{N_{\overline{t_z}}}$ and $\overline{N_{\overline{t_z}}}$ are similarly defined. In addition to the LMI (17) related to the quadratic stability of the considered SNLDI, other LMIs are defined on the matrix P so as to ensure that

- in *Case A* and *Case B*, $\mathscr{E}_P \cap \Pi \neq \emptyset$; for this to hold, it is sufficient to have $l > \underline{l}$ with $\underline{l}$ the length defined in Figure 12;
- in *Case A* and *Case B*, $(\mathscr{E}_P \cap \partial_W \Pi) \subset \mathscr{E}$, with $\partial_W \Pi$ the "West" edge of Π; this constraint, which can be written $(\mathscr{E}_P \cap \partial_W \Pi) = (\mathscr{E}_P \cap \{\xi : \underline{N} \leq \xi_2 \leq \overline{N}\} \cap \{\xi : \xi_1 = \underline{t_z}\}) \subset \mathscr{E}$, is turned into the more suitable form for the $\mathscr{S}$-procedure: $\xi_2 \in [\underline{N_{t_z}}; \overline{N_{t_z}}]$ for all $\xi = (\xi_1, \xi_2)'$ such that $\xi \in \mathscr{E}_P$, $\xi_1 = \underline{t_z}$ and $\xi_2 \in [\underline{N}; \overline{N}]$; notice that the consequent LMI is trivially satisfied when the intersection $(\mathscr{E}_P \cap \partial_W \Pi)$ is empty;
- in *Case A* and *Case B*, $(\mathscr{E}_P \cap \partial_S \Pi) \subset \mathscr{E}$, with $\partial_S \Pi$ the "South" edge of Π; this is equivalent to $(\mathscr{E}_P \cap \{\xi : \underline{t_z} \leq \xi_1 \leq \overline{t_z}\} \cap \{\xi : \xi_2 = \underline{N}\}) \subset \mathscr{E}$ and leads to an LMI similar to the one related to the "West" edge;
- in *Case A*, $\mathscr{E}_P$ must not cross the "East" edge $\partial_E \Pi$ of Π, i.e. $\mathscr{E}_P \subset \{\xi : \xi_1^2 \leq \overline{t}_z^2\}$; in *Case B*, the

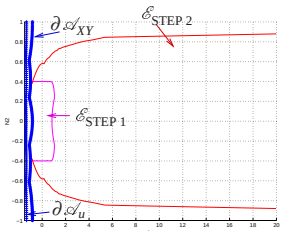

Fig. 13: Application of Algorithm 1

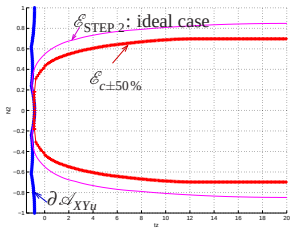

Fig. 14: $\pm 50\,\%$ uncertainty on z^*

relationship $(\mathscr{E}_P \cap \partial_E\Pi) \subset \mathscr{E}$ must hold, viz. $(\mathscr{E}_P \cap \{\xi : \underline{N} \le \xi_2 \le \overline{N}\} \cap \{\xi : \xi_1 = \overline{t}_z\}) \subset \mathscr{E}$;

- in *Case A* and *Case B*, $\mathscr{E}_P$ does not cross the "North" edge $\partial_N\Pi$ of Π; the corresponding LMI on P and other variables can be got through the $\mathscr{S}$-procedure so that $\mathscr{E}_P \subset \{\xi = (\xi_1, \xi_2)' : \xi_2^2 \le \overline{N}^2\}$.

All the above constraints guarantee that for all x_0 in $(\mathscr{E}_P \cap \Pi)$, there exists an instant t_1 such that $x(t)$ belongs to Π for all anterior time $t \in [0, t_1]$ while $x(t_1) \in \mathscr{E}$, so that the convergence is ensured for all x_0 in $(\mathscr{E}_P \cap \Pi)$. To deal with the remaining specifications, the LMIs on P and other variables —hereafter denoted ζ_j_LMI$_k(P,.) \le 0$, $k = 1, \ldots, l_{\zeta_j}$— that were developed in § 4.2.3 and § 4.2.4-B to ensure constraints like $\mathscr{E}_P \subset \mathscr{A}_{\zeta_j}$, are turned into new LMIs which are sufficient for the much less conservative set relationship $(\mathscr{E}_P \cap \Pi) \subset \mathscr{A}_{\zeta_j}$. Typically, LMIs of the following form are obtained through the $\mathscr{S}$-procedure:

$$\exists\ \tau^k_{\zeta_N} > 0,\ \tau^k_{\zeta_{t_z}} > 0,\ \zeta_j\text{\_LMI}_k(P,.) + \tau^k_{\zeta_N} \begin{pmatrix} -W_2 W_2' & \hat{N} W_2 \\ \star & -(\hat{N}^2 - \tilde{N}^2) \end{pmatrix} + \tau^k_{\zeta_{t_z}} \begin{pmatrix} -W_1 W_1' & \hat{t}_z W_1 \\ \star & -(\hat{t}_z^{\,2} - \tilde{t}_z^{\,2}) \end{pmatrix} \le 0, \tag{40}$$

with $\hat{N} = \frac{\overline{N}+\underline{N}}{2}$, $\tilde{N} = \frac{\overline{N}-\underline{N}}{2}$, $\hat{t}_z = \frac{\overline{t}_z+\underline{t}_z}{2}$ and $\tilde{t}_z = \frac{\overline{t}_z-\underline{t}_z}{2}$.

STEP 2 of Algorithm 1 is applied picking $n_\theta = 200$ evenly spread directions $\theta_1, \ldots, \theta_{n_\theta}$ in $[0; 2\pi]$. For each direction, n_Π parallelotopes $\Pi_k = [\underline{t_z}_k; \overline{t_z}_k] \times [\underline{N_k}; \overline{N_k}]$ are selected with $[\underline{N_k}; \overline{N_k}] \subset [-1; 1]$ and $[\underline{t_z}_k; \overline{t_z}_k] \subset [-1.5; 20]$. Figure 13 shows how the inner approximation $\mathscr{E}_{\text{STEP 1}}$ of the multicriteria basin of convergence formerly computed in STEP 1 can be expanded into $\mathscr{E}_{\text{STEP 2}}$. There, $\partial\mathscr{A}_u$ and $\partial\mathscr{A}_{XY}$ respectively term the frontiers of $\mathscr{A}_u = \mathscr{A}_{u_1} \cap \mathscr{A}_{u_2}$ and $\mathscr{A}_{XY} = \mathscr{A}_{X_1} \cap \mathscr{A}_{Y_1} \cap \mathscr{A}_{X_2} \cap \mathscr{A}_{Y_2}$. The new inner approximation $\mathscr{E}_{\text{STEP 2}}$ is noticeably consistent with the fact, acknowledged in [6], that the convergence fails for all initial conditions such that $\nu = \pm 180°$.

The proposed strategy has also been applied to the analysis of the static linear image-based control law $u = -\lambda [J(s^*, \widehat{z^*})]^+ y$, where $\lambda = 0.1$ as before, and $\widehat{z^*} = z^* \pm 50\,\%$. Such a study is highly significant in robotics, because an usual practical goal is to build an image-based control entailing a Jacobian matrix parametrized solely from the 2D data perceived at the reference sensor-target situation —thus the dependence on s^*, viz. on X_1^*, Y_1^*, X_2^*, Y_2^*— without the exact knowledge of the whole target model —from which the uncertainty on the depth z^*. Figure 14 compares the consequent inner approximation $\mathscr{E}_{c\pm 50\%}$ of the multicriteria basin of convergence with $\mathscr{E}_{\text{STEP 2}}$ computed above for the nominal value of z^*. The symbol $\partial\mathscr{A}_{XYu}$ represents the boundary of the set $\mathscr{A}_{XYu} = \mathscr{A}_u \cap \mathscr{A}_{XY}$ in which the actuators and 2D constraints

are satisfied in the most unfavorable case. Note that $\mathscr{E}_{c\pm 50\%}$ is fairly wide despite the constancy of $\widehat{z^*}$ over time is not taken into account.

All these results were confirmed by simulations runs. An *ad hoc* method is proposed in [1] for the determination of initial states from which the camera hits the target plane.

5.2 A method for analysis and synthesis

5.2.1 Basics

This second approach rests on the definition of a fictitious variable $x_f \in \mathbb{R}$ evolving autonomously according to the first-order differential equation

$$\dot{x}_f = -\alpha_f x_f,\ x_f(0) = x_{f0} > 0, \text{ with } \alpha_f > 0, \tag{41}$$

so that $x_f(t)$ lies in $[0; x_{f0}]$ for all t, and converges to 0 as t goes to infinity. Similarly to what was done in § 4, the genuine closed-loop nonlinear system (7) augmented by x_f, i.e. with state vector $\tilde{x}_a \stackrel{\Delta}{=} (\tilde{x}', x_f)'$, can be embedded into an uncertain linear system represented by an SNLDI. The global stability of this SNLDI can be studied through a quadratic Lyapunov function, which leads to the definition of an invariant ellipsoid $\mathscr{E}_P = \{\xi \in \mathbb{R}^{n+m+1} : \xi' P \xi \leq 1\}$. Yet, because of the above property of x_f, every trajectory $\tilde{x}_a(.)$ which starts from an initial state $\tilde{x}_{a0}$ in the "slice" $\mathscr{T}_P \stackrel{\Delta}{=} (\mathscr{E}_P \cap \{\xi_a = (\xi', \xi_f)' \in \mathbb{R}^{n+m} \times \mathbb{R} : \xi_f \in [0; x_{f0}]\})$ stays in $\mathscr{T}_P$. Equivalently, every trajectory $\tilde{x}(.)$ which is issued from an initial state $\tilde{x}_0$ lying in the projection $\mathscr{P}_P \stackrel{\Delta}{=} \{\xi \in \mathbb{R}^{n+m} : \exists \xi_f \in [0; x_{f0}],\ (\xi', \xi_f)' \in \mathscr{T}_P\}$ of $\mathscr{T}_P$ onto the space of the vectors $\tilde{x}$, remains in $\mathscr{P}_P$. Then, the boundedness assumption (11) of Lemma 3.4 and the other specifications are guaranteed by constricting the set $\mathscr{P}_P$ to an admissible area of the $\tilde{x}$-space. As shown in Figure 15, the so obtained invariant set $\mathscr{P}_P$ can be asymmetric w.r.t. the origin, thus circumventing some sources of conservatism.

This whole section still assumes that $\Phi(x) = x$ in (7). The sets Ξ_f and $\mathscr{A}_{\zeta_j}$ keep their former definitions, except that the parallelotope $\Xi_f = \prod_{i=1}^{n} [\underline{x}_i; \overline{x}_i]$ includes 0 but is not necessarily symmetric. While $\tilde{\Xi}_f$ still stands for $\Xi_f \times \mathbb{R}^m$, the augmented parallelotope $\tilde{\Xi}_a$ is defined as $\tilde{\Xi}_a \stackrel{\Delta}{=} \Xi_f \times \mathbb{R}^m \times \mathbb{R}$.

5.2.2 Implication on analysis

Let the genuine closed-loop system (7) be globally linearized under Hypothesis 3.4. If the consequent normalized SNLDI is put into the form of (15), then the following SNLDI can be got for the augmented

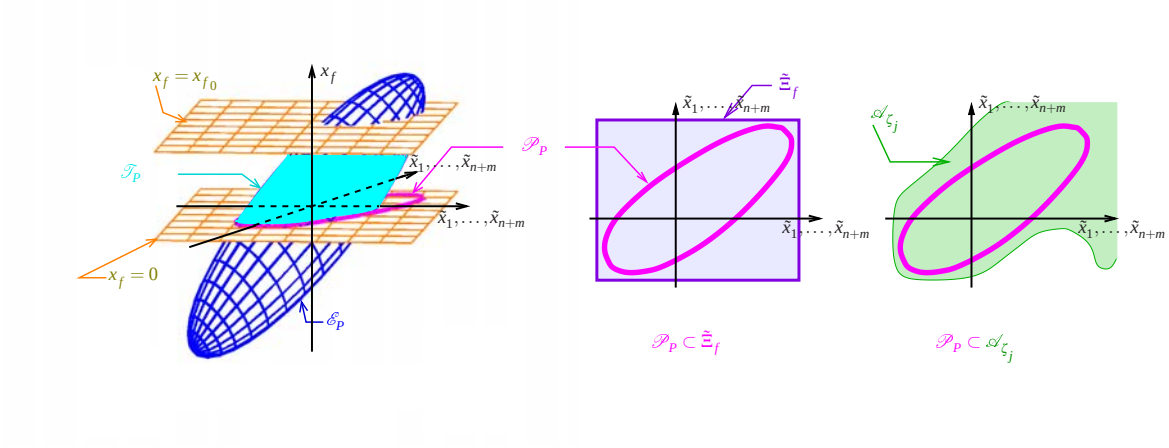

Figure 15: Method for analysis and synthesis based on the definition of an asymmetric invariant set – Basics

closed-loop system:

$$\begin{pmatrix} \dot{\tilde{x}}_a \\ \tilde{q}_a \end{pmatrix} = \begin{pmatrix} \tilde{A}_a & \tilde{B}_{pa} \\ \tilde{C}_{qa} & \tilde{D}_{qpa} \end{pmatrix} \begin{pmatrix} \tilde{x}_a \\ \tilde{p}_a \end{pmatrix}, \; \tilde{p}_a = \Delta \tilde{q}_a \tag{42}$$

$$\text{with} \qquad \Delta \in \blacktriangle(r), \; r = (r_1,\ldots,r_{\mathsf{N}})', \; \tilde{p}_a = \tilde{p}, \; \tilde{q}_a = \tilde{q},$$
$$\tilde{A}_a = \begin{pmatrix} \tilde{A} & 0 \\ 0 & -\alpha_f \end{pmatrix}, \; \tilde{B}_{pa} = \begin{pmatrix} \tilde{B}_p \\ 0_{(1;n_p(r))} \end{pmatrix}, \; \tilde{C}_{qa} = \begin{pmatrix} \tilde{C}_q & 0_{(n_p(r);1)} \end{pmatrix}, \; \tilde{D}_{qpa} = \tilde{D}_{qp}.$$

A Convergence of the camera to the reference situation

A.1 Global asymptotic stability of the SNLDI (42) **and satisfaction of the well-posedness assumption** (12) An application of the results developed in § 4.2.1 enables to conclude that the quadratic stability and the well-posedness of the SNLDI (42) are ensured if

$$\exists\, P>0,\; S\in\mathscr{S}(r),\; G\in\mathscr{G}(r),\; \begin{pmatrix} \tilde{A}_a'P + P\tilde{A}_a + \tilde{C}_{qa}'S\tilde{C}_{qa} & P\tilde{B}_{pa} + \tilde{C}_{qa}'S\tilde{D}_{qpa} + \tilde{C}_{qa}'G \\ \star & \tilde{D}_{qpa}'S\tilde{D}_{qpa} - S + \tilde{D}_{qpa}'G + G'\tilde{D}_{qpa} \end{pmatrix} < 0. \tag{43}$$

As the matrix $\tilde{A}_a$ depends linearly on α_f, the matrix inequality (43) is an LMI (resp. a BMI) when α_f is fixed (resp. when α_f is a decision variable.)

A.2 Satisfaction of the boundedness assumption (11) Define $\overline{x}_{0i} \overset{\Delta}{=} \frac{\overline{x}_i + \underline{x}_i}{2}$, $\overline{x}_{\omega i} \overset{\Delta}{=} \frac{\overline{x}_i - \underline{x}_i}{2}$, $W_i \overset{\Delta}{=} \mathrm{col}_i(I_{n+m})$, and let the matrix P be decomposed into $P = \begin{pmatrix} P_1 & P_2 \\ \star & P_3 \end{pmatrix}$, with $P_1 \in \mathbb{R}^{(n+m)\times(n+m)}$, $P_2 \in \mathbb{R}^{(n+m)\times 1}$, $P_3 \in \mathbb{R}^{+*}$. The constraint $\mathscr{P}_P \subset \tilde{\Xi}_f$, or equivalently $\mathscr{T}_P \subset \tilde{\Xi}_a$, which ensures the

boundedness assumption during the building of the SNLDI (42), is satisfied if:

$$\exists\ \tau_1 \in \mathbb{R}^{+*}, \tau_{f_1} \in \mathbb{R}^{+*}, \ldots, \tau_n \in \mathbb{R}^{+*}, \tau_{f_n} \in \mathbb{R}^{+*},$$
$$\forall i = 1, \ldots, n, \begin{pmatrix} \tau_i W_i W_i' - P_1 & -P_2 & -\tau_i W_i \overline{x}_{0i} \\ \star & -P_3 - \tau_{f_i} & \tau_{f_i} \frac{x_{f_0}}{2} \\ \star & \star & \tau_i(\overline{x}_{0i}^2 - \overline{x}_{\omega i}^2) + 1 \end{pmatrix} \leq 0. \tag{44}$$

The matrix inequalities (44) is are linear (resp. bilinear) in the decision variables when x_{f_0} is fixed (resp. when x_{f_0} is itself a decision variable.) The proof is given in Appendix B.5.

B *A priori* knowledge about the initial sensor-target relative situation The convergence of the camera is ensured from the initial sensor-target situation x_0 (resp. from every initial sensor-target situation in $\mathscr{E}_0 \stackrel{\Delta}{=} \{\xi \in \mathbb{R}^n : \xi = x_0 + Ez,\ z'z \leq 1\}$) if the "slice" $\mathscr{T}_P$ encloses the initial state vector $\tilde{x}_{a_0} \stackrel{\Delta}{=} (x_0', 0'_{(m;1)}, x_{f_0})' \in \mathbb{R}^{(n+m+1)}$ of the augmented closed-loop system (resp. encloses $\tilde{\mathscr{E}}_{a_0} \stackrel{\Delta}{=} \{\xi \in \mathbb{R}^{(n+m+1)} : \xi = \tilde{x}_{a_0} + \tilde{E}_a z,\ z'z \leq 1\}$ with $\tilde{E}_a \stackrel{\Delta}{=} \begin{pmatrix} E & 0_{(n;m+1)} \\ 0_{(m+1;n)} & 0_{(m+1;m+1)} \end{pmatrix} \in \mathbb{R}^{(n+m+1)\times(n+m+1)}$.) Because of the boundedness of the last entry of $\tilde{x}_{a_0}$, the "slice" $\mathscr{T}_P$ encloses the admissible initial states if and only if $\mathscr{E}_P$ does so. A necessary and sufficient condition for $\tilde{x}_{a_0} \in \mathscr{E}_P$ (resp. $\tilde{\mathscr{E}}_{a_0} \subset \mathscr{E}_P$) comes from § 4.2.2 as the matrix inequality on P (resp. on τ_0 and P)

$$\tilde{x}_{a_0}' P \tilde{x}_{a_0} - 1 \leq 0. \quad \left(\text{resp. } \exists\ \tau_0 \in \mathbb{R}^+, \begin{pmatrix} \tilde{E}_a' P \tilde{E}_a - \tau_0 I_{n+m+1} & \tilde{E}_a' P \tilde{x}_{a_0} \\ \star & \tilde{x}_{a_0}' P \tilde{x}_{a_0} - 1 + \tau_0 \end{pmatrix} \leq 0. \right) \tag{45}$$

Note that these equations —which are LMIs (resp. BMIs) if x_{f_0} is fixed (resp. a decision variable)— return to enclose $\tilde{x}_{a_0}$ or $\tilde{\mathscr{E}}_{a_0}$ by the intersection of $\mathscr{E}_P$ with the subspace $\{\xi \in \mathbb{R}^{(n+m+1)} : \xi_{n+1} = \ldots = \xi_{n+m} = 0,\ \xi_{n+m+1} = x_{f_0}\}$.

C Constraints of the type $\zeta_j \in [-\overline{\zeta}_j; \overline{\zeta}_j]$ As previously outlined, each constraint of this kind is taken into account by making $\mathscr{P}_P$ lie into an admissible set $\mathscr{A}_{\zeta_j}$ defined in the $\tilde{x}$-space, or equivalently, by making $\mathscr{T}_P$ lie into $\mathscr{A}_{a_{\zeta_j}} \stackrel{\Delta}{=} \mathscr{A}_{\zeta_j} \times \mathbb{R}$. A reasoning similar to § 5.2.2-A.2 is used to handle constraints like $\zeta_j = Z_{\zeta_j}\tilde{x} \in [-\overline{\zeta}_j; \overline{\zeta}_j]$, leading to the sufficient condition

$$\exists\ \tau_{\zeta_j} \in \mathbb{R}^{+*},\ \tau_{\zeta_{fj}} \in \mathbb{R}^+, \begin{pmatrix} \tau_{\zeta_j} Z_{\zeta_j}' Z_{\zeta_j} - P_1 & -P_2 & 0 \\ \star & -\tau_{\zeta_{fj}} - P_3 & \tau_{\zeta_{fj}} \frac{x_{f_0}}{2} \\ \star & \star & -\tau_{\zeta_j} \overline{\zeta}_j^2 + 1 \end{pmatrix} \leq 0. \tag{46}$$

To deal with constraints like $\zeta_j = Z_{\zeta_j}(\tilde{x})\tilde{x} \in [\underline{\zeta}_j; \overline{\zeta}_j]$, two different methods were developed in § 4.2.4. The matrix inequality (24) obtained through the first method —viz. the global linearization of

$\zeta_j = Z_{\zeta_j}(\tilde{x})\tilde{x}$— here becomes

$$\exists\ \tau_\zeta \in \mathbb{R}^{+*},\ \tau_{\zeta f} \in \mathbb{R}^{+},\ S_\zeta \in \mathscr{S}(r_\zeta),\ G_\zeta \in \mathscr{G}(r_\zeta),\ \tau_\zeta M_{1a} + M_{2a} - M_{0a} + \tau_{\zeta f} M_{3a} < 0, \tag{47}$$

$$\text{with } M_{0a} = \begin{pmatrix} P_1 & P_2 & 0 & 0 \\ \star & P_3 & 0 & 0 \\ \star & \star & 0 & 0 \\ \star & \star & \star & -1 \end{pmatrix},\ M_{1a} = \begin{pmatrix} \tilde{C}'_\zeta \tilde{C}_\zeta & 0 & \tilde{C}'_\zeta \tilde{D}_{p_\zeta} & -\tilde{C}'_\zeta \hat{\xi}_j \\ \star & 0 & 0 & 0 \\ \star & \star & \tilde{D}'_{p_\zeta} \tilde{D}_{p_\zeta} & -\tilde{D}'_{p_\zeta} \hat{\xi}_j \\ \star & \star & \star & \hat{\xi}_j^2 - \tilde{\xi}_j^2 \end{pmatrix},\ M_{3a} = \begin{pmatrix} 0 & 0 & 0 & 0 \\ \star & -1 & 0 & \frac{x_{f_0}}{2} \\ \star & \star & 0 & 0 \\ \star & \star & \star & 0 \end{pmatrix},$$

$$M_{2a} = \begin{pmatrix} \tilde{C}'_{q_\zeta} S_\zeta \tilde{C}_{q_\zeta} & 0 & \tilde{C}'_{q_\zeta} S_\zeta \tilde{D}_{qp_\zeta} + \tilde{C}'_{q_\zeta} G_\zeta & 0 \\ \star & 0 & 0 & 0 \\ \star & \star & \tilde{D}'_{qp_\zeta} S_\zeta \tilde{D}_{qp_\zeta} - S_\zeta + \tilde{D}'_{qp_\zeta} G_\zeta + G'_\zeta \tilde{D}_{qp_\zeta} & 0 \\ \star & \star & \star & 0 \end{pmatrix}.$$

In addition, the matrix inequalities (25) obtained through the inner approximation of $\mathscr{A}_{\zeta_j}$ by quadratic functions must be replaced by

$$\exists\ \tau^1_{\zeta_j} \in \mathbb{R}^{+*}, \tau^1_{\zeta f} \in \mathbb{R}^{+}, \ldots, \tau^{l_{\zeta_j}}_{\zeta_j} \in \mathbb{R}^{+*}, \tau^{l_{\zeta_j}}_{\zeta f} \in \mathbb{R}^{+},$$

$$\forall k = 1, \ldots, l_{\zeta_j},\ \tau^k_{\zeta_j} \begin{pmatrix} \tilde{V}^k_{\zeta_j} & 0 & \tilde{F}^{k'}_{\zeta_j} \\ \star & 0 & 0 \\ \star & \star & \beta^k_{\zeta_j} \end{pmatrix} - \begin{pmatrix} P_1 & P_2 & 0 \\ \star & P_3 & 0 \\ \star & \star & -1 \end{pmatrix} + \tau^k_{\zeta f} \begin{pmatrix} 0 & 0 & 0 \\ \star & -1 & \frac{x_{f_0}}{2} \\ \star & \star & 0 \end{pmatrix} \leq 0. \tag{48}$$

As is the case for (44), the matrix inequalities (46), (47) and (48) are LMIs (resp. BMIs) when x_{f0} is fixed (resp. when x_{f0} is a decision variable.) Their proof is straightforward, using some arguments similar to these mentioned in Appendix B.5 concerning the proof of § 5.2.2-A.2.

5.2.3 Synthesis of a linear static state feedback $u = K_a \tilde{x}_a$

When the synthesis of such a control is of concern, the normalized SNLDI (42) into which the augmented closed-loop system is embedded has the form, $x_a \stackrel{\Delta}{=} (x', x_f)'$ being the augmented open-loop state vector,

$$\begin{pmatrix} \dot{x}_a \\ q \end{pmatrix} = \begin{pmatrix} A_a + B_{ua} K_a & B_{pa} \\ D_{qua} K_a & D_{qpa} \end{pmatrix} \begin{pmatrix} x_a \\ p \end{pmatrix},\ p = \Delta q \tag{49}$$

$$\text{with } \Delta \in \blacktriangle(r),\ A_a = \begin{pmatrix} 0 & 0 \\ 0 & -\alpha_f \end{pmatrix},\ B_{ua} = \begin{pmatrix} B_u \\ 0_{(1;n_u)} \end{pmatrix},\ B_{pa} = \begin{pmatrix} B_p \\ 0_{(1;n_p(r))} \end{pmatrix}, D_{qua} = D_{qu},\ D_{qpa} = D_{qp}.$$

The remarks made at the beginning of § 4.3 concerning Ξ_f, $\tilde{\Xi}_f$, B_u, B_p, D_{qu}, D_{qp}, p, q and Δ still hold, though under the noticeable assumption that $\Xi_f = \prod_{i=1}^{n} [\underline{x}_i; \overline{x}_i]$ is a nonnecessarily symmetric parallelotope including 0.

A Comments concerning the control law $u = Kx$ Following the same reasoning as in § 4.3.1-A, the following matrix inequality is sufficient for the quadratic stability and the well-posedness of the SNLDI (49):

$$\exists\, Q > 0,\ K_a = (K, 0_{(n_u;1)}) \text{ with } K \in \mathbb{R}^{n_u \times n},\ T \in \mathscr{S}(r),\ H \in \mathscr{G}(r),$$
$$\begin{pmatrix} A_aQ + QA_a^{'} + B_{pa}TB_{pa}^{'} + B_{ua}K_aQ + QK_a^{'}B_{ua}^{'} & B_{pa}TD_{qpa}^{'} + QK_a^{'}D_{qua}^{'} + B_{pa}H \\ \star & D_{qpa}TD_{qpa}^{'} - T + D_{qpa}H + H^{'}D_{qpa}^{'} \end{pmatrix} < 0. \qquad (50)$$

This is a BMI. In § 4.3.1-A, a similar inequality could be turned into an LMI through the change of variable $Y = K_aQ$, and the state feedback gain K_a was then deduced from the solution of this LMI by $K_a = YQ^{-1}$. Unfortunately, in the present case, such a change of variable cannot be performed because of the above structure of K_a. The synthesis of a control $u = Kx$ will henceforth be left apart, i.e. the control variable u will also depend on the fictitious variable x_f so that the feedback gain $K_a \in \mathbb{R}^{n_u \times (n+1)}$ has no prescribed structure.

B Convergence of the camera to the reference situation

B.1 Global asymptotic stability of the SNLDI (49) **and satisfaction of the well-posedness assumption** (12) The aforementioned change of variable turns the sufficient condition (50) for the quadratic stability and the well-posedness of the SNLDI (49) into

$$\exists\, Q > 0,\ Y \in \mathbb{R}^{n_u \times (n+1)},\ T \in \mathscr{S}(r),\ H \in \mathscr{G}(r),$$
$$\begin{pmatrix} A_aQ + QA_a^{'} + B_{pa}TB_{pa}^{'} + B_{ua}Y + Y^{'}B_{ua}^{'} & B_{pa}TD_{qpa}^{'} + Y^{'}D_{qua}^{'} + B_{pa}H \\ \star & D_{qpa}TD_{qpa}^{'} - T + D_{qpa}H + H^{'}D_{qpa}^{'} \end{pmatrix} < 0, \qquad (51)$$

which is an LMI on Q, Y, T and H when the value of α_f is fixed, and a BMI on Q, Y, T, H and α_f otherwise. Of course, $K_a = YQ^{-1}$ follows.

B.2 Satisfaction of the boundedness assumption (11) As the matrix inequality (51) is expressed in terms of $Q = P^{-1}$, an equivalent formulation of the sufficient condition (44) for the boundedness assumption is sought for, which does not explicitely involve the variable P. Yet, such an equivalent formulation would remain bilinear in the decision variables. So, the LMI (44) is still united to (51), along with the nonconvex constraint $PQ = I$. As P and Q are positive definite, this last constraint is equivalent to the conjunction of an LMI on P and Q together with a rank constraint, namely,

$$\mathscr{K}(P,Q) = \begin{pmatrix} P & I_{n+1} \\ I_{n+1} & Q \end{pmatrix} \geq 0,\ \operatorname{rank} \mathscr{K}(P,Q) = n+1. \qquad (52)$$

The set of matrix inequalities {(51),(44),(52)} is a Cone Complementarity Problem, which can be efficiently solved with the algorithm [16] of El Ghaoui, Oustry and Ait-Rami.

C *A priori* knowledge about the initial sensor-target relative situation As for analysis, the constraint $x_{a0} \in \mathscr{T}_P$ or $\tilde{\mathscr{E}}_0 \subset \mathscr{T}_P$ is ensured by the matrix inequality (45) on P. To improve the convergence of the cone complementarity linearization algorithm [16], an equivalent formulation of this constraint in terms of Q is introduced, which has the form of (29):

$$\begin{pmatrix} -1 & x_{a0}' \\ \star & -Q \end{pmatrix} \leq 0 \quad \left(\text{resp. } \exists\, \sigma_0 \in \mathbb{R}^+, \begin{pmatrix} -\sigma_0 I_{n+1} & 0_{(n+1;1)} & \tilde{E}_a' \\ \star & \sigma_0 - 1 & x_{a0}' \\ \star & \star & -Q \end{pmatrix} \leq 0 \right). \tag{53}$$

D Avoidance of the actuators saturations and Constraints $\zeta_j = Z_{\zeta_j}(\tilde{x})\tilde{x} \in [\underline{\zeta}_j; \overline{\zeta}_j]$ The j^{th} constraint on the actuators is satisfied by means of the condition $\mathscr{T}_P \subset \mathscr{A}_{au_j}$, with $\mathscr{A}_{au_j} \overset{\Delta}{=} \{\xi \in \mathbb{R}^{n+1} : \xi' K_a' W_j W_j' K_a \xi \leq \overline{u}_j^2\}$. Though less restrictive, this condition does not lead to LMIs. So, $\mathscr{E}_P \subset \mathscr{A}_{au_j}$ is considered instead, which leads to LMIs similar to (30), except that Q and Y are matrices of $\mathbb{R}^{(n+1)\times(n+1)}$ and $\mathbb{R}^{n_u \times (n+1)}$, respectively.

The constraints $\zeta_j = Z_{\zeta_j}(\tilde{x})\tilde{x} \in [\underline{\zeta}_j; \overline{\zeta}_j]$ are ensured by the matrix inequalities (47)/(48).

5.2.4 Synthesis of a nonlinear static state feedback

In the same vein as in § 4.4, the aim is to synthesize the parameters K_a and K_p of the nonlinear state feedback

$$u = \left(K_a + K_p \Delta(x) \left(I - (D_{qp} + D_{qu} K_p)\Delta(x) \right)^{-1} D_{qu} K_a \right) x_a. \tag{54}$$

For the reasons mentioned in § 5.2.3-A, the matrix $K_a \in \mathbb{R}^{n_u \times (n+1)}$ has no predefined structure, i.e. the control signal u also depends on the fictitious variable x_f.

Similarly to § 4.4.1-A, the changes of variables $Y = K_a Q$ and $Y_2 = K_p T$ can exhibit the following condition for the global asymptotic —quadratic— stability and well-posedness of the SNLDI into which the augmented closed-loop system is embedded:

$$\begin{gathered} \exists\, Q > 0,\ Y \in \mathbb{R}^{n_u \times (n+1)},\ Y_2 \in \mathbb{R}^{n_u \times n_p(r)},\ T \in \mathscr{S}(r), \\ \begin{pmatrix} A_a Q + Q A_a' + Y' B_{ua}' + B_{ua} Y & B_{pa} T + B_{ua} Y_2 & Y' D_{qua}' \\ \star & -T & T D_{qpa}' + Y_2' D_{qua}' \\ \star & \star & -T \end{pmatrix} \leq 0. \end{gathered} \tag{55}$$

The boundedness assumption is ensured in the same way as in § 5.2.3-B.2. The set of matrix inequalities {(55),(44),(52)} is a Cone Complementarity Problem, which can be efficiently solved with the algorithm of El Ghaoui, Oustry and Ait-Rami [16].

The *a priori* knowledge about the initial sensor-target situation is taken into account through the LMIs of § 5.2.3-C.

As in § 5.2.3-D for the synthesis of a linear state feedback, ensuring the j^{th} constraint on the actuators by means of the condition $\mathscr{T}_P \subset \mathscr{A}_{a_{u_j}}$ does not lead to LMIs. Likewise, $\mathscr{E}_P \subset \mathscr{A}_{a_{u_j}}$ is considered instead, which leads to LMIs similar to (37), except that the dimensions of Q, Y have changed, $\{D_{qu}, D_{qp}\}$ are replaced by $\{D_{qua}, D_{qpa}\}$, and T is the decision variable involved in (55).

At last, the constraints $\zeta_j = Z_{\zeta_j}(\tilde{x})\,\tilde{x} \in [\underline{\zeta}_j; \overline{\zeta}_j]$ are ensured by the matrix inequalities (47)/(48).

5.2.5 Application to Case Study #1

The above results are applied to the case study which was first considered in § 4.5.1. The criteria are unchanged, except that a tighter 2D constraint is considered. The bounds of the virtual image plane corresponding to a unit focal length $f = 1$ are set to $-\underline{X} = \overline{X} = 0.3\,\text{m}$ and $-\underline{Y} = \overline{Y} = 0.25\,\text{m}$. The initial state $x_0 = (2.06, 4.79, 0.46)'$ is selected so that the camera starts in the vicinity of a wall, fairly far from the target.

When the aim is to synthesize a linear static state feedback $u = K_a \tilde{x}_a$, the SNLDI into which the augmented closed-loop system is embedded is defined under the boundedness assumption $\Xi_f = [\underline{t_y}; \overline{t_y}] \times [\underline{t_z}; \overline{t_z}] \times [\underline{L}; \overline{L}]$ with $\overline{t_y} = 2.2\,\text{m}$, $\underline{t_y} = -0.21\,\text{m}$, $\overline{t_z} = 4.9\,\text{m}$, $\underline{t_z} = -0.3\,\text{m}$, $\overline{L} = 0.49$ and $\underline{L} = -0.02$. Further, selecting $x_{f0} = 0.51$ and $\alpha_f = 0.14$ and solving the problem with the MATLAB LMI Control Toolbox leads to the controller $K_a = \begin{pmatrix} 7.38 & -5.23 & 35.89 & -12.86 \\ -6.74 & 9.18 & -36.51 & -24.03 \\ -5.51 & -0.84 & 65.69 & -29.65 \end{pmatrix}$.

The corresponding camera 3D trajectory is shown in Figure 16. The settling time is about 25 s. The admissible sets represented in Figures 17–18 do enclose the invariant set $\mathscr{P}_P$. Thanks to the asymmetry of $\mathscr{P}_P$, the initial sensor-target situation x_0 can be taken into account despite the 2D constraints are violated at $-x_0$. Nevertheless, as the set $\mathscr{A}_{3D}$ in which the 3D constraints are satisfied is nonconvex while the invariant set $\mathscr{P}_P$ defined by this extension remains convex, some initial relative situations x_0 lying in $\mathscr{A}_{3D}$ cannot be taken into account as soon as γx_0 leaves $\mathscr{A}_{3D}$ for at least one γ in $[0;1]$.

The solution of the problem can even be improved by synthesizing a nonlinear static state feedback of the form (54). Selecting a slightly different parallelotope Ξ_f for the definition of the embedding SNLDI as well as different values for x_{f0} and α_f, leads to a 15 s settling time thanks to a "tighter" fit of $\mathscr{P}_P$ into the admissible sets, see [1].

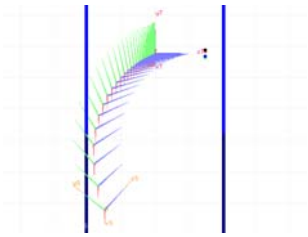

Figure 16: $u = K_a\tilde{x}_a$: Upper view of the 3D camera motion (1 frame/s)

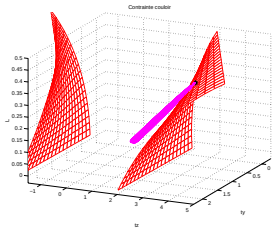

Figure 17: $u = K_a\tilde{x}_a$: Satisfaction of the 3D constraint by the invariant set $\mathscr{P}_P$

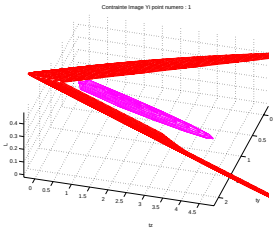

Figure 18: $u = K_a\tilde{x}_a$: Satisfaction of the 2D constraint on Y_1 by the invariant set $\mathscr{P}_P$

5.3 Strengths and weaknesses of the extensions

The analysis method proposed in § 5.1 can partly reduce the global linearization conservatism through the definition in STEP 2 of small-sized parallelotopes Π. As it puts some set relationships only on parts of the used ellipsoids $\mathscr{E}_P$, all the former problems induced by the symmetry or the convexity of these ellipsoids are circumvented. An interesting point is that this feature is obtained with no increase in the complexity of the consequent LMI feasibility/optimization problems. Unfortunately, these results seem difficult to use for the multicriteria analysis of visual feedbacks of order higher than three, and cannot be trivially extended to the synthesis.

The approach described in § 5.2 seems somewhat more generic, in that it can be applied to analysis or synthesis, even for higher-order visual feedbacks. By putting constraints on the invariant slice $\mathscr{T}_P$ or its projection $\mathscr{P}_P$, it enables the reduction of the conservatism coming from the symmetry w.r.t. 0 of ellipsoidal invariant sets. However, as was the case in § 4, this technique is limited by the fact that $\mathscr{P}_P$ is convex. Lastly, the complexity of the consequent feasibility/optimization problems can be strongly influenced, depending on whether (i) (x_{f0}, α_f) are parameters or decision variables, and (ii) x_f is a controller input or not.

6 Related developments

Other Matrix Inequalities, still rooted in the work of El Ghaoui and co-authors, were developed for this multicriteria visual servocontrol problem. Due to space reasons, they are not included in this paper. The reader is referred to [11, 1].

The synthesis of an interesting class of nonlinear rational static state feedback controllers is a tractable

problem. Its application to Case Study #1 enables a 40 % reduction of the settling time compared to § 5.2.5 [11, 1].

The synthesis of output feedback controllers leads to difficult —nonconvex— problems entailing BMIs. Yet, if the scaling matrix G involved in the outer approximation of the closed-loop SNLDI is set to $G = 0_{(n_p(r);n_p(r))}$ —thus inducing some conservatism—, then a solution enjoying nice tractability properties remains theoretically possible. Indeed, an application of the elimination lemma leads to a Cone Complementarity Problem ensuring the existence of a stabilizing controller. The controller further follows from the solution of an LMI problem [13], which can straightly take into account 3D and 2D constraints. Dealing with the actuators saturations still raises very sharp issues if LMIs are sought [1]. All these properties hold when the approach is extended following the guidelines of § 5.2.

A similar tradeoff between tractability and conservatism occurs when the aim is to synthesize a gain-scheduled output controller. However, this case shows three main differences [18, 13, 1]: the consequent problem may get convex, putting contraints on the actuators is easier, and a "pseudo-invariance" property is refered to when dealing with 2D and 3D constraints.

As already noticed —e.g. in § 4.6—, the above method may fail because of well-posedness issues when 2D servos are considered, and/or if 2D constraints are handled through Theorem 4.2 or 4.4. The selection of the mappings $\Phi(.)$ and $\Phi_{\zeta_j}(.)$ in the LFTs (10) and (16) is of paramount importance, and defining them as the identity function is often inappropriate. Instead, a convenient choice should be so that bounding $\Phi(\xi)$ (resp. $\Phi_{\zeta_j}(\xi)$) by a parallelotope Ξ would enable ξ to lie into a tighter subset Ξ_f of a connected component of the set $\mathscr{O}$ onto which (10) (resp. (16)) is well-posed. This is a tricky problem, all the more because the entries of $\Phi(.)$ (resp. $\Phi_{\zeta_j}(.)$) should be kept independent of each other, see § 3.4.

Even when considering such modifications along with the arguments developed in § 5.2, the synthesis of 2D servos has seemed to lead to a blind alley when $G = 0_{(n_p(r);n_p(r))}$. Like in the "easier" state feedback synthesis problem considered in Case Study #1 of § 4.6, the high conservatism induced by this setting of G often prevents the feasibility of the consequent LMI problem or the meaningfulness of its solution.

7 Conclusion

A generic framework has been proposed to the multicriteria analysis and synthesis of kinematic visual-based positioning schemes. A basic "standard" problem has been stated, through the definition of a rational state space representation including uncertainties, if any. The interest of such a formulation is that the problem is not limited to the stabilization part, by the very fact that various criteria —e.g. actuators, 2D or 3D constraints— can be handled through rational additional variables. Thanks to a global linearization step, the problem has been dealt with in the robust linear control framework. Yet, the mere application of

existing robust control results has proved unsatisfactory. The sources of failures have been analyzed, and two extensions have been proposed to partly reduce the conservatism coming from the applicative domain.

The proposed open-loop model shows several potentialities, mainly, a statement of the convergence problem relying upon a sound definition of a state vector, some versatility in handling the criteria, and an ease of enrichment so as to take account of unmodeled properties —see § 2.3. Moreover, it enables a "control system" approach to visual-based localization. Indeed, this last problem can be tackled as the "dual" —in the sense of duality between control and estimation— of visual servoing, in that it consists in estimating/forecasting the relative camera-target situation from the knowledge of the visual data and of the camera command input. An LMI solution has been proposed in [4] based on a slight extension of the results of El Ghaoui and Calafiore [15]. A rational discrete-time open-loop model is set up under zero order hold (ZOH) hypothesis. Its global linearization leads to a Structured Norm-Bounded Recursive Inclusion, so that some "dual" robust filtering techniques apply.

The suggested modeling, however, show several drawbacks. The concealment of the difference between 3D and 2D methodologies into its mathematical structure may induce a loss of intuition compared with other approaches to visual servoing. Moreover, through the used control framework, it makes the synthesis of 2D servos a difficult —nonconvex— problem, which is a severe limitation. To open up a possibility of success, the solution of the raw BMIs for output feedback synthesis could be checked as well as the selection of another rational open-loop model which "bridges the gap" with existing work, e.g. by redefining the visual features or by deliberately disregarding the sensor-target relative situation. Note that the extensions of § 5 may remain useful so as to get rid of the symmetry and convexity properties of the Lyapunov level sets, and that the avoidance of local minima may need special attention.

Significantly better results might be got concerning the synthesis of gain-scheduled output feedbacks, e.g. by enhancing the approach of [38] by the recent work of Scherer [37]. More generally, still in the context of SNLDIs, it would be worth finding LMI relaxations so as to enable the parameters Φ lie into more general sets —e.g., in an ellipsoid rather than in a parallelotope—, to investigate alternate choices of Lyapunov functions, or to allow actuators saturations rather than avoiding them. This last topic is particularly relevant in the kinematic context, for in this case it is likely that a saturated control enlarges the convergence region.

As an overall conclusion, the proposed methods can be helpful for the analysis of any visual-based controller and for the synthesis of 3D servos. Due to their potential conservatism, the synthesis methods might better express themselves —included for 2D servos— when used to propose a systematic tuning of existing controllers, e.g. to select a parameter $\widehat{z^*}$ which can bestow nice properties to the inverse static Jacobian controller $u = -\lambda\,[J(s^*,\widehat{z^*})]^+ y$ seen in Case Study #2, in the vein of [31].

An ongoing work aims at keeping in this robotics context the powerful LMI framework for the analysis and synthesis of control systems. A new LMI approach to the analysis and synthesis of rational systems using biquadratic and polyquadratic Lyapunov functions is being assessed [12]. Homogeneous Polynomial Lyapunov functions as introduced in [7] are planned to be checked as well. Insights gained from works developed in the visual servoing community —e.g. concerning the choice of the visual features, the vector space in which the problem is stated, etc.— will then be included. The aim is obviously to limit the conservatism, so that a multicriteria LMI-based strategy can soon be versatile enough to be embedded on a real robot.

References

[1] D. Bellot. *Contribution à l'analyse et à la synthèse de schémas de commande référencés vision*. Ph.D. thesis (in french), Université Paul Sabatier, LAAS-CNRS, December 2002. Available at `http://www.laas.fr/~danes/RESEARCH/VS/thesisBELLOT.pdf`.

[2] D. Bellot and P. Danès. Handling visual servoing schemes through rational systems and LMIs. In *40th IEEE Conference on Decision and Control (CDC'01)*, pages 3601–3606, Orlando, FL, December 2001.

[3] D. Bellot and P. Danès. Towards an LMI approach to multicriteria visual servoing. In *European Control Conference (ECC'01)*, pages 2930–2935, Porto, Portugal, September 2001.

[4] D. Bellot and P. Danès. An LMI solution to visual-based localization as the dual of visual servoing. In *42nd IEEE Conference on Decision and Control (CDC'03)*, pages 5420–5425, Maui, HI, December 2003.

[5] S. Boyd, L. El Ghaoui, E. Feron, and V. Balakrishnan. *Linear Matrix Inequalities in System and Control Theory*. SIAM, 1994.

[6] F. Chaumette. Potential problems of stability and convergence in image-based and position-based visual servoing. In *The confluence of Vision and Control, LNCIS series*, volume 237, pages 66–78. Springer-Verlag, 1998.

[7] G. Chesi, A. Garulli, A. Tesi, and A. Vicino. Robust analysis of LFR systems through homogeneous lyapunov functions. *IEEE Transactions on Automatic Control*, 49(7):1211–1216, 2004.

[8] G. Chesi and A. Vicino. Visual servoing for large camera displacements. *IEEE Transactions on Robotics*, 20(4):724–735, August 2004.

[9] P.I. Corke and S.A. Hutchinson. A new partitioned approach to image-based visual servo control. *IEEE Transactions on Robotics and Automation*, 17(4):507–515, August 2001.

[10] N.J. Cowan, J.D. Weingarten, and D.E. Koditschek. Visual servoing via navigation functions. *IEEE Transactions on Robotics and Automation*, 18(4):521–533, August 2002.

[11] P. Danès and D. Bellot. Towards an LMI approach to multicriteria visual servoing in robotics — Companion report. Technical Report 05085, LAAS-CNRS, 2005. Available at `http://www.laas.fr/~danes/RESEARCH/VS/companionEJC2k5.pdf`.

[12] P. Danès and D.F. Coutinho. Multicriteria analysis of visual servos via biquadratic lyapunov functions. In *5th Symposium on Robust Control Design (ROCOND'06)*, Toulouse, France, September 2005. IFAC.

[13] S. Dussy. *Approche LMI de la commande robuste multicritère*. Thèse de doctorat de l'Université de Paris IX-Dauphine, UFR Mathématiques de la Décision, March 1998.

[14] S. Dussy and L. El Ghaoui. Measurement-scheduled control for the RTAC problem: an LMI approach. *International Journal of Robust and Nonlinear Control*, 8:377–400, 1998.

[15] L. El Ghaoui and G. Calafiore. Robust filtering for discrete-time systems with bounded noise and parametric uncertainty. *IEEE Transactions on Automatic Control*, 46(7), July 2001.

[16] L. El Ghaoui, F. Oustry, and M. Ait-Rami. A cone complementarity linearization algorithm for static output-feedback and related problems. *IEEE Transactions on Automatic Control*, 42(8):1171–1176, August 1997.

[17] L. El Ghaoui and G. Scorletti. Commande des systèmes rationnels par inégalités matricielles affines. In J. Bernussou, editor, *Commande robuste. Développements et applications*. Hermès, 1996.

[18] L. El Ghaoui and G. Scorletti. Control of rational systems using linear-fractional representations and linear matrix inequalities. *Automatica*, 32(9):1273–1284, 1996.

[19] B. Espiau, F. Chaumette, and P. Rives. A new approach to visual servoing in robotics. *IEEE Transactions on Robotics and Automation*, 8(3):313–326, June 1992.

[20] M.K.H. Fan, A.L. Tits, and J.C. Doyle. Robustness in the presence of mixed parametric uncertainty and unmodeled dynamics. *IEEE Transactions on Automatic Control*, 36(1):25–38, January 1991.

[21] P. Gahinet, A. Nemirovski, A. Laub, and M. Chilali. *LMI Control Toolbox*. The Mathworks Inc., 1995.

[22] J.A. Gangloff and M.F. de Mathelin. Visual servoing of a 6-DOF manipulator for unknown 3-D profile following. *IEEE Transactions on Robotics and Automation*, 18(4):511–520, August 2002.

[23] T. Hamel and R. Mahony. Visual servoing of an under-actuated dynamic rigid-body system: an image-based approach. *IEEE Transactions on Robotics and Automation*, 18(2), 2002.

[24] K. Hashimoto, editor. *Visual Servoing: Real Time Control of Robots Manipulators based on Visual Sensory Feedback*. World Scientific Series in Robotics and Automated Systems. World Scientific Press, Singapore, 1993.

[25] K. Hashimoto and H. Kimura. LQ optimal and nonlinear approches to visual servoing. In K. Hashimoto, editor, *Visual Servoing*, volume 7 of *World Scientific Series in Robotics and Automated Systems*, pages 165–198. World Scientific Press, 1993.

[26] R. Horaud, B. Conio, O. Leboulleux, and Lacolle B. An analytic solution for the perspective-4-point problem. In *Computer vision, Graphics, and Image Processing*, 1989.

[27] S. Hutchinson, G. D. Hager, and P. I. Corke. A tutorial on visual servo control. *IEEE Transactions on Robotics and Automation, Special issue on Visual Servoing*, 12(5):651–670, October 1996.

[28] R. Kelly. Robust asymptotically stable visual servoing of planar robots. *IEEE Transactions on Robotics and Automation*, 12(5):759–766, 1996.

[29] E. Malis and F. Chaumette. Theoretical improvements in the stability analysis of a new class of model-free visual servoing methods. *IEEE Transactions on Robotics and Automation*, 18(2):176–186, April 2002.

[30] E. Malis, F. Chaumette, and S. Boudet. $2\frac{1}{2}$2D visual servoing. *IEEE Transactions on Robotics and Automation*, 15(2):234–246, April 1999.

[31] E. Malis and P. Rives. Robustness of image-based visual servoing with respect to depth distribution error. In *IEEE International Conference on Robotics and Automation (ICRA'03)*, pages 1056–1061, Taipei, Taiwan, 2003.

[32] P. Martinet. Comparison of visual servoing techniques: Experimental results. In *IAPR Workshop on Machine vision Application, MVA'98*, pages 254–257, November 1998.

[33] Y. Mezouar and F. Chaumette. Optimal camera trajectory with image-based control. *International Journal of Robotics Research, Special Issue on Visual Servoing*, 22(10/11), 2003.

[34] N. P. Papanikolopoulos, B. Nelson, and P. K. Khosla. Six degre-of-freedom hand/eye visual tracking with uncertain parameters. *IEEE Transactions on Robotics and Automation*, 11(5):725–732, October 1995.

[35] M. Renaud. Comment définir l'orientation d'un corps? Technical Report 96078 (in french), LAAS-CNRS, March 1996.

[36] C. Samson, M. Le Borgne, and B. Espiau. *Robot Control: The Task Function Approach*. Clarendon Press, Oxford, 1991.

[37] C.W. Scherer. LPV control and full block multipliers. *Automatica*, 37:361–375, 2001.

[38] G. Scorletti and L. El Ghaoui. Improved LMI conditions for gain scheduling and related control problems. *International Journal of Robust and Nonlinear Control*, 8:845–877, 1998.

[39] M. Sznaier, B. Murphy, and O.I. Camps. An LPV approach to synthesizing robust active vision systems. In *Proceedings of the 39th IEEE Conference on Decision and Control*, pages 2545–2550, Sydney, Australia, December 2000.

[40] A. Tannenbaum. On the eye tracking problem: a challenge for robust control. *International Journal of Robust and Nonlinear Control*, 10:875–888, 2000. Special Issue in the memory of G. Zames.

[41] S. Tarbouriech and P. Souères. Advanced control strategy for the visual servoing scheme. *IFAC Symposium on Robot Control, SYROCO 2000*, 2:457–462, September 2000.

[42] B. Thuilot, P. Martinet, L. Cordesses, and J. Gallice. Position based visual servoing: keeping the object in the field of vision. In *IEEE International Conference on Robotics and Automation (ICRA'02)*, pages 1624–1629, 2002.

[43] P. Zanne, G. Morel, and F. Plestan. Robust 3D vision based control and planning. In *IEEE International Conference on Robotics and Automation (ICRA'04)*, pages 4423–4428, 2004.

[44] K. Zhou, J. Doyle, and K. Glover. *Robust and Optimal Control*. Englewood Cliffs, 1995.

A Development of the open-loop model (1)–(2)

Due to space reasons, only an outline of the computations is given.

Notations The equations of rigid body kinematics often entail so-called *extrinsic* quantities such as 3×1 vectors, 3×3 matrices, etc. Rather than handling such expressions directly, if is often convenient first writing equations which involve *intrinsic* quantities, i.e. mathematical entities whose meaning makes no assumption upon the basis in which they are expressed. Developments are therefore pursued as far as possible using intrinsic equations. The equations are projected on a selected basis at the end.

A *vector* $\overrightarrow{v}$ (resp. a *tensor* $\overrightarrow{\overrightarrow{T}}$) is an intrinsic mathematical entity whose extrinsic expression $(\overrightarrow{v})_{(F)}$ (resp. $(\overrightarrow{\overrightarrow{T}})_{(F)}$) in the canonical basis of a frame F [§] is a 3×1 *column vector* (resp. a 3×3 *matrix*.) $\overrightarrow{v}$ can term a position, a translational or rotational vector, etc. Mathematical operations —e.g. addition, scalar product, dot-product on vectors, cross-product on vectors, tensor-vector product, etc.— are then straightly defined upon intrinsic quantities through their extrinsic representations.

Performing the *time-derivation* of a vector $\overrightarrow{v}$ or of a tensor $\overrightarrow{\overrightarrow{T}}$ *with respect to a frame* F means that F is supposed time-invariant during the differentiation. The result is denoted $\left[\frac{\mathrm{d}(\overrightarrow{v})}{\mathrm{d}t}\right]_F$ or $\left[\frac{\mathrm{d}(\overrightarrow{\overrightarrow{T}})}{\mathrm{d}t}\right]_F$, respectively.

Among the main tensors are the *rotation tensor* and the *skew-symmetric tensor*. The rotation tensor $\overrightarrow{\overrightarrow{\mathscr{R}}}_{F_S//F_O}$ characterizes the relative attitude of F_S w.r.t. F_O. Its extrinsic expression in F_O reads as

$$\left(\overrightarrow{\overrightarrow{\mathscr{R}}}_{F_S//F_O}\right)_{(F_O)} = \mathscr{R}_{F_S//F_O} = \left((\overrightarrow{x_S})_{(F_O)}\middle|(\overrightarrow{y_S})_{(F_O)}\middle|(\overrightarrow{z_S})_{(F_O)}\right).$$

As for the skew-symmetric tensor $\overrightarrow{\overrightarrow{v}}$ associated with a vector $\overrightarrow{v}$, it is defined by

$$(\overrightarrow{v})_{(F)} = (a,b,c)' \;\Rightarrow\; \left(\overrightarrow{\overrightarrow{v}}\right)_{(F)} = \begin{pmatrix} 0 & -c & b \\ c & 0 & -a \\ -b & a & 0 \end{pmatrix}.$$

Finally, the formula

$$(\overrightarrow{v})_{(F_1)} = \mathscr{R}_{F_2//F_1}(\overrightarrow{v})_{(F_2)} \quad \left(\text{resp. } (\overrightarrow{\overrightarrow{T}})_{(F_1)} = \mathscr{R}_{F_2//F_1}(\overrightarrow{\overrightarrow{T}})_{(F_2)}\mathscr{R}'_{F_2//F_1}\right)$$

relates the extrinsic expressions of a vector $\overrightarrow{v}$ (resp. of a tensor $\overrightarrow{\overrightarrow{T}}$) within two distinct bases.

These notations are consistent with those used in the body of the paper, see the definition of x_i, y_i, z_i, X_i, Y_i, a_i, b_i, c_i in § 2.1, and of t_x, t_y, t_z in § 2.2.

Analytical expressions

State equation This equation depicts the effect of the camera velocity screw onto the relative sensor-target situation. The camera velocity screw is made of any translational velocity vector of F_S w.r.t. F_O

[§] Let $F=(O_F,\overrightarrow{x},\overrightarrow{y},\overrightarrow{z})$ be any frame, and $B=(\overrightarrow{x},\overrightarrow{y},\overrightarrow{z})$ its associated basis. Though with a slight word and notation misuse, the whole document terms "extrinsic expression of X in frame F" the extrinsic expression in basis B of an intrinsic quantity X, and equally uses the notations $(X)_{(F)}$ or $(X)_{(B)}$.

—e.g. $\left[\frac{\mathrm{d}(\overrightarrow{OS})}{\mathrm{d}t}\right]_{F_O}$ — together with the rotational velocity vector $\overrightarrow{\Omega}_{F_S//F_O}$ of F_S w.r.t. F_O. The control input u of the open-loop model has been defined as its extrinsic expression within the F_S basis, namely,

$$u = \left(\left(\left[\frac{\mathrm{d}(\overrightarrow{OS})}{\mathrm{d}t}\right]_{F_O} \right)'_{(F_S)}, \left(\overrightarrow{\Omega}_{F_S//F_O} \right)'_{(F_S)} \right)' = (V_x, V_y, V_z, \Omega_x, \Omega_y, \Omega_z)'. \tag{56}$$

The translational velocities composition law and the composed derivation formula of a vector read as [35]

$$\left[\frac{\mathrm{d}(\overrightarrow{OS})}{\mathrm{d}t}\right]_{F_O} = \left[\frac{\mathrm{d}(\overrightarrow{OT})}{\mathrm{d}t}\right]_{F_O} + \left[\frac{\mathrm{d}(\overrightarrow{TS})}{\mathrm{d}t}\right]_{F_O} \tag{57}$$

and

$$\left[\frac{\mathrm{d}(\overrightarrow{TS})}{\mathrm{d}t}\right]_{F_O} = \left[\frac{\mathrm{d}(\overrightarrow{TS})}{\mathrm{d}t}\right]_{F_S} + \overrightarrow{\Omega}_{F_S//F_O} \times \overrightarrow{TS}. \tag{58}$$

As the target is assumed motionless in the frame F_O attached to the environment, the time derivative of $\overrightarrow{OT}$ w.r.t. F_O is equal to the null vector. Equations (57) and (58) then lead to

$$\left[\frac{\mathrm{d}(\overrightarrow{ST})}{\mathrm{d}t}\right]_{F_S} = -\left[\frac{\mathrm{d}(\overrightarrow{OS})}{\mathrm{d}t}\right]_{F_O} + \overrightarrow{ST} \times \overrightarrow{\Omega}_{F_S//F_O}. \tag{59}$$

The extrinsic representation of (59) in F_S follows:

$$\begin{pmatrix} \dot{t}_x \\ \dot{t}_y \\ \dot{t}_z \end{pmatrix} = \begin{pmatrix} -1 & 0 & 0 & 0 & -t_z & t_y \\ 0 & -1 & 0 & t_z & 0 & -t_x \\ 0 & 0 & -1 & -t_y & t_x & 0 \end{pmatrix} u. \tag{60}$$

Besides, the rotational velocities composition law and the rotation tensor time-derivation law read as [35]

$$\overrightarrow{\Omega}_{F_T//F_O} = \overrightarrow{\Omega}_{F_T//F_S} + \overrightarrow{\Omega}_{F_S//F_O} \tag{61}$$

and

$$\left[\frac{\mathrm{d}(\overrightarrow{\overrightarrow{\mathscr{R}}}_{F_T//F_S})}{\mathrm{d}t}\right]_{F_S} = \widehat{\overrightarrow{\Omega}}_{F_T//F_S} \overrightarrow{\overrightarrow{\mathscr{R}}}_{F_T//F_S}. \tag{62}$$

The fact that the target is motionless also implies that $\overrightarrow{\Omega}_{F_T//F_O} = \overrightarrow{0}$, so that (61) and (62) combine into

$$\left[\frac{\mathrm{d}(\overrightarrow{\overrightarrow{\mathscr{R}}}_{F_T//F_S})}{\mathrm{d}t}\right]_{F_S} = -\widehat{\overrightarrow{\Omega}}_{F_S//F_O} \overrightarrow{\overrightarrow{\mathscr{R}}}_{F_T//F_S}. \tag{63}$$

The extrinsic form of this equation in frame F_S is then computed. Finally, expressing the matrix $\mathscr{R}_{F_T//F_S}$ —which is also the extrinsic form $\left(\overrightarrow{\overrightarrow{\mathscr{R}}}_{F_T//F_S}\right)_{(F_S)}$— as a function of the 3-tuple (λ, μ, ν) of Bryant angles which parametrize the relative attitude between F_S and F_T [35], leads to

$$\begin{pmatrix} \dot{\lambda} \\ \dot{\mu} \\ \dot{\nu} \end{pmatrix} = \begin{pmatrix} -1 & -\sin\lambda\tan\mu & \cos\lambda\tan\mu \\ 0 & -\cos\lambda & -\sin\lambda \\ 0 & \frac{\sin\lambda}{\cos\mu} & \frac{-\cos\lambda}{\cos\mu} \end{pmatrix} \begin{pmatrix} \Omega_x \\ \Omega_y \\ \Omega_z \end{pmatrix}. \tag{64}$$

Equations (60) and (64) join into (1). Notice that the Jacobian matrix involved in (1) is always full rank. Moreover, its entries are all well-defined, and its singular values are finite, iff $\mu \not\equiv \frac{\pi}{2} [\mathrm{mod}\, 2\pi]$.

Output equation Recall that the position-based case sums up to the trivial equation $y = x$. The determination of the output equation (2) in the image-based case follows the two following steps.

- The coordinates $(\overrightarrow{ST_i})_{(F_S)} = (x_i, y_i, z_i)'$ of the targets spots T_i, $i = 1, \ldots, \mathsf{M}$, in the camera frame F_S are first related to their coordinates $(\overrightarrow{TT_i})_{(F_T)} = (a_i, b_i, c_i)'$ in F_T by the equations

$$\begin{aligned}(\overrightarrow{ST_i})_{(F_S)} &= (\overrightarrow{ST})_{(F_S)} + (\overrightarrow{TT_i})_{(F_S)}, \\ &= (\overrightarrow{ST})_{(F_S)} + \mathscr{R}_{F_T//F_S}(\overrightarrow{TT_i})_{(F_T)}. \end{aligned} \tag{65}$$

  The entries $(t_x, t_y, t_z, \lambda, \mu, \nu)'$ of the state vector appear in this relation through $(\overrightarrow{ST})_{(F_S)}$ and $\mathscr{R}_{F_T//F_S}$.

- The computation of $y = s - s^*$ follows, where the entries of $s = (X_1, Y_1, \ldots, X_{\mathsf{M}}, Y_{\mathsf{M}})'$ and $s^* = (X_1^*, Y_1^*, \ldots, X_{\mathsf{M}}^*, Y_{\mathsf{M}}^*)'$ follow the equations of perspective projection $X_i = f\frac{x_i}{z_i}$, $Y_i = f\frac{y_i}{z_i}$, $X_i^* = f\frac{a_i}{c_i}$ and $Y_i^* = f\frac{b_i}{c_i}$.

Notice that the denominator of each subequation of (2) which expresses the coordinates of the projection S_i of a spot T_i is 0 iff $z_i = \overrightarrow{ST_i}.\overrightarrow{z_S}$ is 0. This case cannot occur, because it would imply that T_i belongs to the plane containing the optical center and orthogonal to the optical axis. Each z_i must indeed be strictly positive so that T_i can be in the camera field of view.

B Proofs

B.1 Proof of "boundedness" constaints

Proof of (19)**,** (22)**,** (28)**,** (30)**:** The constraints to be satisfied have the form

$$||C\tilde{x}||^2 \leq \frac{1}{\upsilon}, \text{ with } \upsilon > 0, \text{ holds for all } \tilde{x} \text{ such that } \tilde{x}'P\tilde{x} \leq 1. \tag{66}$$

Two approaches can be developed so as to prove them.

- Like in [18, 13], it can be noticed that

$$\upsilon C'C - P \leq 0 \tag{67}$$

  (or its "Schur complement equivalent form" similar to [18]-(9)) is a sufficient condition, since this is equivalent to

$$\forall \tilde{x},\ \tilde{x}'C'C\tilde{x} \leq \frac{1}{\upsilon}\tilde{x}'P\tilde{x}.$$

- Besides, rewriting (66) as

$$\begin{pmatrix}\tilde{x}\\1\end{pmatrix}' \begin{pmatrix}C'C & 0\\ 0 & -\frac{1}{\upsilon}\end{pmatrix} \begin{pmatrix}\tilde{x}\\1\end{pmatrix} \leq 0, \text{ with } \upsilon > 0, \text{ holds for all } \tilde{x} \text{ such that } \begin{pmatrix}\tilde{x}\\1\end{pmatrix}' \begin{pmatrix}P & 0\\ 0 & -1\end{pmatrix} \begin{pmatrix}\tilde{x}\\1\end{pmatrix} \leq 0$$

enables a straight application of the $\mathscr{S}$-procedure, which leads to the necessary and sufficient condition

$$\exists \sigma \geq 0, \text{ such that } \begin{pmatrix} C'C & 0 \\ 0 & -\frac{1}{\upsilon} \end{pmatrix} - \sigma \begin{pmatrix} P & 0 \\ 0 & -1 \end{pmatrix} \leq 0.$$

As $C'C$ is positive semi-definite, σ cannot be 0. By setting $\tau = \frac{1}{\sigma}$, one gets the equivalent necessary and sufficient condition to (66)

$$\exists \tau > 0, \text{ such that } \tau \begin{pmatrix} C'C & 0 \\ 0 & -\frac{1}{\upsilon} \end{pmatrix} - \begin{pmatrix} P & 0 \\ 0 & -1 \end{pmatrix} \leq 0,$$

or, equivalently,

$$\exists \tau \geq \upsilon, \text{ such that } \tau C'C - P \leq 0. \tag{68}$$

Yet, (67) and (68) are equivalent. Indeed,

- (67) trivially implies (68);
- if (68) holds, then

  $$\forall \tilde{x}, \ \tau \tilde{x}' C'C\tilde{x} - \tilde{x}'P\tilde{x} \leq 0$$

  and, as $C'C \geq 0$,

  $$\forall \tilde{x}, \ \tau \tilde{x}' C'C\tilde{x} \geq \upsilon \tilde{x}' C'C\tilde{x};$$

  these last two equations thus imply

  $$\forall \tilde{x}, \ \upsilon \tilde{x}' C'C\tilde{x} - \tilde{x}'P\tilde{x} \leq 0,$$

  i.e. (67).

Notice that (68) is equivalent to (19) (resp. (22)) when $C = W_i'$ and $\upsilon = \frac{1}{\rho_i^2}$ (resp. when $C = Z_{\zeta_j}$ and $\upsilon = \frac{1}{\bar{\zeta}_j^2}$.)

The "Schur complement forms" of (67) and (68) can be shown to be respectively equivalent to the LMIs (69) and (70) given below, which involve $Q = P^{-1}$ (recall that $P > 0$ and $Q > 0$):

$$\begin{pmatrix} \upsilon^{-1} I & CQ \\ QC' & Q \end{pmatrix} \geq 0 \tag{69}$$

$$\exists \sigma \in]0; \upsilon^{-1}] \text{ such that } \begin{pmatrix} \sigma I & CQ \\ QC' & Q \end{pmatrix} \geq 0. \tag{70}$$

Notice that (70) is equivalent to (28) when $C = W_i'$ and $\upsilon = \frac{1}{\rho_i^2}$.

Assume that

$$||CK\tilde{x}||^2 \leq \frac{1}{\upsilon}, \text{ with } \upsilon > 0, \text{ holds for all } \tilde{x} \text{ such that } \tilde{x}'P\tilde{x} \leq 1 \tag{71}$$

must be ensured in the context of state feedback synthesis, with $K = YQ^{-1}$, $Q = P^{-1}$. (69) and (70) are straightly equivalent to the LMIs (72) and (73) given below, which involve Y and Q:

$$\begin{pmatrix} \upsilon^{-1} I & CY \\ Y'C' & Q \end{pmatrix} \geq 0 \tag{72}$$

$$\exists \sigma \in]0; \upsilon^{-1}] \text{ such that } \begin{pmatrix} \sigma I & CY \\ Y'C' & Q \end{pmatrix} \geq 0. \tag{73}$$

It can be readily noticed that (72) (resp. (73)) is equivalent to the "additional LMI" given in the right column of [18, p. 1277] when $C = I$ and $\upsilon = \frac{1}{u_{\max}^2}$ (resp. to (30) when $C = W_j'$ and $\upsilon = \frac{1}{\bar{u}_j^2}$.) □

B.2 Proof of results in Section 4.2

Proof of Theorem 4.2: Consider the representation (23). The set membership $\tilde{x} \in \mathscr{C}_{\zeta_j}$ holds if and only if the inequality

$$\begin{pmatrix} \tilde{x} \\ p_\zeta \\ 1 \end{pmatrix}' M_1 \begin{pmatrix} \tilde{x} \\ p_\zeta \\ 1 \end{pmatrix} \leq 0, \text{ with } M_1 = \begin{pmatrix} \tilde{C}_\zeta' \tilde{C}_\zeta & \tilde{C}_\zeta' \tilde{D}_{p_\zeta} & -\tilde{C}_\zeta' \hat{\xi}_j \\ \star & \tilde{D}_{p_\zeta}' \tilde{D}_{p_\zeta} & -\tilde{D}_{p_\zeta}' \hat{\xi}_j \\ \star & \star & \hat{\xi}_j^2 - \tilde{\xi}_j^2 \end{pmatrix}, \tag{74}$$

is satisfied for all p_ζ expressing the relationship $p_\zeta = \Delta_\zeta q_\zeta$ with $\Delta_\zeta \in \blacktriangle(r_\zeta)$ and $q_\zeta = \tilde{C}_{q_\zeta} \tilde{x} + \tilde{D}_{qp_\zeta} p_\zeta$. By Lemma 4.1, whatever $(S_{a_\zeta}, G_{a_\zeta}) \in \mathscr{S}(r_\zeta) \times \mathscr{G}(r_\zeta)$, the set of $(\tilde{x}, p_\zeta)$ which satisfy (23) is included in $\{(\tilde{x}, p_\zeta) : (p_\zeta, q_\zeta) \in \mathscr{W}(S_{a_\zeta}, G_{a_\zeta}),\ q_\zeta = \tilde{C}_{q_\zeta} \tilde{x} + \tilde{D}_{qp_\zeta} p_\zeta\}$, i.e. in the set of $(\tilde{x}, p_\zeta)$ such that

$$\begin{pmatrix} \tilde{x} \\ p_\zeta \\ 1 \end{pmatrix}' M_{a2} \begin{pmatrix} \tilde{x} \\ p_\zeta \\ 1 \end{pmatrix} \geq 0, \text{ with } M_{a2} = \begin{pmatrix} \tilde{C}_{q_\zeta}' S_{a_\zeta} \tilde{C}_{q_\zeta} & \tilde{C}_{q_\zeta}' S_{a_\zeta} \tilde{D}_{qp_\zeta} + \tilde{C}_{q_\zeta}' G_{a_\zeta} & 0 \\ \star & \tilde{D}_{qp_\zeta}' S_{a_\zeta} \tilde{D}_{qp_\zeta} - S_{a_\zeta} + \tilde{D}_{qp_\zeta}' G_{a_\zeta} + G_{a_\zeta}' \tilde{D}_{qp_\zeta} & 0 \\ \star & \star & 0 \end{pmatrix}. \tag{75}$$

Moreover, $\tilde{x} \in \mathscr{E}_P$ is equivalent to

$$\begin{pmatrix} \tilde{x} \\ p_\zeta \\ 1 \end{pmatrix}' M_0 \begin{pmatrix} \tilde{x} \\ p_\zeta \\ 1 \end{pmatrix} \leq 0, \text{ with } M_0 = \begin{pmatrix} P & 0 & 0 \\ \star & 0 & 0 \\ \star & \star & -1 \end{pmatrix}. \tag{76}$$

So, to ensure the relationship $\mathscr{E}_P \subset \mathscr{C}_{\zeta_j}$, it is sufficient that there exists a couple of matrices $(S_{a_\zeta}, G_{a_\zeta}) \in \mathscr{S}(r_\zeta) \times \mathscr{G}(r_\zeta)$ such that (74) holds for all $(\tilde{x}, p_\zeta)$ which satisfy (75) and (76). Applying the $\mathscr{S}$-procedure leads to the following sufficient condition:

$$\exists\ \tau_{a_\zeta} \in \mathbb{R}^+,\ \sigma_\zeta \in \mathbb{R}^+,\ S_{a_\zeta} \in \mathscr{S}(r_\zeta),\ G_{a_\zeta} \in \mathscr{G}(r_\zeta),\ M_1 + \tau_{a_\zeta} M_{a2} - \sigma_\zeta M_0 \leq 0. \tag{77}$$

If $\sigma_\zeta = 0$, satisfying the inequality (77) would require that the matrix $\left(\tilde{C}_\zeta' \tilde{C}_\zeta + \tau_{a_\zeta} \tilde{C}_{q_\zeta}' S_{a_\zeta} \tilde{C}_{q_\zeta}\right)$ be negative semidefinite. However, this matrix is by construction nonzero and positive semidefinite. Consequently, σ_ζ is strictly positive. Multiplying (77) by $\tau_\zeta \stackrel{\Delta}{=} \frac{1}{\sigma_\zeta} \in \mathbb{R}^{+*}$, one gets:

$$\exists\ \tau_{a_\zeta} \in \mathbb{R}^+,\ \tau_\zeta \in \mathbb{R}^{+*},\ S_{a_\zeta} \in \mathscr{S}(r_\zeta),\ G_{a_\zeta} \in \mathscr{G}(r_\zeta),\ \tau_\zeta M_1 + \tau_\zeta\, \tau_{a_\zeta} M_{a2} - M_0 \leq 0. \tag{78}$$

The variables τ_{a_ζ}, S_{a_ζ} and G_{a_ζ} appear in (78) only in the form of the products $(\tau_\zeta \tau_{a_\zeta} S_{a_\zeta})$ and $(\tau_\zeta \tau_{a_\zeta} G_{a_\zeta})$. In addition, if $\tau_{a_\zeta} = 0$, for the inequality (78) to hold, it is necessary that the matrix $(\tilde{D}_{p_\zeta}' \tilde{D}_{p_\zeta})$ be negative definite, which is not the case. Consequently, τ_{a_ζ} is strictly positive, therefore $(\tau_\zeta \tau_{a_\zeta} S_{a_\zeta}) \in \mathscr{S}(r_\zeta)$ and $(\tau_\zeta \tau_{a_\zeta} G_{a_\zeta}) \in \mathscr{G}(r_\zeta)$. Replacing the expressions $(\tau_\zeta \tau_{a_\zeta} S_{a_\zeta})$ and $(\tau_\zeta \tau_{a_\zeta} G_{a_\zeta})$ by the variables $S_\zeta \in \mathscr{S}(r_\zeta)$ and $G_\zeta \in \mathscr{G}(r_\zeta)$ leads to the condition

$$\exists \tau_\zeta \in \mathbb{R}^{+*},\ S_\zeta \in \mathscr{S}(r_\zeta),\ G_\zeta \in \mathscr{G}(r_\zeta),\ \tau_\zeta M_1 + M_2 - M_0 \leq 0. \tag{79}$$

It remains to guarantee the well-posedness of (23), that is —once the matrices $\tilde{C}_\zeta$, $\tilde{D}_{p_\zeta}$, $\tilde{C}_{q_\zeta}$, $\tilde{D}_{qp_\zeta}$ can be computed— to ensure the property $\forall \Delta_\zeta \in \blacktriangle(r_\zeta)$, $\det(I - \tilde{D}_{qp_\zeta} \Delta_\zeta) \neq 0$. As proved in [20], a sufficient condition is the existence of $S_\zeta \in \mathscr{S}(r_\zeta)$ and $G_\zeta \in \mathscr{G}(r_\zeta)$ such that $\tilde{D}_{qp_\zeta}' S_\zeta \tilde{D}_{qp_\zeta} - S_\zeta + \tilde{D}_{qp_\zeta}' G_\zeta + G_\zeta' \tilde{D}_{qp_\zeta} < 0$. Yet, the inequality (79) implies that $\tilde{D}_{qp_\zeta}' S_\zeta \tilde{D}_{qp_\zeta} - S_\zeta + \tilde{D}_{qp_\zeta}' G_\zeta + G_\zeta' \tilde{D}_{qp_\zeta} + D_{p\zeta}' \tilde{D}_{p_\zeta} \leq 0$, so $\tilde{D}_{qp_\zeta}' S_\zeta \tilde{D}_{qp_\zeta} - S_\zeta + \tilde{D}_{qp_\zeta}' G_\zeta + G_\zeta' \tilde{D}_{qp_\zeta} \leq 0$. Consequently, in order to ensure that $\tilde{D}_{qp_\zeta}' S_\zeta \tilde{D}_{qp_\zeta} - S_\zeta + \tilde{D}_{qp_\zeta}' G_\zeta + G_\zeta' \tilde{D}_{qp_\zeta}$ is negative definite, the inequality (79) is made strict, which leads to the condition (24). □

Proof of Theorem 4.3: A vector $\xi \in \mathbb{R}^{(n+m)}$ belongs to the set $\mathscr{B}_{\zeta_j}^k$ if and only if $\begin{pmatrix} \xi \\ 1 \end{pmatrix}' \tilde{N}_{\zeta_j}^k \begin{pmatrix} \xi \\ 1 \end{pmatrix} \leq 0$. Similarly, $\xi \in \mathbb{R}^{(n+m)}$ belongs to $\mathscr{E}_P$ if and only if $\begin{pmatrix} \xi \\ 1 \end{pmatrix}' \begin{pmatrix} P & 0 \\ \star & -1 \end{pmatrix} \begin{pmatrix} \xi \\ 1 \end{pmatrix} \leq 0$. Applying the $\mathscr{S}$-procedure leads to the following necessary and sufficient condition for $\mathscr{E}_P \subset \mathscr{B}_{\zeta_j}^k$:

$$\exists\ \sigma_{\zeta_j}^k \in \mathbb{R}^+,\ \tilde{N}_{\zeta_j}^k - \sigma_{\zeta_j}^k \begin{pmatrix} P & 0 \\ \star & -1 \end{pmatrix} \leq 0. \tag{80}$$

If $\sigma_{\zeta_j}^k = 0$, satisfying the inequality (80) would require that the matrix $\tilde{N}_{\zeta_j}^k$ be negative semidefinite. However, this is not the case lest $\mathscr{B}_{\zeta_j}^k$ would be $\mathbb{R}^{n+m}$. Consequently, $\sigma_{\zeta_j}^k$ is strictly positive. Multiplying (80) by $\tau_{\zeta_j}^k \stackrel{\Delta}{=} \frac{1}{\sigma_{\zeta_j}^k} \in \mathbb{R}^{+*}$, one gets:

$$\exists \tau_{\zeta_j}^k \in \mathbb{R}^{+*}, \quad \tau_{\zeta_j}^k \tilde{N}_{\zeta_j}^k - \begin{pmatrix} P & 0 \\ \star & -1 \end{pmatrix} \leq 0. \tag{81}$$

Finally, $\mathscr{E}_P \subset \mathscr{B}_{\zeta_j} = \bigcap_{k=1}^{l_{\zeta_j}} \mathscr{B}^k_{\zeta_j}$ holds if and only if for all $k = 1,\dots l_{\zeta_j}$, there exists a positive scalar $\tau^k_{\zeta_j}$ such that (81) is true, thus leading to (25). □

B.3 Proof of results in Section 4.3

Proof of Theorem 4.4: As the scalar τ_ζ in the LMI (24) is strictly positive, by applying the Schur lemma this inequality can be turned to

$$\begin{pmatrix} \tilde{C}'_{q_\zeta} S_\zeta \tilde{C}_{q_\zeta} - P & \tilde{C}'_{q_\zeta} S_\zeta \tilde{D}_{qp_\zeta} + \tilde{C}'_{q_\zeta} G_\zeta & 0 & \tilde{C}'_\zeta \\ \star & \tilde{D}'_{qp_\zeta} S_\zeta \tilde{D}_{qp_\zeta} - S_\zeta + \tilde{D}'_{qp_\zeta} G_\zeta + G'_\zeta \tilde{D}_{qp_\zeta} & 0 & \tilde{D}'_{p_\zeta} \\ \star & \star & -\tau_\zeta \tilde{\zeta}_j^2 + 1 & -\hat{\zeta} \\ \star & \star & \star & -\frac{1}{\tau_\zeta} \end{pmatrix} < 0. \tag{82}$$

The matrix S_ζ is positive definite, so S_ζ^{-1} exists and $S_\zeta^{-1} > 0$ as well as $(S_\zeta + G'_\zeta S_\zeta^{-1} G_\zeta) > 0$. Moreover, the block-diagonal structure of $(S_\zeta + G'_\zeta S_\zeta^{-1} G_\zeta)$ and of its inverse implies that both these symmetric positive definite matrices belong to $\mathscr{S}(r_\zeta)$. Stating $T_\zeta \stackrel{\Delta}{=} (S_\zeta + G'_\zeta S_\zeta^{-1} G_\zeta)^{-1} \in \mathscr{S}(r_\zeta)$, the inequality (82) becomes

$$\begin{pmatrix} \tilde{C}'_{q_\zeta} S_\zeta \tilde{C}_{q_\zeta} - P & \tilde{C}'_{q_\zeta} S_\zeta (\tilde{D}_{qp_\zeta} + S_\zeta^{-1} G_\zeta) & 0 & \tilde{C}'_\zeta \\ \star & (\tilde{D}_{qp_\zeta} + S_\zeta^{-1} G_\zeta)' S_\zeta (\tilde{D}_{qp_\zeta} + S_\zeta^{-1} G_\zeta) - T_\zeta^{-1} & 0 & \tilde{D}'_{p_\zeta} \\ \star & \star & -\tau_\zeta \tilde{\zeta}_j^2 + 1 & -\hat{\zeta} \\ \star & \star & \star & -\frac{1}{\tau_\zeta} \end{pmatrix} < 0. \tag{83}$$

The matrix S_ζ being positive definite, applying the Schur lemma to (83) leads to

$$\begin{pmatrix} -P & 0 & 0 & \tilde{C}'_\zeta & \tilde{C}'_{q_\zeta} \\ \star & -T_\zeta^{-1} & 0 & \tilde{D}'_{p_\zeta} & \tilde{D}'_{qp_\zeta} + G'_\zeta S_\zeta^{-1} \\ \star & \star & -\tau_\zeta \tilde{\zeta}_j^2 + 1 & -\hat{\zeta} & 0 \\ \star & \star & \star & -\frac{1}{\tau_\zeta} & 0 \\ \star & \star & \star & \star & -S_\zeta^{-1} \end{pmatrix} < 0, \tag{84}$$

so that, after a permutation of the 2nd and 5th rows and of the 2nd and 5th columns, one gets

$$\begin{pmatrix} -P & \tilde{C}'_{q_\zeta} & 0 & \tilde{C}'_\zeta & 0 \\ \star & -S_\zeta^{-1} & 0 & 0 & \tilde{D}_{qp_\zeta} + S_\zeta^{-1} G_\zeta \\ \star & \star & -\tau_\zeta \tilde{\zeta}_j^2 + 1 & -\hat{\zeta} & 0 \\ \star & \star & \star & -\frac{1}{\tau_\zeta} & \tilde{D}_{p_\zeta} \\ \star & \star & \star & \star & -T_\zeta^{-1} \end{pmatrix} < 0. \tag{85}$$

The matrix T_ζ^{-1} being positive definite, by applying the Schur lemma, the inequality (85) is equivalent to

$$\begin{pmatrix} -P & \tilde{C}'_{q_\zeta} & 0 & \tilde{C}'_\zeta \\ \star & -S_\zeta^{-1} + (\tilde{D}_{qp_\zeta} + S_\zeta^{-1}G_\zeta)T_\zeta(\tilde{D}_{qp_\zeta} + S_\zeta^{-1}G_\zeta)' & 0 & \tilde{D}_{qp_\zeta}T_\zeta\tilde{D}'_{p_\zeta} + S_\zeta^{-1}G_\zeta T_\zeta\tilde{D}'_{p_\zeta} \\ \star & \star & -\tau_\zeta\tilde{\zeta}_j^2 + 1 & -\hat{\zeta} \\ \star & \star & \star & -\frac{1}{\tau_\zeta} + \tilde{D}_{p_\zeta}T_\zeta\tilde{D}'_{p_\zeta} \end{pmatrix} < 0. \tag{86}$$

Define $H_\zeta \stackrel{\Delta}{=} -T_\zeta G_\zeta S_\zeta^{-1}$. So, $H'_\zeta = S_\zeta^{-1}G_\zeta T_\zeta$. Yet, by the matrix inversion lemma,

$$T_\zeta = S_\zeta^{-1} - S_\zeta^{-1}G'_\zeta T_\zeta G_\zeta S_\zeta^{-1}$$

holds, so that

$$\begin{aligned} H'_\zeta &= (S_\zeta^{-1}T_\zeta^{-1} - S_\zeta^{-1}G_\zeta S_\zeta^{-1}G'_\zeta)T_\zeta G_\zeta S_\zeta^{-1} \\ &= (I + S_\zeta^{-1}G'_\zeta S_\zeta^{-1}G_\zeta - S_\zeta^{-1}G'_\zeta S_\zeta^{-1}G_\zeta)T_\zeta G_\zeta S_\zeta^{-1} \\ &= -H_\zeta. \end{aligned}$$

Morover, the block-diagonal structure of H_ζ implies that this matrix belongs to $\mathscr{G}(r_\zeta)$. The second block-diagonal term of (86) can be thus written:

$$\begin{aligned} -S_\zeta^{-1} + (\tilde{D}_{qp_\zeta} + S_\zeta^{-1}G_\zeta)\,T_\zeta\,(\tilde{D}_{qp_\zeta} + S_\zeta^{-1}G_\zeta)' \\ = \tilde{D}_{qp_\zeta}T_\zeta\tilde{D}'_{qp_\zeta} + \tilde{D}_{qp_\zeta}H_\zeta + H'_\zeta\tilde{D}'_{qp_\zeta} - (S_\zeta^{-1} + S_\zeta^{-1}G_\zeta T_\zeta G_\zeta S_\zeta^{-1}) \\ = \tilde{D}_{qp_\zeta}T_\zeta\tilde{D}'_{qp_\zeta} + \tilde{D}_{qp_\zeta}H_\zeta + H'_\zeta\tilde{D}'_{qp_\zeta} - T_\zeta. \end{aligned}$$

So, the inequality (86) becomes[¶]:

$$\begin{pmatrix} -P & \tilde{C}'_{q_\zeta} & 0 & \tilde{C}'_\zeta \\ \star & \tilde{D}_{qp_\zeta}T_\zeta\tilde{D}'_{qp_\zeta} - T_\zeta + \tilde{D}_{qp_\zeta}H_\zeta + H'_\zeta\tilde{D}'_{qp_\zeta} & 0 & \tilde{D}_{qp_\zeta}T_\zeta\tilde{D}'_{p_\zeta} + H'_\zeta\tilde{D}'_{p_\zeta} \\ \star & \star & -\tau_\zeta\tilde{\zeta}_j^2 + 1 & -\hat{\zeta} \\ \star & \star & \star & -\frac{1}{\tau_\zeta} + \tilde{D}_{p_\zeta}T_\zeta\tilde{D}'_{p_\zeta} \end{pmatrix} < 0. \tag{87}$$

[¶]The proof of $H_\zeta \in \mathscr{G}(r_\zeta)$ and the steps leading to the inequality (87) are similar to these of El Ghaoui *et al.* [18, 13] in their proof of (27).

The matrix P being positive definite, the application of the Schur lemma leads to

$$\begin{pmatrix} R_1 & 0 & R_2 \\ \star & -\tau_\zeta \tilde{\zeta}_j^2 + 1 & -\hat{\zeta} \\ \star & \star & R_3 \end{pmatrix} < 0, \tag{88}$$

$$\begin{aligned} \text{with } R_1 &= \tilde{D}_{qp_\zeta} T_\zeta \tilde{D}'_{qp_\zeta} - T_\zeta + \tilde{D}_{qp_\zeta} H_\zeta + H'_\zeta \tilde{D}'_{qp_\zeta} + \tilde{C}_{q_\zeta} Q \tilde{C}'_{q_\zeta}, \\ R_2 &= \tilde{D}_{qp_\zeta} T_\zeta \tilde{D}'_{p_\zeta} + H'_\zeta \tilde{D}'_{p_\zeta} + \tilde{C}_{q_\zeta} Q \tilde{C}'_\zeta, \\ R_3 &= -\tfrac{1}{\tau_\zeta} + \tilde{D}_{p_\zeta} T_\zeta \tilde{D}'_{p_\zeta} + \tilde{C}_\zeta Q \tilde{C}'_\zeta, \\ Q &= P^{-1}. \end{aligned}$$

At last, pre- and post- multiplying (88) by $\mathrm{diag}\,(I, \frac{1}{\tau_\zeta}, 1) > 0$ and applying the Schur lemma leads to

$$\begin{pmatrix} R_1 & 0 & R_2 & 0 \\ \star & -\frac{1}{\tau_\zeta}\tilde{\zeta}_j^2 & -\frac{1}{\tau_\zeta}\hat{\zeta} & \frac{1}{\tau_\zeta} \\ \star & \star & R_3 & 0 \\ \star & \star & \star & -1 \end{pmatrix} < 0. \tag{89}$$

As the variable $\tau_\zeta \in \mathbb{R}^{+*}$ appears in the inequality (89) only under the form $\frac{1}{\tau_\zeta}$, the change of variable $\sigma_\zeta \stackrel{\Delta}{=} \frac{1}{\tau_\zeta} \in \mathbb{R}^{+*}$ can be performed, leading to the expected condition (31). □

Proof of Theorem 4.5: By applying twice the Schur lemma, the inequality (25) becomes

$$\begin{pmatrix} \tau_{\zeta_j}^k \tilde{R}_{\zeta_j}^{k'} \tilde{R}_{\zeta_j}^k - P & \tau_{\zeta_j}^k \tilde{F}_{\zeta_j}^{k'} & 0 \\ \star & \tau_{\zeta_j}^k \beta_{\zeta_j}^k & 1 \\ \star & \star & -1 \end{pmatrix} \leq 0, \tag{90}$$

and, as the matrix $\tau_{\zeta_j}^k I_{(n+m)}$ is positive definite,

$$\begin{pmatrix} -P & \tau_{\zeta_j}^k \tilde{F}_{\zeta_j}^{k'} & 0 & \tilde{R}_{\zeta_j}^{k'} \\ \star & \tau_{\zeta_j}^k \beta_{\zeta_j}^k & 1 & 0 \\ \star & \star & -1 & 0 \\ \star & \star & \star & -\frac{1}{\tau_{\zeta_j}^k} I_{(n+m)} \end{pmatrix} \leq 0. \tag{91}$$

Pre- and post- multiplying (91) by $\mathrm{diag}\left(I_{(n+m)}, \frac{1}{\tau^k_{\zeta_j}}, 1, I_{(n+m)}\right) > 0$ leads to:

$$\begin{pmatrix} -P & \tilde{F}^{k'}_{\zeta_j} & 0 & \tilde{R}^{k'}_{\zeta_j} \\ \star & \frac{1}{\tau^k_{\zeta_j}}\beta^k_{\zeta_j} & \frac{1}{\tau^k_{\zeta_j}} & 0 \\ \star & \star & -1 & 0 \\ \star & \star & \star & -\frac{1}{\tau^k_{\zeta_j}} I_{(n+m)} \end{pmatrix} \leq 0. \tag{92}$$

The matrix P being positive definite, a last application of the Schur lemma on this inequality gives

$$\begin{pmatrix} \frac{1}{\tau^k_{\zeta_j}}\beta^k_{\zeta_j} + \tilde{F}^k_{\zeta_j} Q \tilde{F}^{k'}_{\zeta_j} & \frac{1}{\tau^k_{\zeta_j}} & \tilde{F}^k_{\zeta_j} Q \tilde{R}^{k'}_{\zeta_j} \\ \star & -1 & 0 \\ \star & \star & -\frac{1}{\tau^k_{\zeta_j}} I_{(n+m)} + \tilde{R}^k_{\zeta_j} Q \tilde{R}^{k'}_{\zeta_j} \end{pmatrix} \leq 0 \tag{93}$$

where $Q = P^{-1}$. The variable $\tau^k_{\zeta_j} \in \mathbb{R}^{+*}$ appears in (93) only under the form $\frac{1}{\tau^k_{\zeta_j}}$, so that the change of variable $\sigma^k_{\zeta_j} \stackrel{\Delta}{=} \frac{1}{\tau^k_{\zeta_j}} \in \mathbb{R}^{+*}$ can be done, leading to (32), whatever the ordre m of the controller. □

B.4 Proof of results in Section 4.4

Proof of Theorem 4.6: The reasoning performed by El Ghaoui *et al.* in [18, 13] concerning the quadratic stability and the well-posedness of the closed-loop SNLDI (26) when the aim is to synthesize a linear static state feedback controller, cannot be extended to the synthesis of a nonlinear static state feedback, lest BMIs would be obtained. It is hereafter shown that an LMI condition can be obtained from the analysis LMI (17) if the matrix G is fixed to $G = 0_{(n_p(r);n_p(r))} \in \mathscr{G}(r)$. Though this choice induces extra conservatism, the whole feasibility/optimization problem is kept convex.

Replacing into (17) the matrices involved in the definition of the closed-loop SNLDI by their expressions given in (34), and selecting $G = 0_{(n_p(r);n_p(r))}$, it follows:

$$\begin{pmatrix} K'B'_uP + PB_uK + K'D'_{qu}SD_{qu}K + 2\alpha P & PB_p + PB_uK_p + K'D'_{qu}S(D_{qp} + D_{qu}K_p) \\ \star & (D_{qp} + D_{qu}K_p)'S(D_{qp} + D_{qu}K_p) - S \end{pmatrix} < 0. \tag{94}$$

The matrix S being positive definite, an application of the Schur lemma leads to

$$\begin{pmatrix} K'B'_uP + PB_uK + 2\alpha P & PB_p + PB_uK_p & K'D'_{qu} \\ \star & -S & D'_{qp} + K'_pD'_{qu} \\ \star & \star & -T \end{pmatrix} < 0, \tag{95}$$

where $T \stackrel{\Delta}{=} S^{-1}$. After a pre- and post- multiplication by the symmetric matrix $\mathrm{diag}(Q,T,I) > 0$, with $Q \stackrel{\Delta}{=} P^{-1}$, this inequality becomes

$$\begin{pmatrix} QK^{'}B_u^{'} + B_uKQ + 2\alpha Q & B_pT + B_uK_pT & QK^{'}D_{qu}^{'} \\ \star & -T & TD_{qp}^{'} + TK_p^{'}D_{qu}^{'} \\ \star & \star & -T \end{pmatrix} < 0. \tag{96}$$

Let $Y \stackrel{\Delta}{=} KQ$ and $Y_2 \stackrel{\Delta}{=} K_pT$. The variables Y and Y_2 can be respectively considered as matrices of $\mathbb{R}^{n_u \times n}$ and $\mathbb{R}^{n_u \times n_p(r)}$ with no structure. So, the LMI (36) follows.

As the LMI (36) is equivalent to the inequality (94), by a reasoning similar to the one used in § 4.2.1-B, the feasibility of (36) is sufficient for the well-posedness of the embedding SNLDI (34). In addition, the well-posedness conditions are identical for the SNLDI (34) and for the inclusion (35). □

Proof of Theorem 4.7: The following condition, which is sufficient for $\mathscr{E}_P \subset \mathscr{C}_{u_j}$, is obtained following the above proof of Theorem 4.2 and fixing $G_\zeta = 0$:

$$\exists\ \tau_{u_j} \in \mathbb{R}^{+*},\ S_{u_j} \in \mathscr{S}(r),$$

$$-\tau_{u_j}\overline{u}_j^2 + 1 \leq 0 \tag{97}$$

$$\begin{pmatrix} -P + \tau_{u_j}K^{'}W_jW_j^{'}K + K^{'}D_{qu}^{'}S_{u_j}D_{qu}K & \tau_{u_j}K^{'}W_jW_j^{'}K_p + K^{'}D_{qu}^{'}S_{u_j}(D_{qp} + D_{qu}K_p) \\ \star & \tau_{u_j}K_p^{'}W_jW_j^{'}K_p + (D_{qp} + D_{qu}K_p)^{'}S_{u_j}(D_{qp} + D_{qu}K_p) - S_{u_j} \end{pmatrix} \leq 0. \tag{98}$$

The scalar τ_{u_j} being positive, an application of the Schur lemma turns the inequality (98) into

$$\begin{pmatrix} -P + K^{'}D_{qu}^{'}S_{u_j}D_{qu}K & K^{'}D_{qu}^{'}S_{u_j}(D_{qp} + D_{qu}K_p) & K^{'}W_j \\ \star & (D_{qp} + D_{qu}K_p)^{'}S_{u_j}(D_{qp} + D_{qu}K_p) - S_{u_j} & K_p^{'}W_j \\ \star & \star & -\sigma_{u_j} \end{pmatrix} \leq 0, \tag{99}$$

where $\sigma_{u_j} \stackrel{\Delta}{=} \frac{1}{\tau_{u_j}} > 0$. As the matrix S_{u_j} is positive definite, another application of the Schur lemma to (99) leads to

$$\begin{pmatrix} -P & 0 & K^{'}W_j & K^{'}D_{qu}^{'} \\ \star & -S_{u_j} & K_p^{'}W_j & D_{qp}^{'} + K_p^{'}D_{qu}^{'} \\ \star & \star & -\sigma_{u_j} & 0 \\ \star & \star & \star & -T_{u_j} \end{pmatrix} \leq 0, \tag{100}$$

with $T_{u_j} \stackrel{\Delta}{=} S_{u_j}^{-1} \in \mathscr{S}(r)$. Pre- and post- multiplying (100) by diag(Q, T_{uj}, I, I), one gets

$$\begin{pmatrix} -Q & 0 & Y_1' W_j & Y_1' D_{qu}' \\ \star & -T_{u_j} & T_{u_j} K_p' W_j & T_{u_j} D_{qp}' + T_{u_j} K_p' D_{qu}' \\ \star & \star & -\sigma_{u_j} & 0 \\ \star & \star & \star & -T_{u_j} \end{pmatrix} \leq 0, \tag{101}$$

where $Y_1 = KQ$. Consequently, the condition $\mathscr{E}_P \subset \mathscr{C}_{u_j}$ is guaranteed if there exists $\sigma_{u_j} \in \mathbb{R}^{+*}$ and $T_{u_j} \in \mathscr{S}(r)$ such that the inequalities (97) and (101) hold. The BMI (101) could be turned into an LMI through the change of variable $Y_3 \stackrel{\Delta}{=} K_p T_{u_j}$, so that K_p would be defined from the solution of this LMI by $K_p = Y_3 T_{u_j}^{-1}$. However, $\{(97),(101)\}$ and the inequality (36) which ensures the stability of the SNLDI must be jointly solved. As (36) already implies that $K_p = Y_2 T^{-1}$, the inequality $Y_3 T_{u_j}^{-1} = Y_2 T^{-1}$ may not hold, so that the change of variable $Y_3 = K_p T_{u_j}$ cannot be performed.

If $T_{u_j} = T \in \mathscr{S}(r)$ is selected, with T the decision variable involved in the inequality (36), then, though at the expense of some conservatism, the change of variable $Y_2 = K_p T$ can be performed, leading to the LMIs (37) which can be jointly solved with (36).

Notice that contrarily to what is the case in Theorem 4.2, the inequalities in Theorem 4.7 need not be strict, as the well-posedness of the static inclusion (35) is already ensured by Theorem 4.6. □

B.5 Proof of results in Section 5.2.2

Proof of § 5.2.2-A.2: Define $\xi_a = (\xi', \xi_f)' \in \mathbb{R}^{n+m} \times \mathbb{R}$. The vector ξ_a belongs to $\tilde{\Xi}_a$ if and only if

$$\forall i = 1, \ldots, n, \quad \begin{pmatrix} \xi \\ \xi_f \\ 1 \end{pmatrix}' \begin{pmatrix} W_i W_i' & 0 & -W_i \overline{x}_{0i} \\ \star & 0 & 0 \\ \star & \star & \overline{x}_{0i}^2 - \overline{x}_{\omega i}^2 \end{pmatrix} \begin{pmatrix} \xi \\ \xi_f \\ 1 \end{pmatrix} \leq 0. \tag{102}$$

Besides, $\xi_a \in \mathscr{T}_P$ holds if and only if $\xi_a \in \mathscr{E}_P$ and $\xi_a \in \mathscr{E}_f$. The relationship $\xi_a \in \mathscr{E}_P$ is equivalent to

$$\begin{pmatrix} \xi \\ \xi_f \\ 1 \end{pmatrix}' \begin{pmatrix} P_1 & P_2 & 0 \\ \star & P_3 & 0 \\ \star & \star & -1 \end{pmatrix} \begin{pmatrix} \xi \\ \xi_f \\ 1 \end{pmatrix} \leq 0 \tag{103}$$

while $\xi_a \in \mathscr{E}_f$ holds if and only if $(\xi_f - \frac{x_{f_0}}{2})^2 \leq \frac{x_{f_0}^2}{4}$, i.e.

$$\begin{pmatrix} \xi \\ \xi_f \\ 1 \end{pmatrix}' \begin{pmatrix} 0 & 0 & 0 \\ \star & 1 & -\frac{x_{f_0}}{2} \\ \star & \star & 0 \end{pmatrix} \begin{pmatrix} \xi \\ \xi_f \\ 1 \end{pmatrix} \leq 0. \tag{104}$$

Thus, the set relationship $\mathscr{T}_P \subset \tilde{\Xi}_a$ is true if and only if the n inequalities (102) hold for all the vectors $\xi_a = (\xi', \xi_f)' \in \mathbb{R}^{n+m} \times \mathbb{R}$ which simultaneously satisfy (103) and (104). Applying the $\mathscr{S}$-procedure leads to a sufficient condition in terms of the n matrix inequalities

$$\exists\, \sigma_1 \in \mathbb{R}^+,\ \sigma_{f_1} \in \mathbb{R}^+,\ \ldots, \sigma_n \in \mathbb{R}^+,\ \sigma_{f_n} \in \mathbb{R}^+,\ \forall i = 1, \ldots, n,\ \begin{pmatrix} W_i W_i' - \sigma_i P_1 & -\sigma_i P_2 & -W_i \overline{x}_{0i} \\ \star & -\sigma_i P_3 - \sigma_{f_i} & \sigma_{f_i} \frac{x_{f_0}}{2} \\ \star & \star & (\overline{x}_{0i}^2 - \overline{x}_{\omega i}^2) + \sigma_i \end{pmatrix} \leq 0. \tag{105}$$

If $\sigma_i = 0$, satisfying the inequality (105) would require that the matrix $W_i W_i^{'}$ be negative semidefinite. However, this matrix is by construction nonzero and positive semidefinite. Consequently, σ_i is strictly positive. Making the change of variables $\tau_i \overset{\Delta}{=} \frac{1}{\sigma_i} \in \mathbb{R}^{+*}$ and $\tau_{fi} \overset{\Delta}{=} \frac{\sigma_{f_i}}{\sigma_i} \in \mathbb{R}^+$, and multiplying (105) by τ_i leads to (44). □